

Summary of Professional achievements

Contents:

1. Personal data	2
2. Possessed diplomas, degrees in science/arts	2
3. Information on previous employment in scientific/artistic entities	2
4. Indication of scientific achievement	3
4.a. Title of the scientific/artistic achievement	3
4.b. The series of publications constituting the scientific achievement	3
4.c. Overview of the scientific/artistic objective of the aforementioned publications and the achieved results, together with a discussion of their possible use	5
4.c.1. Methodology	5
4.c.1.1 Introduction.....	5
4.c.1.2 Research motivation	5
4.c.1.3 Research theses	7
4.c.1.4 Research tasks.....	7
4.c.1.5 Research methods	9
4.c.2. The most important scientific results forming the subject of habilitation	12
4.c.2.1 Homogeneous solid solutions	12
4.c.2.1.a. RKKY interactions in the $Zn_{1-x}Mn_xGeAs_2$ crystals	11
4.c.2.1.b. Superexchange interactions in the $Cd_{1-x}Mn_xGeAs_2$ crystals	14
4.c.2.1.c. Homogeneous Mn distribution in the $Cd_{1-x-y}Mn_xZn_ySnAs_2$ crystals	16
4.c.2.1.d. Defects of the $Zn_{1-x}Mn_xGeAs_2$ crystal lattice	17
4.c.2.1.e. Conductivity in the $Cd_{1-x}Mn_xGeAs_2$ crystals	22
4.c.2.1.f. Resistance oscillations in the $Cd_{1-x-y}Mn_xZn_ySnAs_2$ crystals	24
4.c.2.1.g. Summary.....	25
4.c.2.2 Ferromagnetic composites	26
4.c.2.1.a. Control over the magnetoresistive effects in $Zn_{1-x-y}Cd_xMn_yGeAs_2$	26
4.c.2.1.b. Self-organization of clusters in $ZnSnAs_2+MnAs$ composites	31
4.c.2.1.c. High-temperature ferromagnetism in $Zn_{1-x}Mn_xSnSb_2+MnSb$ composites.....	35
4.c.2.1.d. Control of the electrical properties of the $Zn_{1-x}Cd_xGeAs_2$ crystals	40
4.c.2.1.e. Magnetoresistance of the $Zn_{1-x-y}Cd_xMn_yGeAs_2$ composite crystals	44
4.c.2.1.f. Summary.....	45
4.c.3. Conclusions.....	46
4.c.4. Bibliography	47
5. Overview of other scientific - research achievements	50
5.a. Summary of scientific achievements before earning the master's degree	50
5.b. Summary of scientific achievements before receiving the title of doctor	50
5.c. Postdoctoral probation in the Laboratory of Positron Defect Spectroscopy	54
5.d. Summary of scientific achievements while working as an assistant professor, not forming part of habilitation dissertation.....	54
5.e. Development of instrumentation for magnetometric measurements	58
5.f. Future plans and directions of research.....	59

1. Name.

Łukasz Kilański

2. Diplomas, degrees in science/arts – with the name, place and year of obtaining and the title of the doctoral dissertation.

- 2.1. Name of the degree: Doctor of physics
Place of obtaining: Institute of Physics PAS, Warsaw, Poland
Year of obtaining: 2010
Thesis title: „Magnetism of the CuFeS₂ and NaCl structure semiconductor on examples of (Cd,Zn)MnGeAs₂ and GeSnMnEuTe”
- 2.2. Name of the degree: Master of Science
Place of obtaining:: Faculty of Technical Physics, Computer Science and Applied Mathematics, Technical University of Lodz, Poland
Year of obtaining: 2006
- 2.3. Title of diploma: Technician in economy
Place of obtaining: II Secondary Economic School, Lodz, Poland
Year of obtaining: 2001

3. Information on previous employment in scientific/artistic entities.

- 3.1. Name of position: Assistant professor
Place of work: Department of Semiconductor Physics, Institute of Physics, Polish Academy of Sciences, Warsaw, Poland
Period of work: from 25.08.2011 until now
- 3.2. Name of position: Postdoc
Place of work: Department of Applied Physics, Aalto University, Espoo, Finland
Period of work: from 25.08.2010 until 24.08.2011
- 3.3. Name of position: Research assistant
Place of work: Department of Semiconductor Physics, Institute of Physics, Polish Academy of Sciences, Warsaw, Poland
Period of work: from 01.07.2010 until 24.08.2010
- 3.4. Name of position: Scientific internship
Place of work: Department of Applied Physics, Technical University of Helsinki, Espoo, Finland
Period of work: from 01.08.2007 until 31.10.2007
- 3.5. Name of position: PhD student
Place of work: Department of Semiconductor Physics, Institute of Physics, Polish Academy of Sciences, Warsaw, Poland
Period of work: from 01.10.2006 until 17.06.2010

4. Indication of achievement¹ resulting from Article 16 paragraph 2 of the Act dated 14 March 2003 on Academic Degrees and Scientific Title and on Degrees and Title in the arts (Dz. U. No. 65, item. 595 as amended.):

a) Title of the scientific/artistic achievement:

As the scientific achievement I submit a series of 8 publications (H1-H8), all related to the title:

„Magnetic interactions and electronic transport in homogeneous and nanocomposite II-IV-V₂ semiconductors with Mn”

b) The series of publications constituting the scientific achievement:

H1. L. Kilański, K. Szalowski, R. Szymczak, M. Górską, E. Dynowska, P. Aleshkevych, A. Podgórní, A. Avdonin, W. Dobrowolski, I. V. Fedorchenko, and S. F. Marenkin, "Low-dilution limit of Zn_{1-x}Mn_xGeAs₂: Electrical and magnetic properties", Journal of Applied Physics 114, 093908-1-9 (2013)
Impact factor (2013): 2.185
DOI: 10.1063/1.4820475

H2. L. Kilański, M. Górską, E. Dynowska, A. Podgórní, A. Avdonin, W. Dobrowolski, I.V. Fedorchenko, and S.F. Marenkin, "Homogeneous limit of Cd_{1-x}Mn_xGeAs₂ alloy: electrical and magnetic properties" Journal of Applied Physics 115, 133917-1-6 (2014)
Impact factor (2014): 2.183
DOI: 10.1063/1.4870474

H3. L. Kilański, C. Rauch, F. Tuomisto, A. Podgórní, E. Dynowska, W. Dobrowolski, I.V. Fedorchenko, and S.F. Marenkin, "Point defects and p-type conductivity in Zn_{1-x}Mn_xGeAs₂" Journal of Applied Physics 116, 023501-1-7 (2014)
Impact factor (2014): 2.183
DOI: 10.1063/1.4887118

H4. L. Kilański, I. V. Fedorchenko, M. Górską, A. Ślawska-Waniewska, N. Nedelko, A. Podgórní, A. Avdonin, E. Lähderanta, W. Dobrowolski, A.N. Aronov, and S.F. Marenkin, "Magnetoresistance control in granular Zn_{1-x-y}Cd_xMn_yGeAs₂ nanocomposite ferromagnetic semiconductors" Journal of Applied Physics 118, 103906-1-8 (2015)
Impact factor (2015): 2.101
DOI: 10.1063/1.4930047

¹ in the case the achievement is the joint publication/publications, declarations of all its contributors should be provided, defining the individual contribution of each of them in its creation

H5. I.V. Fedorchenko, L. Kilanski, I. Zakharchuk, P. Geydt, E. Lahderanta, P.N. Vasilyev, N.P. Simonenko, A.N. Aronov, W. Dobrowolski, and S.F. Marenkin, "Composites based on self-assembled MnAs ferromagnet nanoclusters embedded in ZnSnAs₂ semiconductor"

Journal of Alloys and Compounds 650, 277-284 (2015)

Impact factor (2015): 3.014

DOI: 10.1016/j.jallcom.2015.08.006

H6. L. Kilanski, M. Górska, A. Ślawska-Waniewska, S. Lewińska, R. Szymczak, E. Dynowska, A. Podgórn, W. Dobrowolski, U. Ralević, R. Gajić, N. Romčević, I.V. Fedorchenko, and S.F. Marenkin,

"High temperature magnetic order in Zn_{1-x}Mn_xSnSb₂+MnSb nanocomposite ferromagnetic semiconductors"

Journal of Physics: Condensed Matter 28, 336004-1-10 (2016)

Impact factor² (2015): 2.209

DOI: 10.1016/j.jallcom.2015.08.006

H7. L. Kilanski, A. Reszka, M. Górska, V. Domukhovski, A. Podgórn, B.J. Kowalski, W. Dobrowolski, I.V. Fedorchenko, A.N. Aronov, and S.F. Marenkin,

"Composite Zn_{1-x}Cd_xGeAs₂ semiconductors: structural and electrical properties"

Journal of Physics: Condensed Matter 28, 495802-1-9 (2016)

Impact factor² (2015): 2.209

DOI: 10.1088/0953-8984/28/49/495802

H8. L. Kilanski, P. Skupiński, S. Lewińska, E. Dynowska, A. Reszka, K. Grasz, R. Szymczak, A. Ślawska-Waniewska, M. Górska, B.J. Kowalski, and W. Dobrowolski, "Homogeneous vs. composite Cd_{1-x-y}Mn_xZn_ySnAs₂ crystals: magnetic interactions and transport properties"

Physical Review B **95**, 035206-1-10 (2017)

Impact factor² (2015): 3.718

DOI: 10.1103/PhysRevB.95.035206

Kilanski Łukasz
27.02.2017v.

² In the case of manuscripts published in 2016 and 2017, due to the lack of "impact factor" for 2016 and 2017 I gave a value for 2015.

c) Overview of the scientific/artistic objective of the aforementioned publications and the achieved results, together with a discussion of their possible use

c.1. Methodology

c.1.1. Introduction

Modern electronics is based essentially on two classes of devices, i.e., instruments for processing and storing information. Information processing is performed using instruments based on semiconductor materials, and storage of information is carried out by instruments whose design uses layered ferromagnetic metals. The main problem that prevents an increase in speed of electronic devices manufactured today is the need for communication between the components processing and storing information. Unequivocal and immediate solution to this problem is to combine the properties of semiconductors and ferromagnetic metals in one material, so that the task of processing and storage of information can be realized by a single device. *Semiconductor Spintronics*³ is considered the most important of the possible solutions to this problem, providing direction of development for hybrid devices that can perform all three of the electronic operations: logic, communication, and storage of information in the same material technology [1-3]. The development of semiconductor spintronics in recent years offers groundbreaking solutions in the field of possible practical applications through the use of a number of phenomena and physical effects that are currently intensively investigated.

c.1.2. Research motivation

Semiconductor spintronics based on semimagnetic semiconductors is being developed for two decades. Since the discovery of ferromagnetism induced by the long-range magnetic interactions mediated by free carriers (RKKY⁴) in materials based on the IV-VI group semimagnetic semiconductors, i.e. $\text{Pb}_{1-x}\text{Sn}_x\text{Mn}_y\text{Te}$ crystals [4], there was a sharp increase in interest in research of ferromagnetism in semimagnetic semiconductors. Currently, conventional, intensively studied, and well understood ferromagnetic semiconductors based on III-V, II-VI and IV-VI groups of the periodic table of elements are of great scientific importance but do not show ferromagnetism at room temperature for homogeneous samples [5,6]. The use of ferromagnetic semiconductors in spintronics devices requires the development of materials with Curie temperature, T_C , higher than room temperature. Most reports in the literature about the magnetic properties of diluted semimagnetic semiconductors show the Curie temperature values significantly lower than 300 K [7], which makes these compounds of little use in practical applications.

One of the proposed solutions to the problem of inapplicability of semiconductor spintronics devices is *the use of hybrid heterogeneous systems* based on composite semiconductor/ferromagnetic cluster materials with a Curie temperature higher than room temperature. Among many groups of the studied semiconductor materials belonging to the II-IV-V₂ group are considered as an important class of materials, as they offer a number of important properties that enable their easy application and integration in the modern electronics. Chemical compounds belonging to the chalcopyrite II-IV-V₂ group of materials are ternary analogues of binary III-V materials, i.e., GaAs and elemental group IV semiconductors, i.e., Si and Ge. The tetragonal chalcopyrite crystal structure is similar to the

³ This term was proposed by S. A. Wolf in 1996, as a name for DARPA initiative for new materials and magnetic devices.

⁴ The abbreviation is derived from the names of discoverers ie Ruderman-Kittel-Kasuya-Yoshida.

zincblende structure. In this way, many of the compounds belonging to the II-IV-V₂ group of semiconductors show a lattice match to their analogs in the III-V group [8]. Thus, they are compatible with the existing technology based on GaAs [9,10]. Chalcopyrite compounds are considered as a potential efficient source of spin-polarized photoelectrons due to the non-degenerate top of the valence band [11]. Moreover, the large values of the nonlinear optical coefficients of the CdGeAs₂ crystals and the direct energy gap at the Γ point of the Brillouin zone [12] makes the II-IV-V₂ materials suitable for applications in nonlinear optics.

The similarity of crystals belonging to the II-IV-V₂ group, containing transition metal ions, to the III-V compounds, i.e., Ga_{1-x}Mn_xAs suggests that for the low concentration of paramagnetic ions in the alloy it seems possible to strengthen long-range magnetic interactions carried by the free carriers, i.e., RKKY interaction. That would lead to the optimization of the magnetic properties of the material for a homogenous ferromagnetic compound. The growth of bulk crystals of ternary arsenides, i.e., Ga_{1-x}Mn_xAs under thermodynamic equilibrium conditions is not limited by the low solubility of Mn ions with $x < 0.001$ [13]. However, in the II-IV-V₂ group compounds the solubility of paramagnetic ions in the bulk crystals grown under thermodynamic equilibrium conditions is significantly higher (of the order up to 5%). Through research devoted to RKKY interactions in II-IV-V₂ crystals it will be possible to control the magnetic properties of the alloy. In Refs. [14,15] published in 2011 and 2012 containing the results showing paramagnetism for the Zn_{0.947}Mn_{0.053}GeAs₂ crystal we showed that indeed the solubility of Mn ions in the selected II-IV-V₂ group crystals is of the order of several mole percent, and this line of research requires considerable work to determine precisely the potential of the homogeneous semimagnetic semiconductors based on materials from the II-IV-V₂ group.

Ferromagnetism at room temperature has been observed in recent years in the case of some representatives of the semiconductors belonging to the II-IV-V₂ group containing Mn [16,17]. There are numerous reports in the literature, which shows the ferromagnetic order in several materials such as Cd_{1-x}Mn_xGeP₂ [18], Zn_{1-x}Mn_xSnAs₂ [19], or Zn_{1-x}Mn_xGeP₂ [20], with the Curie temperatures, T_C , equal to 320 K, 329 K, and 312 K, respectively. Initially, it was proposed in the literature that the ferromagnetic order at room temperature in the materials listed above can be caused by the RKKY interaction [21]. Another explanation was to link the ferromagnetism to the presence of defects which would be responsible for the observed magnetic properties of chalcopyrite alloys doped with Mn ions through superexchange magnetic interactions [22].

In contrast to the above possible explanations my initial experimental studies of the II-IV-V₂ crystals with Mn showed that the ferromagnetism at room temperature with maximum T_C of about 367 K in the Zn_{1-x}Mn_xGeAs₂ crystals [21] and the T_C of about 323 K in the Cd_{1-x}Mn_xGeAs₂ crystals [23] is due to the presence of MnAs clusters with different geometrical parameters. Therefore, there was in the literature a number of conflicting explanations for this phenomenon. That required verification and correction. That was one of my reasons for the choice of the research topics and focusing the research efforts on understanding the structural, magnetic, and electrical properties of this important and prospective group of semiconductors.

c.1.3. Research theses

The development of the knowledge related to the understanding of structural, magnetic, and electrical properties of the selected semiconductor crystals belonging to the II-IV-V₂ group with manganese ions required in 2010 to develop and prove the following research theses:

- T1. The existence of the Mn content range in which the II-IV-V₂ semiconductors exhibit characteristics specific to homogeneous materials and above which they show properties specific to composite materials. This thesis has been verified on the basis of results obtained in the publications [H1-H8].
- T2. The existence in the selected II-IV-V₂ group semiconductors with Mn of long-range and short-range exchange magnetic interactions leading to the appearance of the magnetic coupling. This thesis has been verified in detail in the publications [H1, H2, H8].
- T3. The existence of the phenomena of the carrier localization on the defect centers and the influence of the homogeneous distribution of Mn in the material on the magnetotransport effects in the selected II-IV-V₂ semiconductors with Mn. This thesis was verified in the publications [H1-H3, H8].
- T4. The possibility of preparing Zn_{1-x-y}Cd_xGe_yAs₂ solid solutions and ferromagnetic Zn_{1-x-y}Cd_xGe_yAs₂+MnAs composites with chemical composition dependent magnetic and electrical properties. This thesis was verified in publications [H4, H7].
- T5. The existence of short-range magnetic interactions in the matrix of the selected composite II-IV-V₂ semiconductors through the aggregation of magnetic ions in the clusters. This thesis was verified in the publications [H4-H8].
- T6. The existence of the influence of the clusters on the transport and magnetotransport in the selected II-IV-V₂ group semiconductors obtained in the form of composite materials. This thesis has been verified in the publications [H4-H8].

The selected series of publications enabled me to verify these scientific theses.

c.1.4. Research tasks

The key issue for my research is to describe and understand the structural, magnetic and magnetotransport properties of the selected materials belonging to II-IV-V₂ with Mn. As a part of the experimental work I performed a series of measurements characterizing the properties of the studied semiconductors. The performed research enabled me to carry out the following research objectives:

1. Improvement of the structural properties of crystals focused on eliminating precipitates of foreign crystallographic phases in alloys. An important issue from the point of view of applications is to investigate the phase diagram of II-IV-V₂ compounds in order to estimate the range of compositions for which the resulting crystals have the best structural quality. Essential for the development of the technology of the crystals mentioned above is to study the limits of a uniform dissolution of magnetic impurities in the alloy, the occurrence of segregation of magnetic impurities, and the studies of defects of the crystal lattice. On the other hand, structural investigations take a significant problem of obtaining nanocomposite systems semiconductor - ferromagnetic metal, based on II-IV-V₂ materials.
2. Understanding the physical mechanisms behind the interesting magnetic properties of crystals belonging to the II-IV-V₂ group of periodic table containing magnetic Mn ions. These studies I conducted in the framework of the statutory activity in the IFPAN. This research was also financed by the Ministry of Science and Higher Education of Poland through the awarded Iuventus-Plus grant titled "Ferromagnetic semiconductor nanocomposites based on II-IV-V₂ group: magnetic, electrical and optical properties"

which I headed in 2011. These studies focused on a comprehensive understanding of materials using different magnetometric methods. As a result, the study identified a number of material parameters of crystals, i.e., the critical temperatures, spontaneous magnetization and coercive field, as a function of the relevant parameters, e.g., the chemical composition and electrical parameters.

- a) An extremely important task was to investigate the properties of crystals containing manganese arsenide precipitates, which (as demonstrated by my preliminary studies presented in my doctoral thesis) in several compounds belonging to this group are the cause of the observation of ferromagnetism at room temperature. In particular, I examined the problem of the occurrence of short-range ferromagnetic interactions that accompany long-range magnetic interactions mediated by free charge carriers. These issues are an extremely important step towards the proper understanding of the physical mechanisms that determine the physical properties of the composite crystals.
 - b) I also carried the studies of a number of crystals, in which there were no segregation of magnetic impurities. The presence of precipitates is associated with a significant deterioration in the electrical properties of crystals. Due to the low mobility of carriers the practical use of the crystals, in which the clusters are present, in spintronic devices is questionable. Thus one of the objectives of the studies I assigned to investigation of the crystals with homogeneous distribution of magnetic impurities in the sample volume. The strengthening of the long-range magnetic interactions carried by the free carriers (RKKY) will allow to optimize the magnetic properties of the material in terms of the development of homogenous ferromagnetic material. The experimental data were used by me to estimate the exchange parameters J_{dd} (ion-ion) and $J_{s,pd}$ (paramagnetic ion - free carrier). I estimated also the role of direct and indirect magnetic interactions in the changes in the magnetic properties of crystals with a change in their chemical composition.
3. I took for the first time in this group of materials an important problem from the point of view of their possible use to investigate the possibility of changing the type of conductivity and carrier concentration. I performed detailed studies of the physical mechanisms behind the strong p-type conductivity observed in ZnGeAs_2 crystals. The main objective associated with the optimization of the electronic properties of the aforementioned crystals is to control their carrier concentration and mobility. Increasing the carrier concentration to the level of 10^{20} - 10^{21} cm^{-3} will strengthen the RKKY interaction in the system and allow indirect control of magnetic properties of crystals. A number of publications devoted to studies of crystals belonging to the II-IV- V_2 group confirms the possibility of doping these semiconductors.
 4. Another important goal for me was to study the effect of geometrical parameters of MnAs clusters present in II-IV- V_2 crystals with higher contents of Mn on the electrical properties of the materials. This task has been prepared on the technological side by the appropriately selected temperature of the sample synthesis and fast cooling of the crystals after synthesis. This allowed the aggregation of magnetic impurities in clusters with controlled size. This problem is very interesting from both the basic science and the applications points of view. The materials, in which ferromagnetic clusters are present are an important and intensively developed in recent years group of materials called nanocomposites. Due to the presence of ferromagnetic clusters the granular ferromagnetic materials have a number of significant effects important from the point of view of the possible applications (e.g. the giant or colossal magnetoresistance).

c.1.5. Research methods

Crystal synthesis

Preparation of crystals which are the subject of the research has been carried out in collaboration with two groups of technologists specializing in the growth of bulk semiconductor crystals containing Mn magnetic impurities.

The synthesis of $Zn_{1-x}Mn_xGeAs_2$ (manuscript [H1] and [H3]), $Cd_{1-x}Mn_xGeAs_2$ (manuscript [H2]), $Zn_{1-x-y}Cd_xMn_yGeAs_2$ (manuscript [H4]), $ZnSnAs_2+MnAs$ (manuscript [H5]), $ZnSnSb_2+MnSb$ (manuscript [H6]) and $Zn_{1-x-y}Cd_xMn_yGeAs_2$ (manuscript [H7]) crystals was carried out in the Institute of Inorganic Chemistry of the Russian Academy of Science by prof. S.F. Marenkin, dr. I.V. Fedorchenko, and M.Sc. A.N. Aronov. Participation of the Russian group in my research was consisted of synthesis of dozens of different semiconductor II-IV-V₂ group crystals, some of which contain magnetic manganese ions.

The synthesis of $Cd_{1-x-y}Mn_xZn_ySnAs_2$ crystals (manuscript [H8]) was carried out in the Institute of Physics of the Polish Academy of Sciences in Warsaw by dr. hab. K. Graszka and dr. P. Skupiński.

Studies of the structural properties of crystals

I conducted the analysis of the chemical composition of crystals using the Tracor Spectrace Xray 5000 spectrometer utilizing an energy dispersive X-ray fluorescence (EDXRF⁵) method. This technique is based on the measurement and analysis of the intensity of the secondary X-ray radiation emitted from the crystal. The experimental spectrum is analyzed to determine the chemical composition of the material. The results are obtained in the form of the respective mole fractions of the elements and are very important quantity used throughout the following stages of research.

The crystallographic characterization of the studied crystals was carried out by my colleagues, i.e. Dr. E. Dynowska from IF PAN (manuscripts [H1-H3, H6, H8]), M.Sc. V. Domukhovski from IF PAN (manuscript [H7]) and colleagues from Russia (manuscripts [H4, H5]) using high-resolution X-ray diffraction method (HRXRD⁶). HRXRD measurements were performed using two devices, i.e. highly-resolved X'Pert PRO MPD Panalytical diffractometer and Siemens D5000 diffractometer. The resulting diffraction patterns were analyzed using the indexing and the Rietveld refinement methods. The results enabled the analysis of crystallographic phases present in the crystals and the calculation of the lattice parameters of each of the observed phases.

Structural studies were broadened through measurements of surface morphology of the samples and their chemical microanalysis. These measurements were performed by my colleagues in Russia (manuscript [H4, H5]) and colleagues from IF PAN, i.e. Prof. B.J. Kowalski and M.Sc. A. Reszka (manuscript H7, H8) with the Hitachi SU-70 scanning electron microscope (SEM). This microscope allows for the analysis of chemical composition distribution and a mapping of the chemical element content of the sample surface. In turn in the manuscript [H6] the morphology of crystals was studied with the use of the atomic force microscope (AFM⁷) and magnetic force microscope (MFM⁸). These studies were done in collaboration with the University of Belgrade. AFM and MFM measurements were done at room temperature and at atmospheric pressure.

⁵ energy dispersive x-ray fluorescence

⁶ high resolution x-ray diffraction

⁷ atom force microscopy

⁸ magnetic force microscopy

A very important element of structural studies was positron annihilation spectroscopy measurements published in [H3]. These studies I performed personally during postdoctoral fellowship in the group of Prof. F. Tuomisto at the Aalto University in Espoo (Finland) in the period 2010 - 2011. A group of measurement techniques called positron annihilation spectroscopy allows the studies of parameters of defects present in the crystal lattice. Positrons localize at the negatively charged or neutral defects of the crystal lattice which increases their lifetime. Positron lifetime measurements enable the identification of the type of crystal lattice defects. The process of electron - positron annihilation causes (due to the fulfillment of the conservation of momentum and energy principles) the Doppler broadening of the energy of the emitted photon by the value of projection of the angular momentum of the electron on the direction of the emitted photon. Experimentally it is possible to measure the Doppler broadening of the spectrum emitted during annihilation γ quanta with energy close to 511 keV. Quantitative analysis of the Doppler broadening of the line at 511 keV gives the possibility to identify the chemical environment of the vacancy defects, at which the annihilation of the electron - positron pairs occurs.

Studies of the magnetic properties of crystals

Magnetic properties of the crystals I conducted by using a number of magnetometric techniques. I had direct access to most of the used experimental setups.

Measurements of alternating-field magnetic susceptibility, χ_{AC} , and magnetization, M , measured at a constant magnetic field with induction B were done using the LakeShore 7229 AC Susceptometer/DC Magnetometer setup. This device allowed me to study the magnetic susceptibility by mutual induction technique in a wide temperature range from $T = 1.4$ K to 325 K. The use of mutual induction method enables the measurements of the magnetic susceptibility of the order of 2×10^{-8} emu in the presence of an alternating magnetic field of controlled amplitude, $H_{AC} < 3$ mT, and frequency, $f < 10$ kHz. In turn, the magnetic moment was measured using the Weiss extraction technique in a constant magnetic field with $B \leq 9$ T.

Magnetization measurements were complemented via cooperation within IF PAN with Prof. A. Ślawska-Waniewska, Dr. N. Nedelko, and Dr. S. Lewińska, who have done measurements of magnetization as a function of temperature using the vibrating sample magnetometer (VSM⁹) which allows widening the studied temperature range to the range from 295 K to 550 K

Magnetization measurements were performed in part using Quantum Design MPMS XL-7 SQUID magnetometer. This device allowed the measurements of the magnetization in the temperature range between $2 \text{ K} < T < 380 \text{ K}$ and the magnetic field induction $B \leq 7 \text{ T}$, thus giving the opportunity to study the magnetic phase transition in the temperature range not covered by the LakeShore 7229 magnetometer.

Studies of the magnetic properties of the crystals published in manuscript H1 were broadened by the measurements of the electron paramagnetic resonance (EPR¹⁰). EPR studies of $\text{Zn}_{1-x}\text{Mn}_x\text{GeAs}_2$ crystals and the analysis of the experimental data was carried out by Dr P. Aleshkevych under my supervision.

Studies of the electrical properties of crystals

I performed the measurements of the electron transport with the use of two experimental setups: (i) with a system equipped with the resistive magnet for $B \leq 1.5 \text{ T}$ and (ii) with a system equipped with the superconducting magnet for $B \leq 13 \text{ T}$. I performed the

⁹ vibrating sample magnetometer

¹⁰ electron paramagnetic resonance

measurements of the electrical properties using a standard six-contact method using a direct current. I made a number of studies of the magnetic field dependencies of the resistivity tensor components, ρ_{xx} and ρ_{xy} , in the range of strong magnetic fields with a maximum induction, $B = 13$ T. The magnetotransport studies consisted of the measurements of temperature dependencies of the resistivity ρ_{xx} and the Hall effect. The carrier concentration, n , and the carrier mobility, μ , were calculated as a function of temperature.

c.2. The most important scientific results forming the subject of habilitation

c.2.1. Homogeneous solid solutions

The ability to create solid solutions of Mn in the II-IV-V₂ semiconductor matrix is a very important issue due to the possibility of the control of the RKKY interaction strength in the semimagnetic semiconductors by altering their electrical properties. The test results presented in manuscripts [H1,H2,H8] were motivated by my first observation of paramagnetism related to the Mn ions uniformly dissolved in the Zn_{0.947}Mn_{0.053}GeAs₂ crystals [15]. Unfortunately, despite the presence of up to 5 mol% of Mn uniformly distributed in the ZnGeAs₂ lattice our results indicated that the magnetization of the material is only about 1% of the value, which would result from the chemical composition of the crystals.

c.2.1.a. RKKY interactions in the Zn_{1-x}Mn_xGeAs₂ crystals

The studies of the long-range magnetic interactions in the II-IV-V₂ materials required to carry out systematic studies of the properties of the Zn_{1-x}Mn_xGeAs₂ crystals with $x < 0.053$. The studies presented in the manuscript [H1] focused on acquiring knowledge about the possibility to improve the structural, magnetic, and electrical properties of paramagnetic Zn_{1-x}Mn_xGeAs₂ crystals. I acquired from my coworkers from Russia 15 Zn_{1-x}Mn_xGeAs₂ crystal ingots with the average Mn content, x , in the range of 0 to 0.042.

The structural properties of Zn_{1-x}Mn_xGeAs₂ crystals have been studied in detail using a variety of experimental techniques. I have conducted the EDXRF studies which showed that the obtained Zn_{1-x}Mn_xGeAs₂ crystals have the correct stoichiometry equal to 1-x:x:1:2. The HRXRD studies showed that the Zn_{1-x}Mn_xGeAs₂ crystals with $x = 0.003$ have the chalcopyrite structure, while for $x = 0$ and for the crystals with $x > 0.003$ we observed the presence of the zincblende phase.

The main scientific problem taken in the manuscript [H1] *was to estimate the dominant type of magnetic interactions* and their strength in the Zn_{1-x}Mn_xGeAs₂ crystals. This is the first attempt to verify the theses T1 and T2. For this purpose, I made a study of the alternating-field magnetic susceptibility versus temperature for a series of Zn_{1-x}Mn_xGeAs₂ crystals with different chemical compositions, x , from 0 to 0.043.

The results of the magnetic susceptibility studies are presented in Fig. 1a. I estimated the value of the diamagnetic component of the magnetic susceptibility, $\chi_{\text{dia}} = -2 \times 10^{-7}$ emu/g. All the samples with $0 < x \leq 0.042$ show paramagnetic Curie-Weiss behavior at temperatures $T < 30$ K. Moreover, at temperatures $T > 30$ K the apparent deviation from the behavior described by the Curie-Weiss law is observed. It is not related with the Van-Vleck paramagnetism because the observed contribution has values higher than the order of magnitude of the known literature values for Cd_{1-x}Co_xSe are the order of 10^{-7} emu/g [24]. Therefore, I interpreted this contribution as related to the magnetic ions coupled via the short range magnetic interaction such as the super-exchange Mn-As-Mn magnetic interaction via an anion. Analysis of the temperature dependence of the magnetic susceptibility indicated that the additional contribution to the susceptibility has values varying with the chemical composition of the samples from 3×10^{-7} emu/g to 1×10^{-6} emu/g.

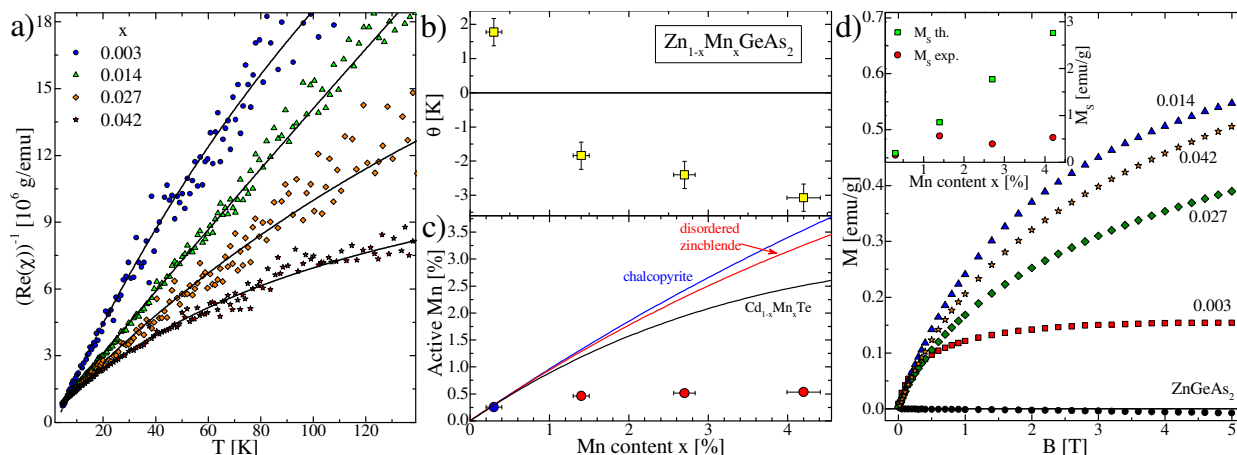


Fig. 1. Results of the magnetometric studies of the $Zn_{1-x}Mn_xGeAs_2$ crystals with different chemical compositions, x , comprising: (a) temperature dependence of the inverse of the real part of the alternating-field magnetic susceptibility (b) the Curie-Weiss temperature and (c) the effective Mn content as a function of the average chemical composition, x , and (d) the $M(B)$ curves recorded at $T = 4.5$ K; inset – the experimentally observed (circle symbols) and the theoretically calculated (square symbols) values of the saturation magnetization dependence on the chemical composition, x .

The analysis of the magnetic susceptibility, which was done using the Curie-Weiss law allowed the calculation of the Curie-Weiss temperature, θ , as a function of the average chemical composition of the crystals (see Fig. 1b). The θ values that I calculated for the $Zn_{1-x}Mn_xGeAs_2$ crystals are small. A very important and interesting result for me is the observed $\theta(x)$ dependence, and in particular the θ sign change between the crystals with $x = 0.003$ and $x = 0.014$. I interpreted this result as a consequence of a change in the sign of the average exchange constant for all Mn ions in the crystal, and therefore, the *change of the dominant type of the magnetic interaction in the system*. It can, therefore, be presumed that in the case of crystals with $x = 0.003$ the magnetic interactions with the positive sign of the magnetic exchange constant are dominant, while in the crystals with $x \geq 0.014$ the magnetic interactions with the negative sign of the magnetic exchange constant play a dominant role, which increases with x . The confirmation of my interpretation required to carry out numerical calculations. These calculations were performed in cooperation with me by Dr. hab. K. Szałowski working at the University of Lodz. Together with Dr. hab. K. Szałowski we showed in the chapter III.D of the manuscript [H1] that in the II-IV- V_2 group semiconductor, in which we assumed two types of magnetic interactions: (i) the long-range RKKY magnetic interactions and (ii) the short range super-exchange Mn-As-Mn magnetic interactions, the experimental $\theta(x)$ dependence can be reproduced theoretically. It is possible via changing the value of the exchange interaction strength for both the above types of magnetic interactions. As a result, the theoretical explanation and confirmation of my initial interpretation of the experimental data became possible.

Furthermore, the results of calculations indicate that in the case of the $Zn_{1-x}Mn_xGeAs_2$ crystal with $x = 0.003$, we have to deal with one type of magnetic interactions i.e. RKKY interaction. This conclusion was verified through the EPR measurements. Analysis of the EPR data obtained at $T = 10$ K showed that for the $Zn_{1-x}Mn_xGeAs_2$ crystal with $x = 0.003$ we observed 30 resonances. This result is interpreted as characteristic of the Mn^{2+} ions, demonstrating splitting of the fine ($S = 5/2$) and the hyperfine ($I = 5/2$) structures. Accordingly, the EPR data were interpreted as the presence of five groups, each consisting of six Mn^{2+} lines. The relative shifting of the line groups is associated with splitting of the

ground state in the zero magnetic field. Thus, we proved that in case of the crystal with $x = 0.003$ Mn ions are in the 2+ charge state. On the other hand, for $x \geq 0.014$ we do not observe either the fine structure or hyperfine structure of the Mn ions due to the blurring of the EPR resonance line. It was only possible to determinate the effective electron g-factor in the material equal to 1.9972. The above results are important in view of verification of thesis T1.

These findings allowed us to use the RKKY model and calculation for the first time for the $Zn_{1-x}Mn_xGeAs_2$ crystals the value of the Mn ion – free conducting carrier magnetic exchange constant, $J_{pd} = (0.75 \pm 0.09)$ eV and verification of thesis T2. This is a significant result in view of the fact that the obtained value is high. This raises hopes of inducing ferromagnetism based on the RKKY interaction in the $Zn_{1-x}Mn_xGeAs_2$ crystals.

Based on the experimentally determined values of the Curie constant, C , we calculated the effective Mn content in the alloy as a function of the average Mn content, x (see Fig. 1c). This value is important in determining the effectiveness of doping the non-magnetic material with magnetic ions and therefore verification of thesis T1. It turns out that only in the case of the $Zn_{1-x}Mn_xGeAs_2$ crystal with $x = 0.003$ the effective Mn content is close to the average value calculated based on the EDXRF spectra analysis. For chemical compositions higher than $x = 0.003$ the calculated effective Mn content in the alloy does not increase along with x and reaches a maximum value not exceeding $x \approx 0.005$. This means that despite the lack of manganese precipitations in the $Zn_{1-x}Mn_xGeAs_2$ crystal the possibilities of doping with Mn ions can be significantly reduced. It forced me to search for the other II-IV-V₂ group materials, for which the observed effective concentration of the Mn ions will be higher. I continued the verification of theses T1 and T2 for the $Cd_{1-x}Mn_xGeAs_2$ and $Cd_{1-x-y}Mn_xZn_ySnAs_2$ crystals (manuscripts [H3] and [H8]) in order to improve the magnetic properties with respect to the results observed for the $Zn_{1-x}Mn_xGeAs_2$ crystals.

The problem of the physical mechanisms responsible for the presence of the short-range magnetic interactions in the $Zn_{1-x}Mn_xGeAs_2$ crystals I solved in cooperation with dr. hab. K. Szałowski. Cooperation led to the calculation of the relationship between the average chemical composition, x , and the composition effective chemical content, x_θ , in the material, wherein some Mn ions are coupled antiferromagnetically via the super-exchange magnetic interaction. The theoretical calculated curves determined in this way are not similar to the experimental curves (see Fig. 1c). This means that the additional paramagnetic contribution observed by me in the $Zn_{1-x}Mn_xGeAs_2$ crystals is also connected with the presence of clusters more complex than the short-range coupled double or triple Mn systems in these samples.

The studies of the magnetic properties of the $Zn_{1-x}Mn_xGeAs_2$ crystals I continued with a series of measurements of the magnetization $M(B)$ curves (see Fig. 1d). I did not observe a presence of magnetic hysteresis in any of the studied samples. In the case of the $Zn_{1-x}Mn_xGeAs_2$ crystal with $x = 0.003$ the observed shape of the $M(B)$ curve is a shape typical of paramagnetic material. The experimental $M(B)$ curves for this sample can therefore be fitted with the Brillouin function. On the other hand, in the case of the $Zn_{1-x}Mn_xGeAs_2$ crystals with $x \geq 0.014$ I observed that the $M(B)$ curves have a shape deviating from the shape of the typical paramagnetic material. The $M(B)$ curves for the crystals with $x \geq 0.014$ were fitted by me using the modified Brillouin function called Gaj function [25], the function containing additional phenomenological factor T_0 . The obtained T_0 constant values (between -1.95 K and -1.5 K) and the saturation magnetization, M_S , values (inset to Fig. 1d) were determined by fitting the experimental data. The $M_S(x)$ dependence is very similar to the effective Mn content as a function of x dependence determined based on the analysis of the Curie-Weiss law. The measurement results and the conclusions drawn on the basis of the results of magnetic susceptibility and magnetization are close to each other.

The results summarized in the manuscript [H1] allowed me to show that, despite the fact that the solubility of magnetic ions in the $Zn_{1-x}Mn_xGeAs_2$ crystals is high and has values at least $x = 0.053$ the analysis of data and detailed research allowed me to demonstrate that the effective concentrations of the Mn ions in this material are almost an order of magnitude lower than the nominal value estimated by the EDXRF data. I allowed verification of thesis T1 and forced me to look for other representatives of the II-IV-V₂ group of semiconductors, for which it will be possible to obtain a homogeneous bulk diluted semimagnetic semiconductors.

c.2.1.b. Superexchange interactions in the $Cd_{1-x}Mn_xGeAs_2$ crystals

In the next step I focused the studies towards verification of thesis T1 and T2 via the studies of $Cd_{1-x}Mn_xGeAs_2$ crystals with the chemical compositions determined by the method EDXRF, ranging from $x = 0$ to $x = 0.037$. The experimental results and the analysis of the obtained data were published in the manuscript [H2]. *The $Cd_{1-x}Mn_xGeAs_2$ crystals have a much better crystalline quality than the $Zn_{1-x}Mn_xGeAs_2$ crystals.* We observed the presence of diffraction patterns predicted by the diffraction theory, but experimentally never observed before [26,27]. The excellent quality of the $Cd_{1-x}Mn_xGeAs_2$ crystals allowed the publication of a separate paper focused on the HRXRD results and its analysis in a journal specialized in publishing X-ray research manuscripts [28]. Additionally, we published in collaboration with Prof. N. Romcevic from the Belgrade University an extensive manuscript about the Raman spectroscopy results. As a result, we were able to identify the presence of anti-substitutional Ge_{As} defects and a small fraction of $CdAs_2$ and Cd_3As_2 precipitates [29]. Also we observed that with increasing the Mn content in the $Cd_{1-x}Mn_xGeAs_2$ crystals their lattice parameters, a and c , show a monotonic dependence as a function of x . It should be emphasized that the slope coefficients of the $a(x)$ and $c(x)$ dependences obtained by us have similar values to those in the literature [30]. These relationships are important indication which might attest to the fact that Mn substitutes Cd positions in the semiconductor crystal lattice, and it is highly probable that the studied solid solutions of Mn ions in the $CdGeAs_2$ semiconductor matrix are homogeneous. This result is important in view of verification of thesis T1.

Magnetic properties of the $Cd_{1-x}Mn_xGeAs_2$ crystals are the consequence of their excellent crystal quality. The results of the studies of the magnetic susceptibility were published in the manuscript [H2] and have been summarized in Fig. 2a. All the $Cd_{1-x}Mn_xGeAs_2$ crystals with $0 < x \leq 0.037$ showed the paramagnetic Curie-Weiss behavior. This confirms the belief that the Mn^{2+} ions are likely to be homogeneously diluted in the semiconductor matrix. We did not observe in any of the $Cd_{1-x}Mn_xGeAs_2$ crystals the presence of additional contributions to the magnetic susceptibility other than the diamagnetic component. It is an important result allowing verification of thesis T1 and T2 but requires further studies.

All the experimental dependences of the inverse of the magnetic susceptibility versus temperature are linear. This means that no magnetic clusters are present in these crystals. I calculated for the first time for this chemical compound the value of the diamagnetic susceptibility of the $CdGeAs_2$ crystal lattice equal to $\chi_{dia} = -2.5 \times 10^{-7}$ emu/g. I conducted an analysis of the data mentioned above based on the Curie-Weiss law, which allowed me to determine the Curie-Weiss temperature, θ , and the Curie constant, C , for each of the studied crystals (see Table 1). The θ values are negative, rising along with x . This is an important result, which indicates that in the $Cd_{1-x}Mn_xGeAs_2$ crystals short range magnetic interactions are present, and the value of their exchange parameter may be a decreasing function of x . Similar $\theta \approx -3$ K values were observed in the literature using the EPR technique [31]. The second parameter, which is obtained from the analysis of the magnetic susceptibility data is

Table 1. Parameters obtained from the analysis of the magnetometric data obtained for the $\text{Cd}_{1-x}\text{Mn}_x\text{GeAs}_2$ crystals with different chemical compositions, x .

x	C (10^{-5}) [emu·K/g]	x_θ	θ [K]	J/k_B [K]	M_S [emu/g]	x_m	T_0 [K]
0.004	7.0±0.2	0.005±0.001	-0.08±0.02	-0.46	0.27±0.02	0.005±0.001	0.061±0.012
0.013	9.4±0.2	0.007±0.001	-0.41±0.03	-1.69	0.43±0.03	0.008±0.002	0.63±0.12
0.024	28±2	0.021±0.002	-2.4±0.2	-3.26	2.0±0.2	0.037±0.005	2.8±0.5
0.037	66±3	0.050±0.005	-3.1±0.3	-1.77	2.7±0.3	0.050±0.008	2.0±0.4

the Curie constant, C . Assuming that in a semiconductor we have Mn^{2+} ions with the total magnetic momentum equal to $J = S = 5/2$, we can estimate the effective magnetic ion content x_θ in the studied crystals (see Table 1). The comparison of the x and x_θ values permits the unambiguous conclusion that the majority of the Mn ions in the $\text{Cd}_{1-x}\text{Mn}_x\text{GeAs}_2$ crystals are in the high-spin state. This confirms my earlier observations of the fact that Mn ions in the $\text{Cd}_{1-x}\text{Mn}_x\text{GeAs}_2$ crystals are allocated in substitutional Cd positions and *forms a homogeneous solid solution*. I also noticed that with the increase of x the divergence between x and x_θ increases which may indicate the emergence of the short-range magnetic interactions in the system under study. These magnetic interactions, however, are not related to the presence of either macroscopic or nanoscopic MnAs clusters in the crystals. Besides the crystal with $x = 0.037$ for all the other samples $x < x_\theta$ which means probably that I observed the antiferromagnetic short-range magnetic interactions leading to a strong magnetic coupling of the Mn ions and the lack of their contribution to the magnetic susceptibility. This is an important result because of the need to verify the thesis T2.

The experimental $\chi(T)$ dependences for $T \gg \theta$ were used to estimate the strength of the nearest neighbors magnetic interactions J . The calculated values of J/k_B (k_B - Boltzmann constant) are summarized in Table 1. The obtained J/k_B parameters are negative and have small values not exceeding 3 K. The values of J/k_B I obtained are characteristic of antiferromagnetic superexchange interaction via the anion [32,33]. The literature review indicated that the J/k_B values obtained by me are lower than the values reported for the II-VI compounds with Mn [34]. It turns out, however, that the type of anion has a decisive impact on the value of the superexchange constant, J [34]. This means that the J/k_B value for the $\text{Cd}_{1-x}\text{Mn}_x\text{GeAs}_2$ crystals should be compared with counterparts among the ternary alloys belonging to the III-V. The materials with similar properties may be $\text{In}_{1-x}\text{Mn}_x\text{As}$, where the carrier concentration is of the order of 10^{19} cm^{-3} and the observed $J/k_B = -1.6 \text{ K}$ [35] and $\text{Ga}_{1-x}\text{Mn}_x\text{N}$, where the carrier concentration is less than 10^{18} cm^{-3} and the observed $J/k_B = -1.9 \text{ K}$ [36]. These selected examples of materials have the exchange constant values J similar to the values obtained for the studied $\text{Cd}_{1-x}\text{Mn}_x\text{GeAs}_2$ crystals. An important finding is the fact that the superexchange interaction in chalcopyrite structure semimagnetic semiconductors strongly depends on the type of chemical bonding.

The last part of the verification of thesis T1 and T2 are the magnetization $M(B)$ studies for the $\text{Cd}_{1-x}\text{Mn}_x\text{GeAs}_2$ crystals (see Fig. 2b). The $M(B)$ dependencies obtained for the samples with $x \leq 0.013$ exhibit saturation for $B \geq 5 \text{ T}$ while for $x > 0.013$ the saturation magnetization was not observed. Therefore, I conducted the analysis based on fitting the experimental results with the modified Brillouin function comprising phenomenological temperature, T_0 . As a result of the data analysis I obtained two fitting parameters for each of the crystals, i.e., the saturation magnetization, M_S , and the so-called Gaj temperature, T_0 (see Table 1). The resulting T_0 are positive and their values correspond to the negative θ temperatures within the

limits of the experimental errors in the determination of both quantities. The changes in the T_0 values with changes in x are similar to those in θ with an exception of the crystal with $x = 0.037$. This is probably due to an increasing role of the short-range magnetic interactions for simple Mn clusters. In turn the M_S values increase with x . I used the M_S values to estimate the effective Mn content x_m (see Table 1), which I compared with x and x_θ . It turns out that for low $x \leq 0.013$ we have $x \approx x_m$, for $x = 0.024$ we observe the inequality $x \approx x_\theta \leq x_m$, and for $x = 0.037$ we observe inequality $x < x_\theta \approx x_m$. It is important that the conclusions based on the results of magnetic susceptibility measurements are consistent with those made during the studies based on the magnetization of the $\text{Cd}_{1-x}\text{Mn}_x\text{GeAs}_2$ crystals. In this way I have shown in the manuscript [H2] that there exist II-IV-V₂ group materials, which can be compared and classified as diluted magnetic semiconductors, and their magnetic properties raise hopes for further progress towards obtaining homogeneous ferromagnetic materials based on II-IV-V₂ group semiconductors, in which the RKKY interactions dominate.

c.2.1.c. Homogeneous Mn distribution in the $\text{Cd}_{1-x-y}\text{Mn}_x\text{Zn}_y\text{SnAs}_2$ crystals

The verification of thesis T1 and T2 I continued for several chemical compounds, i.e. $\text{Zn}_{1-x-y}\text{Cd}_x\text{Mn}_y\text{GeAs}_2$, $\text{Zn}_{1-x}\text{Mn}_x\text{SnAs}_2$, and $\text{Zn}_{1-x}\text{Mn}_x\text{SnSb}_2$. Unfortunately, these materials or their current growth technology do not allow to obtain uniform crystals. Therefore, I decided to look for a possibility to change the growth technology of these materials. This allowed the studies of a number of $\text{Cd}_{1-x-y}\text{Mn}_x\text{Zn}_y\text{SnAs}_2$ crystals with variable Mn and Zn contents, x from 0.013 to 0.170 and y from 0.002 to 0.051, respectively. We have also conducted the HRXRD research. The results showed a very good quality of the crystalline $\text{Cd}_{1-x-y}\text{Mn}_x\text{Zn}_y\text{SnAs}_2$. Only in the crystals with $x \geq 0.074$ we observed diffraction peaks of low intensity characteristic of MnAs precipitations. This means that for $x < 0.074$ it is possible to grow samples with uniform dissolution of manganese ions in the crystal lattice of the semiconductor. Thus, within the studies devoted to verification of theses T1 and T2 I focused on the studies of the $\text{Cd}_{1-x-y}\text{Mn}_x\text{Zn}_y\text{SnAs}_2$ crystals with $x \leq 0.025$. The results of the studies of homogeneous $\text{Cd}_{1-x-y}\text{Mn}_x\text{Zn}_y\text{SnAs}_2$ crystals were published by me in the manuscript [H8].

The results of studies of magnetic susceptibility published in the manuscript [H8] showed that the samples with $x \leq 0.025$ are characterized by the paramagnetic Curie-Weiss type behavior. Therefore, by analogy with $\text{Cd}_{1-x}\text{Mn}_x\text{GeAs}_2$ crystals I state that the Mn^{2+} ions are likely to be uniformly diluted in the semiconductor lattice and are in a high-spin state. The linear dependence of the inverse of the magnetic susceptibility versus the temperature allows me to state that in the $\text{Cd}_{1-x-y}\text{Mn}_x\text{Zn}_y\text{SnAs}_2$ samples with $x \leq 0.025$ there are no additional contributions to the magnetic susceptibility of the crystals aside of the diamagnetic component, and therefore there is no aggregation of the Mn ions in the macroscopic clusters.

In view of the verification of thesis T2 I have conducted the analysis of the experimental data on the basis of the Curie-Weiss law. For the non-magnetic $\text{Cd}_{0.99}\text{Zn}_{0.01}\text{SnAs}_2$ sample I calculated the value of the diamagnetic susceptibility $\chi_{\text{dia}} = -2.5 \times 10^{-7}$ emu/g. This enabled me to perform the analysis of experimental data, which allowed me to find the Curie-Weiss temperature, θ , and the Curie constant, C , for each of the crystals (see Table 2). The data presented in Table 2 show that the values of the temperature θ are small, decreasing with x . This means that in the $\text{Cd}_{1-x-y}\text{Mn}_x\text{Zn}_y\text{SnAs}_2$ crystals the short range magnetic interactions have the smallest strength of all the paramagnetic II-IV-V₂ group crystals I studied. Decreasing $\theta(x)$ dependence is a result of the increasing probability of forming Mn pairs or more complex clusters. The Curie constant values, C , I used to estimate the effective magnetic ion content x_θ (see Table 2). Comparison of x with x_θ permits the unambiguous conclusion that a large part of Mn ions in the studied $\text{Cd}_{1-x-y}\text{Mn}_x\text{Zn}_y\text{SnAs}_2$ samples is not in the 2+ charge state, i.e. in a

Table 2. Parameters obtained from the analysis of the magnetometric data for the $\text{Cd}_{1-x-y}\text{Zn}_x\text{Mn}_y\text{SnAs}_2$ crystals with different chemical compositions, x and y .

x	y	C (10^{-4}) [emu·K/g]	x_θ	θ [K]	M_S [emu/g]	x_m
0.013	0.051	0.27±0.02	0.002±0.0002	0.03±0.01	0.18±0.02	0.0024±0.0002
0.019	0.036	0.49±0.04	0.004±0.0004	0.05±0.01	0.41±0.04	0.0056±0.0005
0.025	0.028	1.7±0.1	0.015±0.001	-0.9±0.1	1.2±0.1	0.016±0.002

high-spin state. It is therefore likely that *the Mn ions in these crystals are not located in substitutional Cd positions* forming homogeneous solid solution. Low x_θ values in these crystals are not related to the macroscopic or nanoscopic MnAs clusters. It is more likely that I observe short-range magnetic interactions leading to a strong antiferromagnetic coupling of Mn ions and their lack of contribution to the magnetic susceptibility.

The last part of verification of thesis T1 and T2 for the $\text{Cd}_{1-x-y}\text{Mn}_x\text{Zn}_y\text{SnAs}_2$ crystals was to make measurements of magnetization $M(B)$, presented in detail in the manuscript [H8]. The most important observations are: (i) the shape of the curves is typical of paramagnetic material in the entire temperature range, (ii) no signatures of the presence of the magnetic hysteresis which could indicate the presence of a magnetic order was observed, and (iii) I observed the saturation of the $M(B)$ curves at $T = 4.5$ K at $B \geq 5$ T. In view of the above arguments it was justified to perform the analysis of the results based on a fitting of the experimental data to the modified Brillouin function with the diamagnetic component connected to the semiconductor lattice. As a result of the data analysis I obtained for each of the crystals the value of the saturation magnetization, M_S , summarized in Table 2. The M_S values gathered in Table 2 are an increasing function of x . The obtained M_S values I used for the estimation of the effective content of manganese ions, x_m , in the crystals (summarized in Table 2). I compared the obtained x_m values with x and x_θ . It turns out that for all the studied crystals the inequality $x > x_\theta \approx x_m$ is fulfilled. It is very important that thanks to this conclusion, the interpretation based on the magnetic susceptibility results is consistent with those made during the magnetization studies. Thus, in manuscript [H7] I have shown a third example of the II-IV-V₂ group materials which can be classified as semimagnetic semiconductors.

c.2.1.d. Defects of the $\text{Zn}_{1-x}\text{Mn}_x\text{GeAs}_2$ crystal lattice

Knowledge of the magnetic properties and semimagnetic semiconductors should be correlated with their electrical properties. I conducted the magnetotransport studies of the $\text{Zn}_{1-x}\text{Mn}_x\text{GeAs}_2$ crystals with different chemical compositions. The results of this research are published in the papers [H1] and [H3]. The aim of the study of transport properties of $\text{Zn}_{1-x}\text{Mn}_x\text{GeAs}_2$ crystals was to find a correlation between the structural, magnetic, and electric properties of $\text{Zn}_{1-x}\text{Mn}_x\text{GeAs}_2$ crystals and therefore a positive verification of thesis T3.

The temperature dependence of the resistivity for $\text{Zn}_{1-x}\text{Mn}_x\text{GeAs}_2$ crystals showed that at $T > 50$ K all the studied samples are characterized by an increasing, almost linear $\rho_{xx}(T)$ dependence. The increase in the resistivity observed at $T > 50$ K is typical of degenerate semiconductors. In turn, at $T \approx 50$ K I observed the presence of minimum in the $\rho_{xx}(T)$ dependence and at $T < 50$ K the $\rho_{xx}(T)$ dependence is a decreasing function of the temperature. The presence of the minimum in the $\rho_{xx}(T)$ dependence I attribute to the influence of the scattering by magnetic impurities.

I conducted research of the Hall effect as a function of the temperature and the magnetic field. The results have shown that the Hall resistance ρ_{xy} is a linear function of the magnetic field throughout the investigated range of temperatures. All the studied $\text{Zn}_{1-x}\text{Mn}_x\text{GeAs}_2$ crystals are characterized by strong p-type conductivity with carrier concentration in the range from 10^{19} cm^{-3} up to 10^{20} cm^{-3} . Strong p-type conductivity in the crystals is due to the presence of negatively charged defects, the structure of which has to be studied. It is possible and is also likely that, in the material, there are other, more complex negatively charged defects, which contribute to a strong p-type conductivity. A very important result is the observation of a lower carrier concentration in the case of the crystal with $x = 0.003$, which showed the chalcopyrite structure. The structural disorder of the samples with zincblende structure leads to an increase in the carrier concentration to a level of 10^{20} cm^{-3} in the sample with $x = 0.042$. This should be combined with the magnetic properties of crystals which show that with the increase of x most of the Mn ions do not substitute Zn positions in the crystal lattice and may form negatively charged defects in the crystal lattice.

Also noteworthy from the point of view of verification of thesis T3 are the observed temperature dependencies of the carrier concentration. The $n(T)$ dependencies observed for the majority of the investigated crystals are decreasing at $T < 50 \text{ K}$, reaching a minimum at $T \approx 50 \text{ K}$, and at $T > 50 \text{ K}$ show a slight increase with increasing temperature. Interpretation of the $n(T)$ dependence is possible in conjunction with the interpretation of the $\mu(T)$ dependences described in detailed for the studied $\text{Zn}_{1-x}\text{Mn}_x\text{GeAs}_2$ crystals in manuscripts [H1] and [H3]. The $\mu(T)$ dependence exhibits a maximum at $T \approx 50 \text{ K}$. Accordingly, the increasing $\mu(T)$ dependence at $T < 50 \text{ K}$ is a confirmation of the fact that at low temperatures there is a strong scattering at the negatively ionized defect centers. The effect of this scattering on the $\mu(T)$ relationship is not dominant. In turn, at $T > 50 \text{ K}$ the carrier mobility decreases as a function of temperature, which is a typical behavior if the dominant scattering mechanism of conduction carriers is phonon scattering.

I conducted an analysis of the observed temperature dependencies of the carrier mobility based on the phenomenological exponential relations of the mobility components of the total $\mu(T)$ dependence described by the Matthiessen rule. The low temperature $\mu(T)$ dependences were fitted with the exponential temperature functions, with exponent values ranging from 0.11 to 0.55. Literature data for the p-type GaAs show that the $\mu(T)$ relationship can be fitted with $\propto T^{2.2}$ when one type of defect i.e. the ionized carrier scattering centers are affecting the carrier conductivity of the samples. I obtained much lower temperature exponent values. That clearly indicates the presence in the studied crystals of more than one type of defects responsible for the increasing $\mu(T)$ dependence at $T < 50 \text{ K}$. On the other hand, the $\mu(T)$ dependence at $T > 50 \text{ K}$ can be described by an exponential temperature dependence with the exponent values ranging from -0.5 to -0.8. In the case of acoustic phonon scattering mechanism the $\propto T^{3/2}$ dependence is expected, while in the case of the optical phonon scattering the $\propto T^{1/2}$ dependence should be observed. The obtained temperature exponent values for the $\text{Zn}_{1-x}\text{Mn}_x\text{GeAs}_2$ crystals are closer to the values characteristic of the optical phonon scattering, which indicates that this type of phonon scattering mechanism dominated the processes of carrier scattering in the samples I investigated.

I continued the studies of carrier localization in the $\text{Zn}_{1-x}\text{Mn}_x\text{GeAs}_2$ crystals through a series of magnetotransport measurements in the range of strong magnetic fields $B \leq 13 \text{ T}$. It allowed me to shed light on the possible correlation between the structural and the magnetic

properties and the electrical properties of the studied crystals. All the $\rho_{xy}(B)$ dependencies are linear over the entire measured temperature and magnetic field ranges. On the other hand, the measurements of the magnetoresistance, i.e. $\rho_{xx}(B)$ curves showed significant differences in the results between individual crystals with different Mn contents, x . Selected magnetoresistance results collected and interpreted in detail in the manuscript [H1] are presented in Fig. 2.

In the case of the ZnGeAs_2 crystal not containing magnetic impurities I observed only a small positive

magnetoresistance which was square as a function of the magnetic field with amplitudes not exceeding 1%. This effect I interpreted as a classical magnetoresistance effect resulting from the movement of charge carriers around the cyclotron orbits in the presence of an external magnetic field. On the other hand, in the case of the $\text{Zn}_{1-x}\text{Mn}_x\text{GeAs}_2$ crystals at low temperatures $T < 30$ K I observed that both the value (of the order of magnitude greater) as well as the shape of the magnetoresistance curves observed in the case of currently investigated crystals are different than was the case for the paramagnetic $\text{Zn}_{1-x}\text{Mn}_x\text{GeAs}_2$ sample with $x = 0.053$, which I studied in 2009 [15]. It is therefore clear that the physical mechanism responsible for the observed magnetoresistance at $T < 30$ K is not related to the spin disorder scattering mechanism, as I previously interpreted for the crystal with $x = 0.053$ [15]. In turn, at $T > 30$ K for all the studied $\text{Zn}_{1-x}\text{Mn}_x\text{GeAs}_2$ crystals I observed only the classical magnetoresistance with small values, which was square as a function of the magnetic field, similarly as for the ZnGeAs_2 sample containing no Mn.

The shape of the magnetoresistance curves strongly depends on the chemical composition and temperature of the studied $\text{Zn}_{1-x}\text{Mn}_x\text{GeAs}_2$ samples. I observed the largest amplitude of the magnetoresistance in the case of the crystal with the chalcopyrite structure with $x = 0.003$. It is thus possible that the amount of the Mn ions in the alloy and the degree of structural disorder have strong influence on the amplitude of the magnetoresistance. In the case of the crystal with $x = 0.003$ at $T < 30$ K I observed only the negative contribution to the magnetoresistance. In turn, for the crystals with $x \geq 0.014$ at $T < 30$ K I observed two contributions to the magnetoresistance: (i) in the area of low magnetic fields with induction $B < 3$ T I observed a large positive contribution to the magnetoresistance, and (ii) in the area of strong magnetic fields $B \geq 3$ T I observed the presence of a dominant negative contribution to the magnetoresistance. The negative contribution to the magnetoresistance may have the same physical mechanism as that observed for the crystal with $x = 0.003$.

The most important and also the most difficult problem when trying to interpret the results of the magnetoresistance measurements in the $\text{Zn}_{1-x}\text{Mn}_x\text{GeAs}_2$ crystals was predicting the

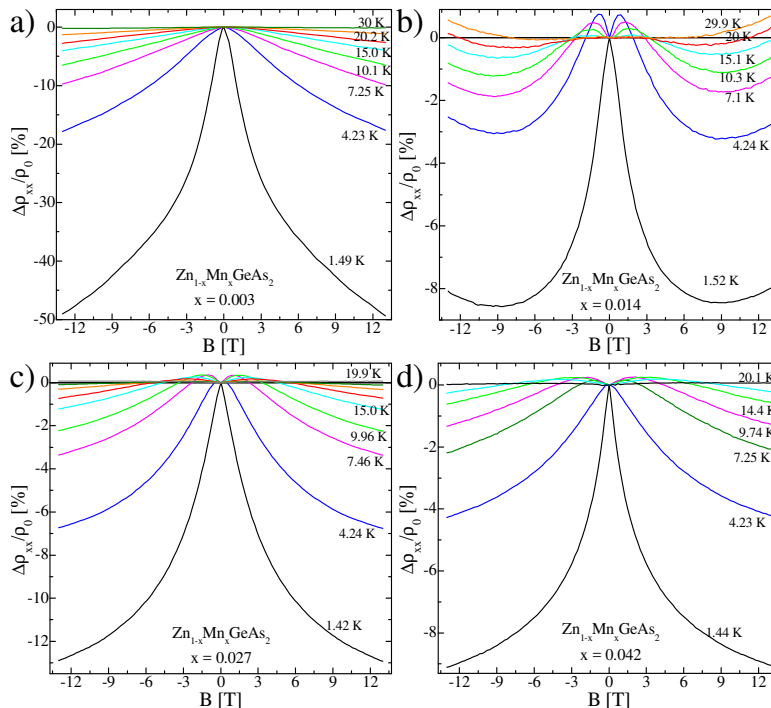


Fig. 2. Selected magnetoresistance curves obtained for the selected $\text{Zn}_{1-x}\text{Mn}_x\text{GeAs}_2$ crystals with different chemical composition.

most likely physical mechanism that is responsible for the effects observed in the manuscript [H1] at $T < 30$ K. I conducted the scaling to a power law analysis of the experimental data according to the $\Delta\rho_{xx}/\rho_0 \propto B^m$ relation. The analysis to the power law showed that the value of the exponent m has changed in the studied samples from 0.6 to 0.8. The Moriya-Kawabata theory of spin-fluctuations [37,38] provides $m = 1$ or 2 in the case of scattering on the spin disorder for materials which are weak ferromagnetic or paramagnetic materials, respectively. Therefore, the scattering on the spin-fluctuations is not the dominant mechanism responsible for the observed in these samples magnetoresistance effects at $T < 30$ K. In addition to the above analysis I made an analysis of the convergence between the $M(B)$ dependencies and the magnetoresistance curves. This analysis excluded the linear or quadratic dependence between the magnetoresistance and the magnetization of the material. This is another proof that the magnetic order in the studied samples is not responsible for the observed magnetoresistance effects.

Another important phenomenon, which may be responsible for the magnetoresistance effects is the weak localization phenomenon [39]. A number of studies shows that in the presence of spin-orbit interaction phenomenon the weak localization can show a complex behavior and dependent on a number of material parameters [40]. For this reason, unfortunately, I could not make fits of the experimental magnetoresistance curves to the theory of weak location. The $k_F l$ product for all the $Zn_{1-x}Mn_xGeAs_2$ crystals I studied is close to 1, which means that the localization is significant in this system. In addition, weak localization theories predict in low diffusivity systems (less than $0.5 \text{ cm}^2/\text{s}$) the existence of both positive and negative contributions to the magnetoresistance with the shape similar to that observed experimentally for the investigated crystals. In addition, I observed the reduction of the size of the magnetoresistance with increasing x and especially correlations with x_0 and x_m as a consequence of the destruction of the weak location phenomenon for the increasing number of magnetically active Mn ions. Accordingly, I finally assign the observed magnetoresistance effects in the $Zn_{1-x}Mn_xGeAs_2$ crystals at $T < 30$ K to *the weak localization phenomenon*. Localization is therefore strong in the II-IV-V₂ materials as I showed in the manuscript [H1] and leads to positive verification of the thesis T3.

The strong p-type conductivity observed by me in the $Zn_{1-x}Mn_xGeAs_2$ crystals is associated with the presence of significant concentrations of different types of negatively charged defects in the semiconductor crystal lattice. Identification of the types of defects observed in the $Zn_{1-x}Mn_xGeAs_2$ crystals is a very important issue; important for me also because of the need to verify the thesis T3. To overcome this problem I used a positron annihilation spectroscopy technique, which is a specialized technique to identify the dominant types of point defects in solids. It is therefore a very important technique for identifying defects in the structure of the p-type semiconductor in which the negatively charged defects usually dominate. Positron annihilation studies of the $Zn_{1-x}Mn_xGeAs_2$ crystals, the data analysis, and the theoretical calculations I made during the postdoctoral fellowship at the University of Aalto in Espoo in Finland.

The positron studies of the $Zn_{1-x}Mn_xGeAs_2$ crystals consisted of the measurements of the temperature dependence of the positron lifetime spectra and the Doppler broadening of the electron-positron annihilation line. Selected results of the positron studies, which were published by me in the manuscript [H3] are presented in Fig. 3. Temperature changes in the positron lifetime spectra are best illustrated by the so-called average lifetime, τ_{av} , which is mathematically the center of mass of the spectrum. It is essential that the observed $\tau_{av} > 255 \pm 5$ ps, e.g. are higher than the calculated positron lifetime in the defect-free $ZnGeAs_2$

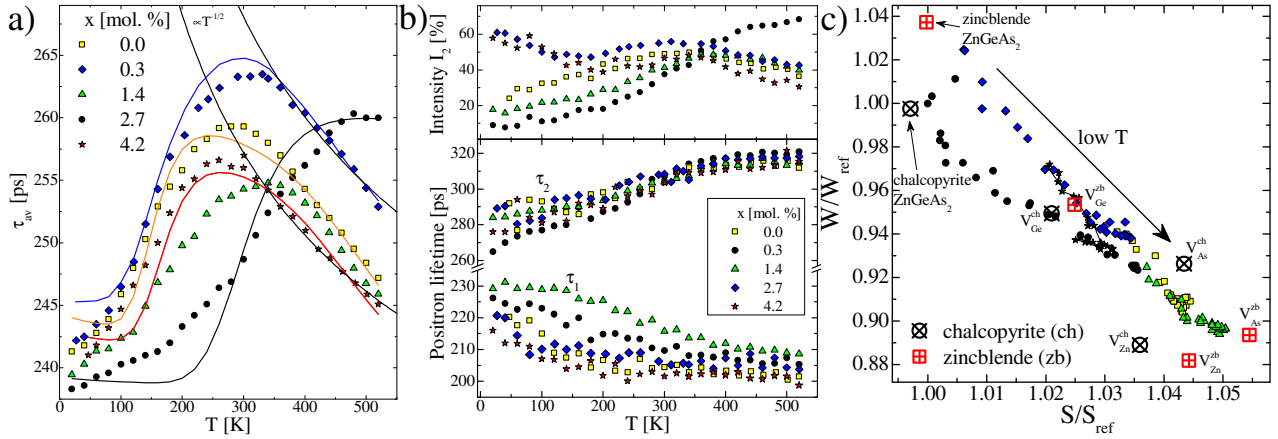


Fig. 3. The results of the positron studies of the $\text{Zn}_{1-x}\text{Mn}_x\text{GeAs}_2$ crystals with different chemical composition comprising: (a) the temperature dependence of the average positron lifetime, (b) temperature dependences of the components of the positron lifetime spectra, and (c) the Doppler parameters obtained at different temperatures.

crystal [41]. This means that the positrons in the $\text{Zn}_{1-x}\text{Mn}_x\text{GeAs}_2$ crystals I studied in manuscript [H3] are trapped by vacancy type or other point defects. In the case of the $\text{Zn}_{1-x}\text{Mn}_x\text{GeAs}_2$ crystal with $x = 0.003$ I observed the increasing $\tau_{av}(T)$ dependence for $T < 450$ K and the saturation of $\tau_{av}(T)$ at higher temperatures. Such a shape of the $\tau_{av}(T)$ dependence indicates the trapping of positrons in the vacancies, which are electrically neutral. This result is consistent with the previously investigated $\text{Zn}_{1-x}\text{Mn}_x\text{GeAs}_2$ crystals with $x \geq 0.053$ [41]. On the other hand, in the case of the crystals with the zincblende structure I observed $\tau_{av}(T = 10 \text{ K}) \rightarrow 255$ ps and the increasing $\tau_{av}(T)$ dependence at $T < 300$ K which is due to the positron trapping at defects which are shallow positron traps that do not form an open volume in the crystal. On the other hand the decreasing $\tau_{av}(T)$ at $T > 300$ K dependence having the $\propto T^{-1/2}$ character points to the trapping of positrons in the negatively charged vacancies. Hence I discovered two types of defects having a negative charge, which are responsible for the strong p-type conductivity in these crystals. Comparison of $\tau_{av}(T = 300 \text{ K})$ indicated a generally increasing $\tau_{av}(x)$ dependence. With increasing the amount of Mn in the sample the concentration of electrically active defects increases.

In the next step I made a more complex analysis of the positron lifetime spectra aiming at the identification of several components of the spectra with different values, τ_i , and different intensities, I_i . This analysis has enabled me to distinguish two lifetimes, τ_1 and τ_2 , and the intensity, I_2 . The results of the data analysis I made are presented in Fig. 5b. Separation of the positron lifetime spectra into two very distinct components reaffirmed previous conclusions that I raised based on the analysis of the $\tau_{av}(T)$ dependence.

I also performed the analysis of the $\tau_{av}(T)$ based on the positron trapping model on defects [42]. The application of the above model enabled me to reproduce the experimental $\tau_{av}(T)$ dependence and to estimate the concentration and energy binding of defects that I have discovered. The estimated defects binding energies have values close to 90 meV and 170 meV for defects in the zincblende and the chalcopyrite crystal structures, respectively. This means that in the chalcopyrite crystal structure in addition to neutral vacancies negatively charged ion defects are also present. The estimated concentrations of defects amounted to $3 \times 10^{15} \text{ cm}^{-3}$ for the negatively charged cationic vacancies in the zincblende structure samples and $2.5 \times 10^{17} \text{ cm}^{-3}$ and $7.5 \times 10^{17} \text{ cm}^{-3}$ for ion defects in the samples with zincblende and chalcopyrite structures, respectively. These results, particularly concentrations of defects are too small to allow full explanation of the carrier concentration with the order of $10^{19} - 10^{20}$

cm^{-3} . Thus it is possible that in this material there are also present other types of defects not detected by the positron lifetime spectroscopy.

I made further studies of the structure of defects present in the $\text{Zn}_{1-x}\text{Mn}_x\text{GeAs}_2$ crystals studied in the manuscript [H3] with the use of the Doppler broadening spectroscopy of the electron-positron annihilation line. The results of these measurements are typically presented in the form of so-called $W(S)$ plane, where W and S are the parameters determined based on the number of counts in the spectrum in the region near and far from the 511 keV annihilation energy. Detailed description of the analysis of the experimental results is presented in detail in the manuscript [H3]. For the purpose of this text I present only the final experimental points obtained on the $W(S)$ plane in Fig. 5c. In addition, in collaboration with Dr. C. Rauch from the Aalto University I have carried out a series of ab-initio density of electronic states calculations which allowed the use of density functional theory to model the annihilation of positrons. In particular the calculation packages [43] made available to me by Prof. F. Tuomisto allowed me to calculate the theoretical values of the S and W parameters for perfect ZnGeAs_2 crystals with the chalcopyrite and zincblende structures, as well as the modeling of the above parameters for a number of different cation or anion defects (open symbols in Fig. 5c). Experimental points with increasing temperature pass the points calculated for the V_{Ge} vacancies and head in the direction of the other two types of defects. This means that I can make the *final identification of three types of defects* in the $\text{Zn}_{1-x}\text{Mn}_x\text{GeAs}_2$ crystals: (i) the negatively charged ion traps that do not form an open volume in the crystal, (ii) the neutral defects in the form of As vacancies, and (iii) the negatively charged Zn vacancies. The temperature changes of the positron parameters that I observed are the result of the fact that different types of defects have different temperature dependencies of the trapping coefficients and different binding energies. I was able, therefore, to identify a number of defect states in the $\text{Zn}_{1-x}\text{Mn}_x\text{GeAs}_2$ crystals and indicate the defects, which are at least partly responsible for the observed strong p-type conductivity in these samples. This contributed significantly to the positive verification of the thesis T3.

c.2.1.e. Conductivity in the $\text{Cd}_{1-x}\text{Mn}_x\text{GeAs}_2$ crystals

High-quality $\text{Cd}_{1-x}\text{Mn}_x\text{GeAs}_2$ crystals are a very important in view of the research of thesis T3 due to the fact that the structural quality of the semiconductor generally has a significant influence on its electrical properties. Therefore I conducted a series of transport and magnetotransport studies of the $\text{Cd}_{1-x}\text{Mn}_x\text{GeAs}_2$ crystals. I did not observed a presence of nonlinearities in the $\rho_{xy}(B)$ dependence which is a signature that in the $\text{Cd}_{1-x}\text{Mn}_x\text{GeAs}_2$ crystals there is either no or negligible two-carrier transport and anomalous Hall effect. Based on the magnetotransport results I have calculated the temperature dependencies of the carrier concentration and the mobility, presented in detail in manuscript [H2] and Figs. 4a and 4b. High structural quality of the $\text{Cd}_{1-x}\text{Mn}_x\text{GeAs}_2$ crystals involves *a considerable improvement in the electrical properties* over previously studied samples, i.e. all the crystals behave as semiconductors. The obtained Hall effect measurements results showed that all the $\text{Cd}_{1-x}\text{Mn}_x\text{GeAs}_2$ crystals I studied and published in the manuscript [H2] are p-type semiconductors with low concentrations of conducting holes, $n = (eR_H)^{-1} < 10^{16} \text{ cm}^{-3}$. Moreover, the shape of the temperature dependence of the carrier concentration $n = (eR_H)^{-1}$ (e - elementary charge, R_H – the Hall constant) and the temperature dependence (see Fig. 4a) characteristic of thermally activated carrier transport. This result is in opposition to the transport in typical degenerated semiconductor materials, which I observed for the $\text{Zn}_{1-x}\text{Mn}_x\text{GeAs}_2$ crystals studied in manuscripts [H1] and [H3]. The data collected in Fig. 4a allowed me to estimate the value of the activation energy of the conductivity, E_a , for each of

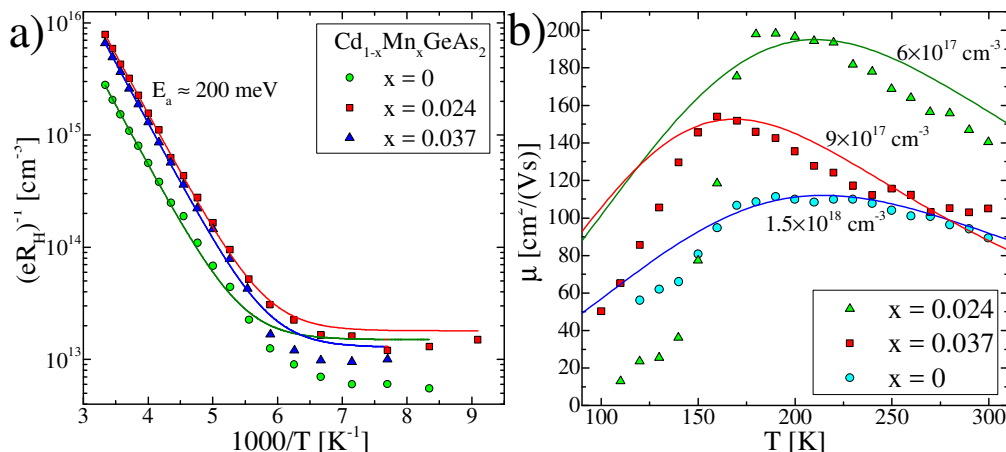


Fig. 4. Results of the magnetotransport studies of the $\text{Cd}_{1-x}\text{Mn}_x\text{GeAs}_2$ crystals with different chemical compositions comprising: (a) the carrier concentration $n = (e \cdot R_H)^{-1}$ as a function of the inverse of the temperature and (b) the temperature dependence of the carrier mobility.

the crystals. The estimated E_a values for all the studied samples are similar, of about 200 meV. I obtained similar E_a values for both a pure CdGeAs_2 crystal and crystals containing Mn which means, in line with previous conclusions, that the Mn ions which are in positions of substitutional impurities are isoelectronic dopants and do not take an active part in the creation of conducting carriers in this material. Thus, it is highly likely that they substitute Cd positions in the CdGeAs_2 lattice. It is therefore evident that the other types of defects, e.g. anti-site defects or Frenkel defects, whose creation energy is lower than for the vacancy type cation defects [44], are responsible for the observed acceptor states.

As a result of the magnetotransport studies I obtained the temperature dependence of the carrier mobility shown in Fig. 4b. The collected data indicated that, at $T > 180$ K the scattering of the charge carriers on phonons is dominant in the material. The observed at $T \approx 180$ K maximum μ values does not depend on the amount of Mn in the crystals. That is in accordance with the previously raised conclusion that Mn ions are not involved in the carrier scattering. For $T < 180$ K I observed the decreasing $\mu(T)$ dependence, which can be fitted with the $\propto T^{-1/2}$ dependence. This allows the interpretation that the concentration of the scattering centers is independent of temperature due to the effect of compensation. I carried out the analysis of the $\mu(T)$ dependence done by means of an empirical model assuming the presence of two-bands under low magnetic field approximation [43]. Based on a simple model I recreated the experimental $\mu(T)$ dependence for all the studied $\text{Cd}_{1-x}\text{Mn}_x\text{GeAs}_2$ crystals. The used model allowed me to estimate the concentration of the scattering centers responsible for the observed $\mu(T)$ dependence at $T < 180$ K. The obtained concentration of scattering centers is in the range from $6 \times 10^{17} \text{ cm}^{-3}$ up to $1.5 \times 10^{18} \text{ cm}^{-3}$. The estimated concentrations of ionic defects are not increasing with x . This confirmed earlier findings that an increase in the amount of Mn in the crystals does not lead to the creation of defects. The conducted analysis allowed to confirm the existence of the free charge carriers localization phenomena at the defect centers which allowed for a positive verification of the thesis T3.

I performed a detailed study of the magnetoresistance in the $\text{Cd}_{1-x}\text{Mn}_x\text{GeAs}_2$ crystals in order to verify the thesis T3. However, for $T < 100$ K the studied crystals did not conduct electrical current, and at $T > 100$ K I observed only the presence of classical magnetoresistance, square as a function of the magnetic field, associated with the carrier movement along the cyclotron orbits.

c.2.1.f. Resistance oscillations in the $\text{Cd}_{1-x-y}\text{Mn}_x\text{Zn}_y\text{SnAs}_2$ crystals

I made a number of studies of magnetotransport properties of high-quality paramagnetic $\text{Cd}_{1-x-y}\text{Mn}_x\text{Zn}_y\text{SnAs}_2$ crystals with $x < 0.025$ in order to verify thesis T3. The results of these studies were published by me in manuscript [H7] and summarized in Fig. 5. The results of the studies show the presence of the plateaus in the magnetic field dependence of the Hall effect, $\rho_{xy}(B)$, for all the studied samples at magnetic fields higher than 3 T and temperatures lower than 50 K. This is a proof that the data obtained on the basis of the Hall effect studies at low fields can be analyzed on the basis of patterns resulting from the classical Drude theory and the data interpretation and analysis are justified.

I conducted a series of the Hall effect measurements for all the $\text{Cd}_{1-x-y}\text{Mn}_x\text{Zn}_y\text{SnAs}_2$ crystals. The results and their analysis indicate that all of the studied $\text{Cd}_{1-x-y}\text{Mn}_x\text{Zn}_y\text{SnAs}_2$ crystals are n-type semiconductors with electron concentrations of about $1\text{-}2 \times 10^{18} \text{ cm}^{-3}$. The temperature dependences of the carrier concentration show little change with T which is indicative of the fact that our samples are degenerate semiconductors and the thermal activation of conducting carriers does not play a major role in the electron transport in this material. The carrier concentration varies with the change of the Mn content in the samples. These changes, however, are small and are not monotonic with x .

The mobility of electrons, μ , shows no clear and well-defined trend as a function of the Mn content, x . I observe, however, a general decrease of μ with x . I can therefore speculate that this decrease is associated with the presence of an increasing number of defects in the samples containing high Mn content. The highest value of the carrier mobility I observed equals to $\mu = 7100 \text{ cm}^2/(\text{V}\cdot\text{s})$ for the sample with $x = 0.025$ and $y = 0.028$. The carrier mobility values, observed in the samples studied in the manuscript [H8], to my knowledge, are the highest for the group of II-IV- V_2 semiconductors. In this way I have reached a significant progress in improving the electrical properties of group II-IV- V_2 materials. The $\mu(T)$ dependences for all the $\text{Cd}_{1-x-y}\text{Mn}_x\text{Zn}_y\text{SnAs}_2$ crystals are almost constant in the temperature range from 4.5 K to 30 K and decreasing for temperatures from 30 K to 380 K. Decreasing $\mu(T)$ dependencies are characteristic of the phonon carrier scattering. I made an analysis of the $\mu(T)$ dependence using a phenomenological temperature dependent model and obtained the scaling of the experimental curves with the $T^{-1/2}$ dependence. This relation indicates that the scattering of carriers at the optical phonons is a major process responsible for the observed $\mu(T)$ dependence.

For all the $\text{Cd}_{1-x-y}\text{Mn}_x\text{Zn}_y\text{SnAs}_2$ crystals I observed the presence of the Shubnikov - de Haas oscillations (SDH) at $T < 50$ K (see Fig. 7). The oscillating nature of the $\rho_{xx}(B)$ curves is visible on the background of the parabolic dependence in all the studied in the manuscript [H8] paramagnetic samples with $x \leq 0.025$. The contribution to the magnetoresistance proportional to the square of the magnetic field must be subtracted in order to further analyze the data. Simultaneous observation of oscillations $\rho_{xx}(B)$ and plateaus in the

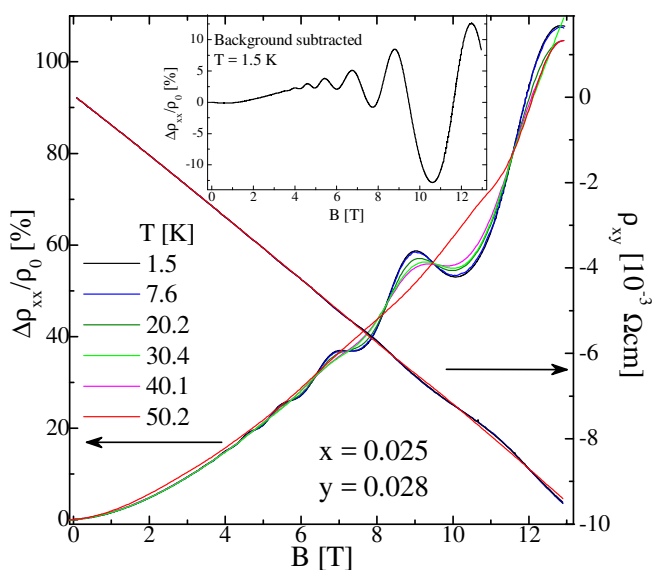


Fig. 5. Selected results of the magnetotransport studies for the $\text{Cd}_{0.947}\text{Mn}_{0.025}\text{Zn}_{0.028}\text{GeAs}_2$ crystal.

$\rho_{xy}(B)$ dependence in these samples confirmed *the presence of the quantization of energy levels in magnetic fields* with induction higher than $B = 3$ T.

I made an analysis of the frequency of SDH oscillations to calculate the carrier concentration in the material. The estimated carrier concentrations are close to those obtained based on the analysis of the results of the low field Hall effect measurement. This is an important result, indicating that a scattering coefficient for our samples is indeed close to 1, and the Hall-effect analysis has been performed correctly. The second step in the analysis of the SDH oscillations was based on the theoretical modeling of the temperature dependence of the amplitude of each oscillation. This analysis has enabled me to estimate a very important material parameter for the $\text{Cd}_{1-x-y}\text{Mn}_x\text{Zn}_y\text{SnAs}_2$ crystals, i.e. the electron effective mass m^* . As a result I obtained the effective mass values which are for all our samples similar and equal to about $0.11 \cdot m_0 - 0.12 \cdot m_0$, where m_0 is the mass of an electron in vacuum. The values of the effective mass for CdSnAs_2 are known in the literature with values from $0.04 \cdot m_0$ to $0.06 \cdot m_0$ [24].

c.2.1.g. Summary

The first part of the studies that I conducted was focused on the verification of the theses T1-T3 in the manuscripts H1, H2, H3, and H8. I showed on the example of the three materials the positive verification of these three research theses and made important conclusions:

- I have shown that for a number of semiconductors belonging to the II-IV- V_2 group with Mn the uniform dissolution of magnetic impurities is possible in the $\text{Zn}_{1-x}\text{Mn}_x\text{GeAs}_2$ ($0 < x \leq 0.042$), $\text{Cd}_{1-x}\text{Mn}_x\text{GeAs}_2$ ($0 < x \leq 0.037$) and $\text{Cd}_{1-x-y}\text{Mn}_x\text{Zn}_y\text{SnAs}_2$ ($0 < x \leq 0.025$) crystals. Changing the semiconductor host has a major influence on the efficiency of doping with Mn ions and the degree of disorder of the magnetic material.
- I have shown that depending on the type of the II-IV- V_2 semiconductor matrix the values of the effective chemical compositions calculated using magnetometric methods changes. Only for (i) $\text{Zn}_{1-x}\text{Mn}_x\text{GeAs}_2$ with $x = 0.003$, (ii) $\text{Cd}_{1-x}\text{Mn}_x\text{GeAs}_2$ with $x \leq 0.013$, and (iii) $\text{Cd}_{1-x-y}\text{Mn}_x\text{Zn}_y\text{GeAs}_2$ with $x \leq 0.013$, most of the Mn ions are in the Mn^{2+} charge state with $J = S = 5/2$. For higher Mn content in these crystals I have shown the presence of Mn ions short-range coupled into simple clusters that do not form foreign crystalline phases.
- I discovered the existence of long-range RKKY interactions in the $\text{Zn}_{1-x}\text{Mn}_x\text{GeAs}_2$ crystals with $x \leq 0.042$ and short-range superexchange interactions in the $\text{Cd}_{1-x}\text{Mn}_x\text{GeAs}_2$ crystals with $x \leq 0.037$. I calculated the value of the RKKY exchange parameter in the $\text{Zn}_{1-x}\text{Mn}_x\text{GeAs}_2$ crystal with $x = 0.003$ equal to $J_{\text{pd}} = (0.75 \pm 0.09)$ eV. In the case of the $\text{Cd}_{1-x}\text{Mn}_x\text{GeAs}_2$ crystals with $x \leq 0.037$ I calculated the value of the superexchange parameter of the magnetic interaction via an anion, J/k_B , varying with the amount of Mn in the crystals in the range from -0.46 to -3.26 K.
- I have shown that the type of the II-IV- V_2 semiconductor matrix has a significant influence on the type and character of the conductivity of homogeneous crystals. I examined the p-type conductivity with carrier concentrations of the order of 10^{19} cm^{-3} to 10^{20} cm^{-3} in $\text{Zn}_{1-x}\text{Mn}_x\text{GeAs}_2$ crystals with $x \leq 0.042$. In turn, the $\text{Cd}_{1-x}\text{Mn}_x\text{GeAs}_2$ crystals with $x \leq 0.037$ are characterized by the n-type conductivity with the carrier concentration values $n < 10^{16} \text{ cm}^{-3}$ and the $\text{Cd}_{1-x-y}\text{Mn}_x\text{Zn}_y\text{SnAs}_2$ crystals with $x \leq 0.025$ showed the n-type conductivity with carrier concentration values in the range of $1-2 \times 10^{18} \text{ cm}^{-3}$.
- The electrical conductivity of homogeneous crystals exhibits characteristics specific of degenerate semiconductors for the $\text{Zn}_{1-x}\text{Mn}_x\text{GeAs}_2$ and $\text{Cd}_{1-x-y}\text{Mn}_x\text{Zn}_y\text{SnAs}_2$ crystals. On the other hand, in the case of the $\text{Cd}_{1-x}\text{Mn}_x\text{GeAs}_2$ crystals I observed the thermally activated transport of charge carriers specific to semiconductors. It should be emphasized that the

above-mentioned electrical properties of the II-IV-V₂ crystals with Mn have a complex nature and several phenomena that have simultaneous impact on them are observed.

- I have demonstrated that, depending on the type of semiconductor, I observe different defects which are responsible for the creation and scattering of carriers in the material. I conducted a detailed study of the defect structure in the Zn_{1-x}Mn_xGeAs₂ crystals showing the existence of negatively charged ion traps, the negatively charged Zn vacancies, and the electrically neutral As vacancies.
- I have shown that the crystal lattice defects are responsible for the observed $\rho_{xx}(T)$, $n(T)$, and $\mu(T)$ dependencies. I observed significant fluctuations in the carrier mobility between the: (i) Zn_{1-x}Mn_xGeAs₂ with $\mu < 40 \text{ cm}^2/(\text{V}\cdot\text{s})$, (ii) Cd_{1-x}Mn_xGeAs₂ with $\mu < 200 \text{ cm}^2/(\text{V}\cdot\text{s})$, and (iii) Cd_{1-x-y}Mn_xZn_ySnAs₂ crystals with $\mu < 7100 \text{ cm}^2/(\text{V}\cdot\text{s})$.
- I examined the presence of the phenomena of the carrier localization on the defect states in the Zn_{1-x}Mn_xGeAs₂ crystals via the magnetoresistive effects at $T < 30 \text{ K}$. I have demonstrated, moreover, that the increasing concentration of magnetic impurities in the material leads to the suppression of the weak localization phenomenon in the Zn_{1-x}Mn_xGeAs₂ crystals.
- I discovered the magnetotransport oscillations in the form of the the Shubnikov-de Haas oscillations for the Cd_{1-x-y}Mn_xZn_ySnAs₂ crystals with high carrier mobility. Based on the Shubnikov-de Haas oscillations I estimated the carrier concentration and the value of the carrier effective mass of about $0.11 \cdot m_0$ - $0.12 \cdot m_0$.

c.2.2. Ferromagnetic composites

Parallel to the work focused on the studies of the properties of homogeneous semimagnetic semiconductors based on the chemical compounds belonging to the II-IV-V₂ group of the periodic table doped with magnetic Mn ions I undertook an extensive research of ferromagnetic composites based on the above group of semiconductor materials aiming verification of theses T4-T6. Exceeding the solubility limit of Mn in II-IV-V₂ material leads to creation of the semiconductor - ferromagnetic metal granular system. I started the studies of ferromagnetic composites based on the II-IV-V₂ materials as a graduate student in the IF PAN. As a result of these studies I published several publications which are a good introduction to an extensive study of this subject. Preliminary manuscripts I developed as an assistant professor in the IF PAN. I published the selected results of my work focused on the studies of ferromagnetic composites in the manuscripts [H4-H6] and [H8].

c.2.2.a. Control over the magnetoresistive effects in Zn_{1-x-y}Cd_xMn_yGeAs₂

Research of the composite ferromagnetic-semiconductor systems based on the materials belonging to the group II-IV-V₂ of the periodic table I began during PhD studies. I showed in my doctoral dissertation that the presence of MnAs clusters in the ZnGeAs₂ [14] or CdGeAs₂ [23] semiconductor matrix causes giant negative or positive linear magnetoresistance, respectively. The initial and very interesting results led to my interest in the ability to control the magnetotransport properties of ferromagnet-semiconductor composite II-IV-V₂ crystals intentionally grown with the MnAs clusters. I made a detailed study of a series of Zn_{1-x-y}Cd_xMn_yGeAs₂ crystals with variable Cd and Mn contents, x and y . The results of the studies of the structural, magnetic and electrical properties are published in the manuscript [H4]. My earlier work on the possibility of obtaining Zn_{1-x}Cd_xGeAs₂ solid solutions [47] indicated that this system can exist only in a limited content of Cd from 0 to 0.18 and from 0.82 to 1. This gave us the base to attempt the synthesis of the good quality Zn_{1-x}Cd_xGeAs₂ crystals containing MnAs precipitates. This enabled me to conduct specific studies of the

structural, magnetic and electrical properties of a range of samples with different concentrations of MnAs clusters in the semiconductor lattice.

I started the studies of $\text{Zn}_{1-x-y}\text{Cd}_x\text{Mn}_y\text{GeAs}_2$ samples necessary for the verification of the thesis T4 from the structural characterization. The EDXRF studies showed that the $\text{Zn}_{1-x-y}\text{Cd}_x\text{Mn}_y\text{GeAs}_2$ had the average contents of Cd, x , from 0.18 or 0.83, and Mn content changing in the range from $y = 0.033$ to 0.109. Colleagues from Russia performed the structural studies using the HRXRD method. The results and the data analysis made using the Rietveld refinement method clearly show the presence of the following phases in our crystals: (i) in the crystals with $x \approx 0.18$ we detected the chalcopyrite phase similar to ZnGeAs_2 , [46] (ii) for the samples with $x \approx 0.83$ we detected the chalcopyrite-like phase similar to that of CdGeAs_2 [46], and (iii) we have detected the presence of the hexagonal MnAs phase in all the studied crystals. The presence of hexagonal MnAs precipitates in the samples was confirmed by the SEM studies, which revealed the presence of MnAs clusters of the size smaller than $1 \mu\text{m}$. Only a small fraction of MnAs clusters present in the samples was of the size exceeding $1 \mu\text{m}$, and only for such large precipitates their shape looked like a hexagon.

In view of the need to verify the thesis T5 I conducted detailed studies of the magnetic properties of the $\text{Zn}_{1-x-y}\text{Cd}_x\text{Mn}_y\text{GeAs}_2$ crystals by a series of measurements using different magnetometric techniques. The research revealed that all the samples show the paramagnet – ferromagnet transition at the temperature about $T \approx 310 \text{ K}$. At low temperatures I have not found a presence of a significant paramagnetic contribution to the total magnetic susceptibility. This means that the method of synthesis prevented the uniform dissolution of Mn in the semiconductor lattice and the vast majority of magnetic ions in the material remains in the MnAs clusters.

Correct determination of the Curie temperature and the analysis of the magnetic properties on the basis of the Curie-Weiss law required broadening of the range of temperatures at which the magnetometric measurements were made by the studies of the magnetic properties in the range of temperatures above room temperature. I used the results of the magnetization as a function of temperature measurements obtained using the VSM magnetometer by my collaborators at low magnetic fields $B \leq 50 \text{ mT}$ to determine the temperature dependencies of the dc-field magnetic susceptibility χ_{dc} . The selected results of the magnetization measurements are presented in Fig. 8. The calculated $\chi_{\text{dc}}(T)$ dependences have been used by me to determine the Curie temperature, T_C , for all the studied samples. The T_C values change little between the samples in the range from 306 K to 313 K. *Ferromagnetic ordering of the crystals is related to the presence of MnAs clusters.* I observed only minor changes of T_C with the Cd content, x , varying from 0.12 to 0.83. It is associated with the deformation of the MnAs clusters due to stress. Deformation manifests itself by the change of the MnAs lattice parameters between the two above-mentioned series of samples with $x \approx 0.12$ and 0.83. Deformation of the clusters is known as one of the main factors responsible for the changes in the T_C

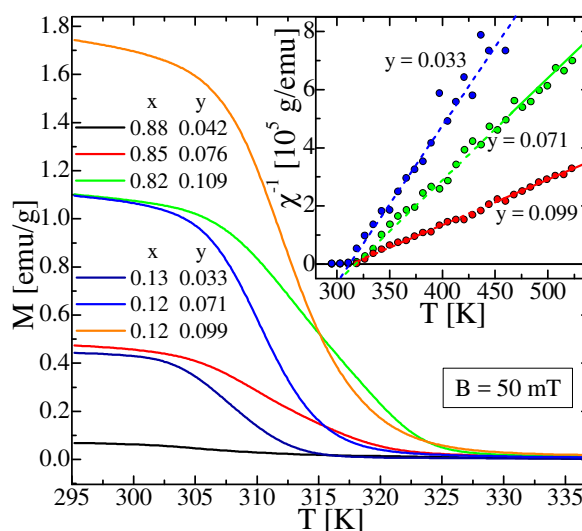


Fig. 6. Temperature dependence of the magnetization and the magnetic susceptibility (inset) obtained for the selected $\text{Zn}_{1-x-y}\text{Cd}_x\text{Mn}_y\text{GeAs}_2$ crystals.

[48,49].

Further verification of the thesis T4 requires the analysis of the inverse of the magnetic susceptibility, χ_{dc} (see the inset to Fig. 6). In the temperature range well above T_C , i.e. in the paramagnetic region χ_{dc} behaves according to the Curie-Weiss law. Data analysis enabled me to estimate the values of two parameters i.e. the Curie-Weiss temperature, θ , and the Curie constant, C . I used the obtained C values to calculate the effective Mn content in the samples, y_θ . The obtained results indicate that for the case of all our crystals the inequality $y_\theta < y$ is true. There are two possible explanations for this behavior. First, the modified Curie-Weiss law is applicable only for T much higher than T_C . Because of the experimental equipment limitations and because of the risk of annealing the samples it was not possible to carry out measurements at $T > 600$ K. It is therefore possible that, in the temperature range from 450 K to 600 K and in the low magnetic field region the magnetic moments of manganese ions are isolated and aligned along the direction of the magnetic field, and their contribution to the magnetic susceptibility is only partial. Secondly, a large portion of the manganese ions in the material can be in the charge state different from Mn^{2+} , which is a high-spin state with the total magnetic momentum equal to $J = S = 5/2$. The second parameter determined by me during the data analysis, i.e. the Curie-Weiss temperature, θ , has values similar to T_C , indicating a lack of strong magnetic frustration in our samples, which could lead to a difference between the T_C and θ . These results represent an important contribution to the studies of the thesis T4.

I continued the studies of the magnetic properties of the $Zn_{1-x-y}Cd_xMn_yGeAs_2$ crystals through a number of measurements of the magnetization $M(B)$ curve. The magnetization at $T = 4.5$ K for the samples with $x \approx 0.012$ exhibits saturation for $B < 9$ T. It enabled me to estimate the saturation magnetization, M_S , a quantity important to estimate the effective Mn content, y_m . On the other hand, in the case of the samples with $x \approx 0.083$ the $M(B)$ curves do not show saturation. Lack of magnetization saturation of the $M(B)$ curves is the result of a large magnetic frustration and the presence of strong antiferromagnetic interactions in the samples with $x \approx 0.083$. The obtained y_m values, gathered in the manuscript [H4], show that $y_m \approx y$ and $y_m > y_\theta$. The likely explanation for this behavior is that some of the Mn ions occupy interstitial positions and/or create nano-clusters. Such Mn ions interact antiferromagnetically with other Mn ions and may not give a full contribution to the magnetic susceptibility. On the other hand, in a high magnetic field region during magnetization measurements the antiferromagnetic coupling is too weak and the magnetic moments of Mn ions are aligned along the the direction of the magnetic field giving the full contribution to the magnetization which results in $y_m \approx y$.

I made a number of measurements of the hysteresis of the magnetization for all the studied $Zn_{1-x-y}Cd_xMn_yGeAs_2$ crystals. I observed the presence of a well-defined magnetic hysteresis loop only for the samples with $x \approx 0.83$. The difference in the shapes of the $M(B)$ loops between the samples with $x \approx 0.12$ and 0.83 is associated with the change of the domain structure of the MnAs clusters, which in turn is closely associated with the structural disorder and geometrical parameters of the clusters.

The most important element of the studies of the properties of composite $Zn_{1-x-y}Cd_xMn_yGeAs_2$ crystals containing MnAs clusters was to study their electrical properties aiming at the verification of the thesis T6. At first I have made a series of studies of the $\rho_{xx}(T)$ dependencies for $B = 0$ T. The obtained $\rho_{xx}(T)$ dependencies for a group of samples with $x \approx 0.012$ are a decreasing function of temperature, while for the samples with $x \approx 0.085$ the $\rho_{xx}(T)$ curves are increasing functions of the temperature at low temperatures, reach a

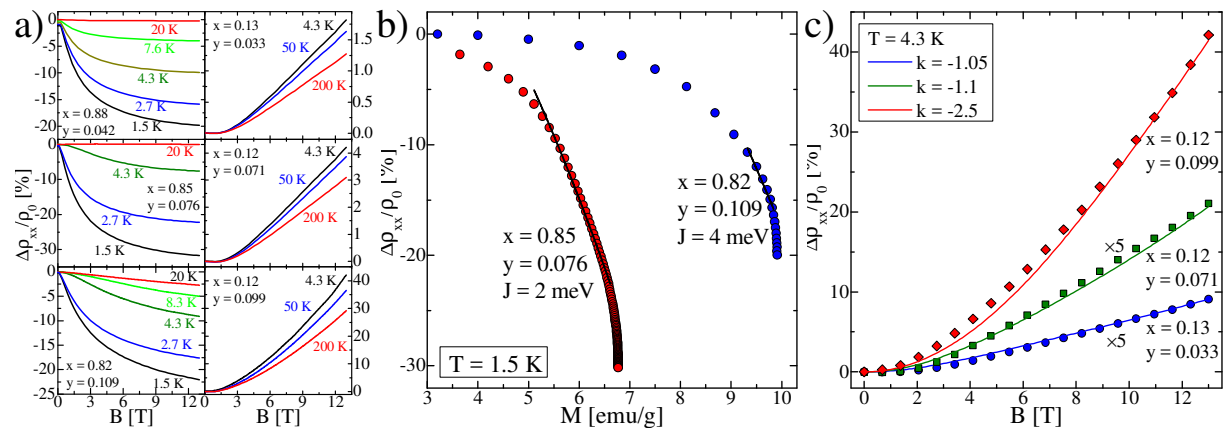


Fig. 7. Results of the magnetotransport investigations of the $\text{Zn}_{1-x-y}\text{Cd}_x\text{Mn}_y\text{GeAs}_2$ crystals with different chemical compositions comprising: (a) the resistance, ρ_{xx} , as a function of the magnetic field obtained at different temperatures, (b) the magnetoresistance as a function of the magnetization obtained for the selected crystals at $T = 1.5$ K, and (c) the magnetoresistance as a function of the applied magnetic field obtained for the selected samples at $T = 4.3$ K (points) and calculated based on the effective medium approximation model (lines).

maximum, and subsequently decrease as a function of temperature. Decreasing $\rho_{xx}(T)$ dependence, which I observed for a group of samples with $x \approx 0.012$ can not be interpreted as a thermally activated transport, because the experimental dependence $\rho_{xx}(T)$ does not fulfill the activation law. Thus, the experimental observation is a result of the presence of a large number of defects in the material and the opening of the second metallic conductivity channel. I observed more complex $\rho_{xx}(T)$ dependencies for the samples with $x \approx 0.085$. It is likely that the observed $\rho_{xx}(T)$ curves are the result of the presence of structural defects.

The Hall effect studied as a function of the temperature allowed me to determine the temperature dependence of the carrier concentration n and the mobility μ . The results of measurements show that for all the samples both n and μ show almost no temperature dependence. This means that the carrier transport in the studied samples is not due to thermal activation. Samples with $x \approx 0.085$ are p-type ($n = 0.8\text{-}1.9 \times 10^{18} \text{ cm}^{-3}$) and samples with $x \approx 0.012$ are n-type ($n = 5.5\text{-}11 \times 10^{19} \text{ cm}^{-3}$). This is a result of the change of the dominant type of electrically active defects in the material. These defects are a source of conducting electrons or holes in this alloy. All the $\text{Zn}_{1-x-y}\text{Cd}_x\text{Mn}_y\text{GeAs}_2$ crystals I studied show low carrier mobility values ($\mu \leq 11 \text{ cm}^2/(\text{V}\cdot\text{s})$) at room temperature and no $\mu(T)$ dependence. This confirms earlier observations that the crystals studied in [H4] are strongly defected.

The next stage of the studies of the electrical properties of the $\text{Zn}_{1-x-y}\text{Cd}_x\text{Mn}_y\text{GeAs}_2$ crystals was done in the range of strong magnetic fields. The $\rho_{xy}(B)$ dependencies for all the crystals were linear suggesting no anomalous Hall effect or effects associated with two types of conducting carriers in the material. In turn, the magnetoresistance measurements have a much more complicated character (see Fig. 7a). For all the samples with $x \approx 0.085$ the magnetoresistance exhibits negative values at $T < 20$ K, and positive values proportional to B^2 at $T > 20$ K. The negative magnetoresistance shows a decline in amplitude with increasing temperature. The $M(B)$ curves for the samples with $x \approx 0.085$ did not show saturation at $B \leq 13$ T. It is therefore clear that the magnetoresistance of the alloy is not exclusively related to the presence of MnAs clusters. Magnetoresistance observed in the samples with a high content of Cd, $x \approx 0.085$ shows a behavior similar to that observed for $\text{ZnGeAs}_2:\text{MnAs}$ [14], while for the group of samples with a low content of Cd, $x \approx 0.012$, the magnetoresistance shows a behavior similar to that observed for $\text{CdGeAs}_2:\text{MnAs}$ [23]. It is therefore possible

that the physical mechanism leading to the appearance of different magnetoresistance effects is related not only with the cation type.

I conducted an analysis to determine the dominant physical mechanism responsible for the negative magnetoresistance in the studied $\text{Zn}_{1-x-y}\text{Cd}_x\text{Mn}_y\text{GeAs}_2$ samples. There are many different mechanisms that can lead to a negative magnetoresistance in the semiconductor containing magnetic dopants. The Moriya-Kawabata theory of spin fluctuations [37,38] predicts that the negative magnetoresistance should scale as B or B^2 for either weak ferromagnetic or paramagnetic metals, respectively. I made the data analysis that shows that the magnetoresistance can be fitted to the power law for the value of the scaling factor of approximately 0.76. Since the value of the exponent for our samples differs from 1 or 2, I exclude the spin fluctuations mechanism as being responsible for the observed magnetoresistance. Furthermore, the magnetoresistance as a function of the magnetization, M , which is normalized to the saturation magnetization, M_S , (see Fig. 7b) is neither square nor cubic. This is further proof that the negative magnetoresistance comes from processes that are not closely related to the scattering of charge carriers by magnetic impurities.

The negative magnetoresistance in granular systems, i.e. Ni-SiO₂ [50] is a known phenomenon, which is usually described by the theory of spin-polarized electrons. Negative magnetoresistance values have been reported for many systems and can take both significant values of the order of 60% [14], and small values not exceeding 1% [51]. The $\rho_{xx}(B)$ dependence of the ferromagnetic metal with the clusters can be described within the framework of the molecular theory and the model described by Helman and Abeles [52]. I made an analysis of the $\rho_{xx}(M)$ curves using the model with two required experimental fitting parameters, i.e. the exchange constant, J , and the polarization of the carriers, P . We took the P value for the MnAs cluster equal to 45%. The value was found in the literature [52] and used in order to reduce the number of fitting parameters of the fitting procedure to J parameter only. The results of the data analysis are presented in Fig. 7b. The data show that the magnetoresistance curves can not be reproduced in the whole range of magnetic field values using the adopted model. This is a clear indication of the presence of additional physical mechanisms responsible for the magnetoresistance curves at low temperatures. It is highly likely that the weak localization phenomenon investigated in frame of the thesis T3 and observed for homogeneous $\text{Zn}_{1-x}\text{Mn}_x\text{GeAs}_2$ samples with $x < 0.043$ in the manuscript [H1] may occur at low temperatures in the $\text{Zn}_{1-x-y}\text{Cd}_x\text{Mn}_y\text{GeAs}_2$ samples. Moreover, at higher magnetic fields the classical positive magnetoresistance can affect the shape of the $\rho_{xx}(B)$ curves. However, the analysis has allowed me to assess the value of the exchange constant inside the MnAs grains embedded in the semiconductor matrix. The resulting J values increase with the amount of Mn in the samples in the range from $J \approx 1$ meV for $y = 0.042$ up to 4 meV for $y = 0.109$. I can therefore speculate that the increase in J versus the amount of Mn in the samples is associated with changes in the structural and magnetic properties of the ferromagnetic MnAs clusters. The obtained J values are higher by more than an order of magnitude than the values obtained by me earlier for the $\text{Zn}_{1-x}\text{Mn}_x\text{GeAs}_2$ crystals with $J < 0.1$ meV [14]. Higher J values are responsible for the higher temperatures at which I observed the negative magnetoresistance in the $\text{Zn}_{1-x-y}\text{Cd}_x\text{Mn}_y\text{GeAs}_2$ samples.

For the samples with $x \approx 0.012$ the $\rho_{xx}(B)$ curves are positive in the entire range of magnetic fields. In addition, above 3 T the $\rho_{xx}(B)$ dependence is either nearly linear with the magnetic field for the samples with $y = 0.033$ and $y = 0.071$ or almost square with the magnetic field for the sample with $y = 0.099$. The amplitude of the magnetoresistance observed at $T = 4.3$ K increases with the amount of manganese in the crystals from about

1.5% for the sample with $y = 0.033$ to about 40% for the sample with $y = 0.099$. The positive magnetoresistance is observed at temperatures up to 200 K, and it shows a slow decrease with increasing temperature. Most of the Mn ions in our samples are located in the MnAs clusters and is therefore evident that the increase in y results in an increase in the concentration of the MnAs clusters. It is therefore possible that the observed positive magnetoresistance has its source in the same physical mechanism as in the $\text{Cd}_{1-x}\text{Mn}_x\text{GeAs}_2$ crystals [23].

The presence of a positive linear magnetoresistance is known and is attributed to the non-uniformity, i.e. the presence of regions with the conductivity different from that of the base material. The linear magnetoresistance can have either a large value of about 1000% in MnAs-GaAs [53], or less than 1% in the case of thin Ni layers [50]. The magnetoresistance in these systems can be described by a model called effective medium approximation (EMA¹¹) [54,55]. The EMA model is used to reproduce the experimental curves with the use of the ratio between the Hall constants in the matrix and clusters, k . I carried out an analysis of the magnetoresistance curves using the EMA model aiming to reproduce the experimental curves $\rho_{xx}(B)$ for different k values (see Fig. 7c). I obtained the best fits for negative k values which indicate that the clusters have the opposite sign of the Hall constant (n-type) than the matrix. The absolute k values increases with Mn content, y , demonstrating an increasing difference between the carrier concentration in the matrix and in the MnAs clusters.

As I showed above the studies of $\text{Zn}_{1-x-y}\text{Cd}_x\text{Mn}_y\text{GeAs}_2$ crystals allowed me to *show the ability to control the magnetotransport effects* by changing the composition of the non-magnetic impurities in the alloy and therefore the positive verification of these T4 and T6. I accomplished the research program focused on the controlled introduction of the short-ranged magnetic interactions into the II-IV-V₂ semiconductor matrix (thesis T5) and the control of their magnetotransport properties by changing the chemical composition.

c.2.2.b. Self-organization of clusters in ZnSnAs_2 +MnAs composites

The problem of obtaining control over the deployment and geometrical parameters of the clusters still remained unsolved. We performed a series of growth tests and studies of a number of II-IV-V₂ + MnAs crystals obtained using different growth parameters. My work did not yield tangible results until the growth of the ZnSnAs_2 +MnAs composites with different cluster content in the alloy. The results of detailed studies structural, magnetic and electrical properties of these crystals were published in the manuscript [H5]. The composite ZnSnAs_2 -MnAs crystals were synthesized in a way that ensures the smallest MnAs cluster size.

As a part of the characterization of the structural properties of the ZnSnAs_2 -MnAs samples our colleagues from Russia performed a series of HRXRD, SEM, AFM, and MFM measurements. Samples without MnAs comprise 30% of the cubic modification of the ZnSnAs_2 lattice (I-42D). On the other hand the samples with MnAs do not

contain this phase but the ferromagnetic MnAs phase was detected. The most important results of the structural

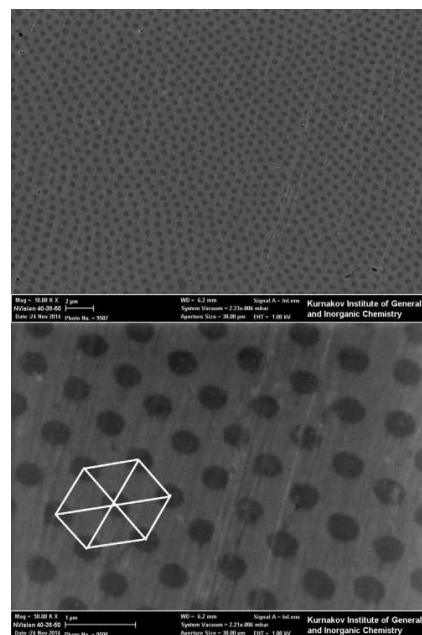


Fig. 8. SEM images of the surface of the ZnSnAs_2 -MnAs composite.

¹¹ effective medium approximation

characterization seem to be SEM images of samples (see Fig. 8). SEM images show that MnAs clusters are present in the ZnSnAs_2 lattice. The average size of the MnAs clusters is about 250 nm. This is a very important result because in the case of slow-cooling after the sample synthesis the MnAs clusters have sizes hundred times larger, in the range of 25-30 μm [56]. Ferromagnetic ordering of the MnAs clusters was confirmed by my colleagues by the AFM and the MFM measurements, as a result of which we obtained clear images of the domain structure of clusters at $T < 340$ K. For all the studied samples the distribution of the MnAs clusters in the ZnSnAs_2 semiconductor matrix is not accidental and the organization of their mutual position was observed. It is important that the *MnAs clusters organize in hexagons*. Thanks to this phenomenon, we managed to achieve the goal of research included in the thesis T5 involving the controlled introduction of the short-range magnetic interactions in the II-IV-V₂ semiconductors through the control of geometrical parameters of clusters. Obtaining such valuable samples was a strong motivation to perform research related to the thesis T6, i.e. the studies of influence of the structural properties of composite systems on their magnetic and electrical properties.

I made a series of studies of magnetic properties of the ZnSnAs_2 -MnAs samples with different MnAs content varying from 0 to 47 mol% with a few selected magnetometric methods, to which I had direct access. The results of the performed studies were published in [H5]. At first I conducted a series of studies of the temperature dependence of the alternating-field magnetic susceptibility (see Fig. 9b). Measurements done for the non-magnetic ZnSnAs_2 crystal allowed the estimation of the diamagnetic contribution of the crystal lattice to the magnetic susceptibility, equal to $\chi_{\text{dia}} = -2 \times 10^{-7}$ emu/g. The obtained results showed that all the samples with MnAs are characterized by the presence of paramagnet - ferromagnet transition at $T > 300$ K. At $T < 300$ K the magnetic susceptibility shows small changes with temperature. In particular, at low temperatures I observed the paramagnetic contribution to the magnetic susceptibility resulting from the presence of isolated Mn ions homogeneously dissolved in the ZnSnAs_2 semiconductor lattice. This means that the method of synthesis has led to a uniform dissolution of Mn in semiconductor lattice but at the same time the contribution is small enough that the vast majority of magnetic ions in the material remains in the MnAs clusters. The purpose of research (thesis T5) was therefore in my opinion reached.

The studies of the $\text{Re}(\chi_{\text{ac}})(T)$ have been supplemented by my colleagues via the magnetization $M(B)$ measurements at $B < 10$ mT and at temperatures from 300 K to 600 K. I used the magnetization results to calculate the magnetic susceptibility for temperatures from 300 K to 600 K (see Fig. 9b). I used the temperature dependence of the magnetic susceptibility to determine the Curie temperature, T_C (see Fig. 9b). The observed T_C values slightly increase as a function of the MnAs concentration. That is associated with changes in the structural parameters of MnAs clusters, especially with the changes of lattice parameters of the clusters.

Further verification of the thesis T5 was made possible by the analysis of the magnetometric data in the range of high temperatures (well above T_C), where for all the studied samples magnetic ions are in a paramagnetic state and the temperature dependence of the magnetic susceptibility can be analyzed using the Curie-Weiss law. The data analysis indicated that the magnetic susceptibility of the ZnSnAs_2 -MnAs samples obeys the Curie-Weiss law and it is possible to determine the Curie-Weiss temperature, θ , and the Curie constant, C . The calculated values of θ satisfy the condition $\theta \approx T_C$. This points to the dominance of one type of magnetic interactions in the material, i.e. the interaction in the

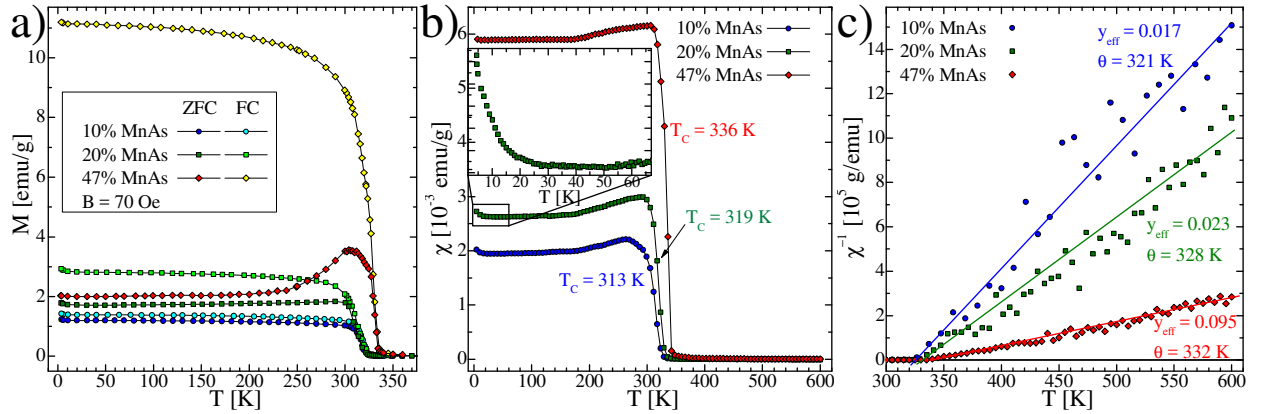


Fig. 9. Results of the magnetometric studies for the $\text{ZnSnAs}_2\text{-MnAs}$ composites with different chemical compositions comprising: (a) temperature dependencies of the magnetization measured under conditions of the sample cooled in the presence of a magnetic field $B = 70$ Oe, and cooled at $B = 0$ Oe, (b) the magnetic susceptibility as a function of temperature and (c) the temperature dependence of the inverse of the real part of the magnetic susceptibility.

ferromagnetic MnAs clusters and negligible strength of the other magnetic interactions, which might be the source of the magnetic frustration in the system. In turn I used the calculated values of the C constant to estimate the effective Mn content, y_{eff} , in the samples. For all the nanocomposites studied in the manuscript [H5] the y_{eff} values are increasing as a function of the average MnAs cluster content in the samples.

I studied the magnetization $M(B)$ curves using two magnetometers at $T < 400$ K. The selected magnetization measurements presented in the manuscript [H5] indicate that the $M(B)$ curves obtained at $T < T_C$ have shapes similar to that at $T = 4.5$ K for all samples. Above T_C the $M(B)$ curves are typical of a paramagnetic material. At $T < T_C$ the $M(B)$ curves show the Brillouin shape with the saturation for $B > 4$ T. It allowed me to estimate the value of the saturation magnetization, M_S , which is an increasing function of the MnAs concentration in the samples. That coincides with the analysis of the Curie constant, C . I observed the presence of the magnetization hysteresis loop at temperatures below T_C . The temperature dependencies of the coercive field, B_C , and the remanence magnetization, M_R , indicate that both B_C and M_R are very low for the samples with 10% and 20% MnAs. However, for the sample with 47% MnAs I observed much broader and well-defined magnetization hysteresis loops with $B_C = 12$ mT and $M_R = 2$ emu/g. This underlines the fact that the domain structure of clusters was changed with increasing concentration of MnAs clusters in the nanocomposite. The shape and parameters characterizing the magnetic hysteresis loop do not show large changes with increasing temperature up to $T \approx T_C$, where the hysteresis loop disappears. This is another proof that the magnetic ions in the MnAs clusters in the material show the ferromagnetic order. In this way I showed that the concentration of MnAs clusters in the ZnSnAs_2 allows control of the magnetic properties of the nanocomposite and at the same time in manuscript [H5] I added another big contribution to the detailed verification of the thesis T5.

The phenomenon of geometric self-organization of the MnAs clusters creates very important opportunities for the verification of the thesis T6, i.e. the search for the correlations between the presence and structural properties of clusters and the electrical properties of nanocomposites. Consequently, an important element of the studies of the properties of composite $\text{ZnSnAs}_2\text{-MnAs}$ crystals was to study the transport and magnetotransport properties. These studies consisted of a series of measurements that I did myself.

I started the studies of transport properties of the $\text{ZnSnAs}_2\text{-MnAs}$ crystals from the measurements of the $\rho_{xx}(T)$ dependence for $B = 0$ T. The resistance values observed for the

ZnSnAs₂ sample are higher than the values obtained for the ZnSnAs₂-MnAs samples. Furthermore, the $\rho_{xx}(T)$ dependence has a different shape in the pure ZnSnAs₂ compound than in the nanocomposite samples. This is an important pointing to the fact that the addition of MnAs to the ZnSnAs₂ semiconductor drastically changes the electrical transport of the material.

Measurements of the Hall effect, i.e. $\rho_{xy}(B)|_{T=\text{const.}}$ clearly indicated that the Hall effect is a linear function of the magnetic field in the whole investigated temperature range (the contribution from the anomalous Hall effect was not present). This allowed me a simple and precise determination of the $n(T)$ and $\mu(T)$ dependencies for all the samples studied in the manuscript [H5]. All the samples are p-type semiconductors. The carrier concentration in the nanocomposite ZnSnAs₂-MnAs samples is much higher than in the ZnSnAs₂ sample. Acceptor concentration in all the samples exceeds the value characteristic of the metal-insulator transition defined by the Mott criterion [57]. Therefore, all the studied samples lie on the metallic side of the metal-insulator transition due to the presence of MnAs nanoclusters. On the other hand, I observed two orders of magnitude smaller n for the ZnSnAs₂ sample than in the nanocomposite ZnSnAs₂-MnAs samples. This is an important property indicating that during the preparation of a nano-composite alloy the creation of a large number of structural defects, which are electrically active, occurred.

Based on the results of the Hall effect measurements I have calculated the temperature dependence of the carrier mobility gathered in the manuscript [H5]. The mobility, μ , is the order of magnitude higher for the ZnSnAs₂ sample than the values observed in the ZnSnAs₂-MnAs samples. This is due to lower quality of the crystals containing MnAs clusters. In addition, the studies have shown that the $\mu(T)$ dependence for the ZnSnAs₂ sample has a different character than those observed in the ZnSnAs₂-MnAs samples. For the ZnSnAs₂ crystal I observed the decreasing $\mu(T)$ dependence for T from 4.5 K to 75 K, and then increasing $\mu(T)$ for T from 75 K to 300 K. The observed $\mu(T)$ dependence is difficult to explain given the traditional carrier scattering mechanisms in semiconductors, assuming one type of carriers (holes) in the material. It is therefore very likely, as demonstrated in the literature for the ZnSnAs₂ layers that the observed $\mu(T)$ and $n(T)$ dependencies are the result of two conduction channels, i.e. the holes in the valence and in the acceptor band [58]. Interpretation of the transport data for the ZnSnAs₂-MnAs samples is even more complicated than in the case of a pure ZnSnAs₂ compound, suggesting the existence of the auxiliary conduction channel or additional type of carriers associated with the MnAs and having a concentration and mobility, which differ significantly from those of pure ZnSnAs₂ compound. Thus, the differences between the transport data observed for the sample without MnAs and nanocomposite samples should be addressed supposedly to the contribution of an additional type of carriers related to the MnAs clusters.

The complicated nature of the electron transport present in the ZnSnAs₂-MnAs crystals required further research in the area of strong magnetic fields (see Fig. 10). The obtained magnetoresistance curves indicate that there are at least three mechanisms involved in the $\rho_{xx}(B)$ dependencies in the studied ZnSnAs₂-MnAs crystals. The $\rho_{xx}(B)$ curves observed for the pure ZnSnAs₂ sample show high (around 30% at $B = 13$ T) positive linear magnetoresistance at $T < 4.3$ K and classical positive magnetoresistance at $T > 4.3$ K. The low temperature linear positive magnetoresistance is most likely related with large spatial variations in the conductivity of the material, due to the polycrystalline structure of the samples. The presence of grain boundaries, in which the conductivity is locally disrupted with respect to the bulk of the crystal, can cause a positive linear magnetoresistance in

semiconductors, observed, e.g., in InSb [59]. Above 4.3 K (up to 300 K) the magnetoresistance shows the square dependence on the magnetic field and results from classical mechanism associated with the orbital motion of the charge carriers in the magnetic field.

I observed more complex behavior of the magnetoresistance for the nanocomposite ZnSnAs₂-MnAs samples. I observed three effects at low temperatures $T < 50$ K: (i) negative magnetoresistance at $T < 10$ K, (ii) positive magnetoresistance at temperatures from 10 K to about 50 K, and (iii) the negative magnetoresistance observed again at $T > 50$ K. The negative magnetoresistance observed at $T < 10$ K may be associated with the phenomenon of weak localization as it disappears at low temperatures and is not visible at strong magnetic fields. At temperatures from $T = 10$ K to 50 K I observed the positive linear magnetoresistance not showing saturation. The physical reason of this effect may be the same as for pure ZnSnAs₂ sample and is associated with microscopic variations in the conductivity due to the presence of grain boundaries in the polycrystalline material. Above 50 K up to room temperature I observed only slight negative magnetoresistance. The origin of this effect may be related to the presence of the MnAs clusters in the ZnSnAs₂-MnAs samples. The effect is small due to the low carrier mobility in these samples. *The complex nature of the magnetoresistive effects* can lead to the thesis that the electrical properties of ZnSnAs₂-MnAs nanocomposites can be controlled in a wide range of values. That contributes to the positive verification of the thesis T6. The studies of the ZnSnAs₂-MnAs nanocomposites presented by me in the manuscript [H5] constituted an important step for understanding the structural, magnetic and electrical nanocomposite systems exhibiting disorder as well as the phenomenon of self-organization.

c.2.2.c. High-temperature ferromagnetism in Zn_{1-x}Mn_xSnSb₂+MnSb composites

The next step and the task that I set for myself on the way to verify theses T5 and T6 was to investigate the structural, magnetic, and electrical properties of the II-IV-V₂-MnSb composites. The motivation to undertake research focused on materials containing different type of clusters than MnAs was primarily due to the need to examine whether also for other types of precipitations the spectacular magnetotransport effects will be observed as they were in the case of composites with MnAs. To this end, our colleagues from Russia have done for us the synthesis of a series of Zn_{1-x}Mn_xSnSb₂ crystals with different Mn contents.

As the first part of the above crystals research program I performed measurements of the average chemical composition by the EDXRF technique. The analysis of the obtained EDXRF spectra showed that the studied samples had an average Mn content, x , varying in the range from 0.027 to 0.138 and the correct stoichiometry of the Zn_{1-x}Mn_xSnSb₂ alloy equal to

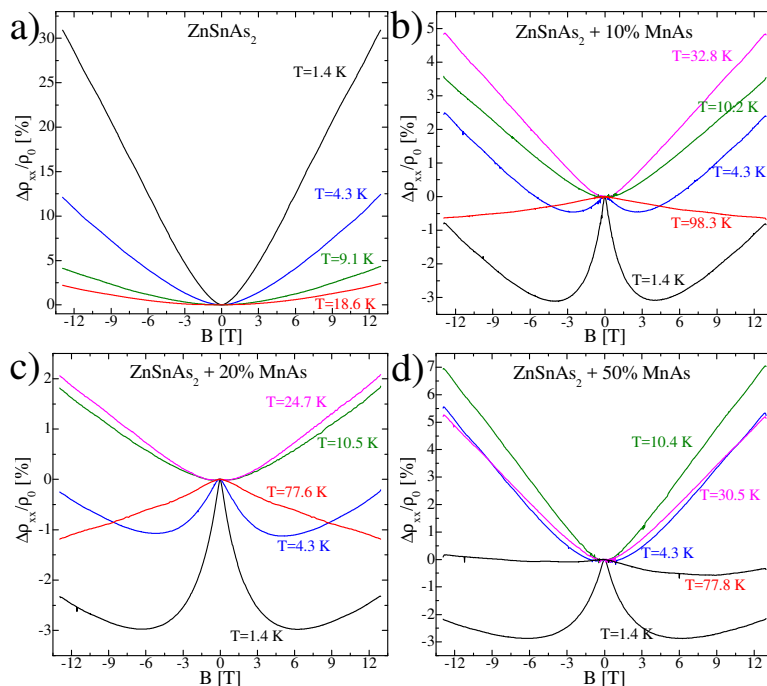


Fig. 10. Selected magnetoresistance curves obtained for the ZnSnAs₂-MnAs crystals with different chemical compositions.

1-x:x:1:2. In collaboration with Dr. E. Dynowska from IF PAN we performed the studies with the use of the HRXRD method aiming at the phase analysis of the crystals. Phase analysis revealed that the samples were not uniform. In addition to the main chalcopyrite ZnSnSb_2 phase we identified the presence of the hexagonal MnSb phase, the rhombohedral SnSb phase, and the orthorhombic ZnSb phase in all the studied samples. It is associated with a limited range of temperatures at which the ZnSnSb_2 crystals may be synthesized. The presence of the MnSb clusters in this material needs further studies of the magnetic and electrical properties aiming at a verification of the theses T5 and T6. We conducted a series of AFM-MFM measurements. The obtained results showed the presence of a strong signal from the ferromagnetic MnSb clusters. AFM-MFM studies allowed us to determine that the examined samples have the MnSb precipitates of a similar size distribution and diameters comprised between 10 and 20 μm . The characterized composite material is an interesting subject to study magnetic properties due to the high-temperature ferromagnetism, which should be accompanied by the presence of the MnSb clusters in the ZnSnSb_2 .

The verification of the thesis T5 required carrying out detailed studies of the magnetic properties of $\text{Zn}_{1-x}\text{Mn}_x\text{SnSb}_2+\text{MnAs}$ crystals. The studies of the magnetic properties were carried out mostly by me using several magnetometric methods, to which I had direct access. The results of the above research I published in the manuscript [H6] and the selected results are presented in Fig. 11. The results showed that all the samples are characterized by the presence of magnetic order. At low temperatures I observed the paramagnetic contribution to the susceptibility due to the presence of isolated Mn ions dissolved uniformly in the ZnSnSb_2 semiconductor lattice. The presence of this contribution means that the method of synthesis has enabled a uniform dissolution of Mn in the semiconductor lattice but at the same time the

contribution is small enough that the vast majority of magnetic ions in the material remain in the MnSb clusters. The results of the $\text{Re}(\chi_{ac})(T)$ dependence studies have to be supplemented with the measurements of the magnetization $M(B)$ at $B < 10$ mT in order to identify the magnetic order present in the crystals using the SQUID and VSM magnetometers and in the temperature range from 320 K to 600 K. I used the magnetization results to determine the constant-field magnetic susceptibility, χ_{DC} , for each studied temperature (see Fig. 11a). The studies showed at high temperature of about 540 K the presence of the magnetic transition in the system. The ZFC and FC $\chi_{DC}(T)$ curves for all the studied samples are of similar shape at temperatures

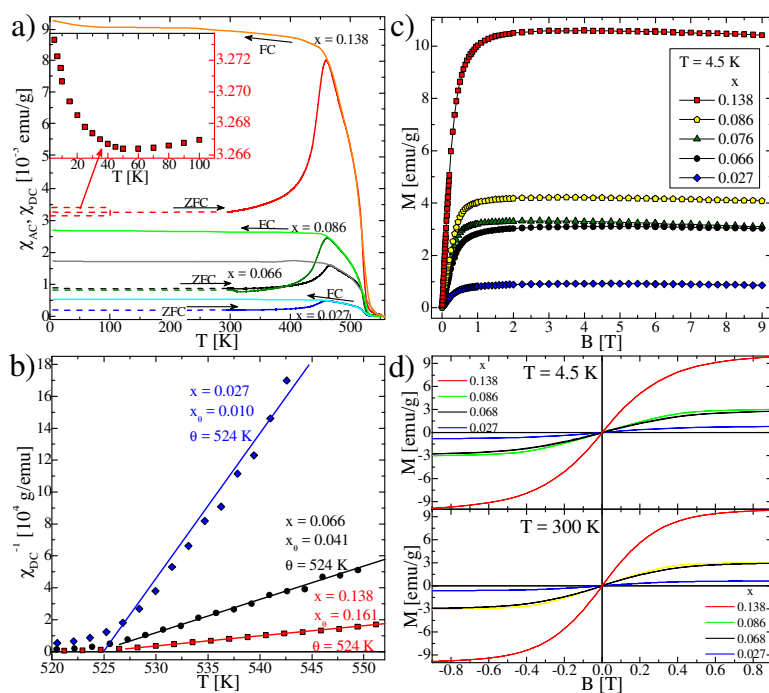


Fig. 11. Results of the magnetometric studies of the $\text{Zn}_{1-x}\text{Mn}_x\text{SnSb}_2+\text{MnSb}$ crystals with different chemical compositions comprising: (a) temperature dependence of the magnetic susceptibility measured under conditions of sample cooled in the presence of the magnetic field $B = 2$ mT and cooled at $B = 0$ mT, (b) the reciprocal magnetic susceptibility as a function of temperature, (c) magnetization curves measured at $T = 4.5$ K, and (d) magnetization hysteresis curves obtained at $T = 4.5$ K and $T = 300$ K.

Table 3. Parameters obtained as a result of the magnetometric data analysis obtained for the $Zn_{1-x}Mn_xSnSb_2+MnSb$ crystals with different chemical compositions, x .

x	T_C [K]	T_{CG} [K]	θ [K]	C (10^{-4}) [emu·K·g $^{-1}$]	x_θ	M_S [emu/g]	x_m
0.027	522±1	462±1	526±1	1.0±0.1	0.010±0.002	0.86±0.04	0.013±0.001
0.066	522±1	466±1	524±1	4.2±0.3	0.041±0.004	2.9±0.2	0.045±0.005
0.076	522±1	464±1	525±1	4.5±0.3	0.044±0.004	3.0±0.2	0.046±0.005
0.086	521±1	463±1	525±1	4.8±0.4	0.048±0.005	4.1±0.3	0.062±0.006
0.138	521±1	459±1	524±1	16±1	0.161±0.016	10.4±0.6	0.159±0.016

higher than 500 K. Therefore, I probably observed the paramagnet - ferromagnet transition at a temperature of about 520 K. The calculated Curie temperatures for this transition (see Table 3) are similar for all the studied samples, suggesting that this transition is due to the presence of MnSb clusters [60]. Therefore, it is true that at least a part of the MnSb clusters present in the samples shows ferromagnetic properties with a well-defined paramagnet - ferromagnet phase transition. Literature data for MnSb indicate that the Curie temperature may vary between 600 K for annealed MnSb crystals [60], and 565 K observed for the MnSb crystals cooled quickly after growth [60]. The relatively low T_C values which I have calculated for the studied $Zn_{1-x}Mn_xSnSb_2+MnSb$ crystals stem from the fact that the MnSb precipitates present in them are small and are related to the conditions of technological synthesis of crystals.

The second magnetic effect indicating a change in the magnetic state of the samples I studied occurred in the temperature range between 455 and 465 K. This effect is visible as a maximum in the ZFC $\chi_{DC}(T)$ curves. Below $T \approx 460$ K I observed bifurcation between the ZFC and FC $\chi_{DC}(T)$ curves for all the studied samples. These two properties show that in addition to the ferromagnetic order a part of the MnSb clusters present in the examined samples can show cluster-glass type behavior associated with a random distribution of orientation of the clusters, which are coupled magnetically by a short-range dipole magnetic interaction and/or long-range RKKY magnetic interaction. In the case of a transition to the cluster-glass type state the ZFC $\chi_{DC}(T)$ curves should extrapolate to 0 emu·g $^{-1}$ for $T \rightarrow 0$ K, whereas in the case of the studied samples the $\chi_{DC}(T)$ relationship does not extrapolate to zero at low temperatures. This may be due to isolated ferromagnetic MnSb clusters, which give almost constant non-zero contribution to the magnetic susceptibility at low temperatures. The presence of the ferromagnetic MnSb clusters masks the behavior of the cluster-glass type regions containing the isolated MnSb clusters. Another explanation of the observed effects is that the ZFC-FC curves as a function of temperature together with the peak in the ZFC $\chi_{DC}(T)$ curve near the magnetic transition temperature may be considered as due to the presence of the Hopkinson effect. This effect was observed in the case of the MnSb clusters [61] and other granular systems [62]. However, the lack of peaks in the $\chi_{DC}(T)$ dependencies is an important indication that I did not observe the Hopkinson effect in the studied samples. Another possible interpretation of the behavior of the $\chi_{DC}(T)$ curves may be associated with the presence of ferrimagnetism of the MnSb clusters, which was observed in the InSb-MnSb system, and also manifests itself as a maximum in the $\chi_{DC}(T)$ dependence [63, 64]. In the cluster-glass type system showing frustrated ground magnetic state the ZFC $\chi_{DC}(T)$ curves should have a maximum near the magnetic transition temperature, and the FC $\chi_{DC}(T)$ curve showed no such maximum. Furthermore, the ZFC $\chi_{DC}(T)$ curves do not show any thermal fluctuations to be observed in the superparamagnetic system. It is therefore very likely that I observed the cluster-glass state of the $Zn_{1-x}Mn_xSnSb_2+MnSb$ crystals. I have calculated for

each sample the temperature of the transition to the cluster-glass state, T_{CG} , as a point of inflection of the ZFC $\chi_{DC}(T)$ curve (see Table 3). The T_{CG} temperature (like the Curie temperature, T_C) does not depend on the chemical composition of the crystals, pointing to the fact that the structural properties of the MnSb clusters present in the $Zn_{1-x}Mn_xSnSb_2+MnSb$ crystals are similar for all the studied crystals. The presence of two types of magnetic ordering of the MnSb clusters is the result that brings an interesting contribution to the verification of the thesis T5.

The presence of two different magnetic states of the MnSb clusters is known for the InSb-MnSb system, in which the MnSb clusters are in the form of crystallographically oriented bars [65]. The large magnetic anisotropy of the MnSb bars is responsible for the change in the shape of the $\chi_{DC}(T)$ curves, when the magnetization is measured along or across the preferred orientation of the MnSb bars. A large magnetic anisotropy was also observed in the epitaxial GaAs-MnSb layers [66]. It is therefore obvious that the presence of a large magnetic anisotropy present in the MnSb clusters in the $Zn_{1-x}Mn_xSnSb_2+MnSb$ crystals I studied is responsible for *the appearance of either the ferromagnetic state or cluster-glass state*.

Another element of the magnetometric studies of the $Zn_{1-x}Mn_xSnSb_2+MnSb$ crystals aimed to verify the thesis T5 consisted of the analysis of the $\chi_{DC}(T)$ dependencies at high temperatures ranging from 550 K to 600 K, using the Curie-Weiss law. As a result of the data analysis I estimated the values of two parameters: θ and C (see Table 3). The calculated θ values satisfy the condition $\theta \approx T_C$. This indicates a dominance of the ferromagnetic interaction of the MnSb clusters. The estimated C values I used to determine the effective concentration of the Mn ions in the crystals, x_θ . For all the crystals except $x = 0.138$ we observed that $x_\theta < x$. There are two explanations for this phenomenon. The first is due to the fact that in the temperature range from 450 K to 600 K and under low magnetic field the magnetic moments of the manganese ions are not free and oriented along the direction of the field, and their contribution to the magnetic susceptibility is partial. The second explanation is that a large portion of the manganese ions in the material can be in a charge state different from the Mn^{2+} state wherein $J = S = 5/2$.

I conducted the research of the $M(B)$ dependencies of the $Zn_{1-x}Mn_xSnSb_2+MnSb$ crystals at $T < 400$ K (see Fig. 11c and 11d). The observed $M(B)$ curves have a similar shape as at $T = 4.5$ K for all the samples. I observe the Brillouin shape of the $M(B)$ curves with the saturation magnetization for $B > 2$ T. It allowed me to determine the value of the saturation magnetization, M_S , for each crystal and then calculate the effective Mn content, x_m , in the samples. The obtained x_m values, summarized in Table 3, show that $x_m \approx x_\theta$ within the limits of the errors in the estimation of the above two values. This is an important result which confirms the fact that the analysis of the $\chi_{DC}(T)$ curves based on the Curie-Weiss gave close and reliable results. It is also a proof that the interpretation based on the obtained x_θ values is correct. I made the measurements of the $M(B)$ dependencies in order to observe the presence of the magnetization hysteresis loop at temperatures below T_C . Both the coercive field, B_C , and remanence magnetization, M_R , have very low values for all the studied samples. It is associated with the observed cluster-glass type behavior of the studied samples. Both the shape and parameters characterizing the magnetization hysteresis did not show significant changes as the temperature increases to $T \approx T_C$, where the hysteresis loop disappears. It is associated with the existence of the strong magnetic interactions of the magnetic MnSb clusters in the material. Thus, in the manuscript [H6] I obtained the last scientific results necessary for a detailed verification of the thesis T5.

The presence of the cluster-glass and the ferromagnetic order at high temperatures observed in the $\text{Zn}_{1-x}\text{Mn}_x\text{SnSb}_2+\text{MnSb}$ crystals is very interesting due to the ability to observe correlations between the properties of clusters and the electrical properties of samples, i.e. the verification of the thesis T6.

I started the studies of the electrical properties of the $\text{Zn}_{1-x}\text{Mn}_x\text{SnSb}_2+\text{MnSb}$ crystals from the measurements of the $\rho_{xx}(T)$ for $B = 0$ T. The $\rho_{xx}(T)$ curves obtained for all the samples show the metallic behavior at temperatures higher than 50 K, in the temperature range from 10 K to 50 K the resistance is a decreasing function of temperature, i.e. I observe the metal-insulator transition. On the other hand, at temperatures below 10 K I observed fast decrease of the $\rho_{xx}(T)$ dependence with decreasing T . I observed therefore the complex shape of the $\rho_{xx}(T)$ dependence, analysis of which requires broader studies using the Hall effect. Measurements of the $\rho_{xy}(B)|_{T=\text{const.}}$ dependencies indicated that the Hall effect is a linear function of the magnetic field in the whole considered temperature range (no anomalous Hall effect was observed in this material). This allowed me a simple and precise determination of the $n(T)$ and $\mu(T)$ dependencies for all the crystals investigated in the manuscript [H6]. All the studied $\text{Zn}_{1-x}\text{Mn}_x\text{SnSb}_2+\text{MnSb}$ crystals are p-type semiconductors. I observed a high carrier concentration in all examined samples with the value of about $5 \times 10^{20} \text{ cm}^{-3}$ for the sample with $x = 0.138$ to about $1.3 \times 10^{22} \text{ cm}^{-3}$ for the sample with $x = 0.027$. Such high concentrations of holes in semiconductors are usually associated with high concentration of defects in the material and were observed by me in the $\text{ZnSnAs}_2+\text{MnAs}$ samples in the manuscript [H5]. I observed two different behaviors of the $n(T)$ dependencies i.e. the increasing $n(T)$ for the samples with $x \leq 0.066$ and the decreasing $n(T)$ dependencies for the samples with $x > 0.066$. This does not mean that the samples with $x \leq 0.066$ show thermally activated conductivity, because: (i) the amount of changes observed in the $n(T)$ dependence is small, and (ii) I observed the metallic behavior of the $\rho_{xx}(T)$ dependencies for $T > 50$ K. All test samples are therefore degenerate semiconductors and lie on the metallic side of the metal-insulator transition.

I calculated the $\mu(T)$ dependencies, where μ does not exceed $35 \text{ cm}^2/(\text{V}\cdot\text{s})^{-1}$ obtained for the sample with $x = 0.138$. The carrier mobility μ is inversely proportional to the carrier concentration, n . This means that the defects responsible for the high n values in the studied samples are also effective electron scattering centers. The $\mu(T)$ dependencies for the $\text{Zn}_{1-x}\text{Mn}_x\text{SnSb}_2+\text{MnSb}$ samples with $x \leq 0.066$ show a different nature than those observed in the samples with $x > 0.066$. For the samples with low Mn content $x \leq 0.066$ the $\mu(T)$ dependencies increase with temperature for T from 4.5 K to 75 K, reaching a maximum at $T \approx 75$ K, and then decreases at temperatures from 75 K to 300 K. The increasing $\mu(T)$ dependence was observed previously for the $\text{Zn}_{1-x}\text{Mn}_x\text{GeAs}_2$ crystals in the manuscripts [H1] and [H3] and for the $\text{Cd}_{1-x}\text{Mn}_x\text{GeAs}_2$ crystals in manuscript [H2]. Such a shape of the $\mu(T)$ curve is a characteristic feature observed for the carrier scattering at the electrically charged defects which is the main scattering mechanism of the charge carriers in the material. Decreasing $\mu(T)$ dependence observed at T of 75 K to 350 K is characteristic of the carrier scattering by phonons. In contrast, for the samples with the Mn content, $x > 0.066$, I observed the increasing $\mu(T)$ dependence in the whole considered temperature range, the behavior difficult to explain by conventional scattering mechanisms in semiconductors, if only one type of carriers (holes) is taken into account. I accepted the explanation of the observed effects as similar to that shown in the literature for the ZnSnAs_2 layers in which the observed $\mu(T)$ and $n(T)$ dependencies may be satisfactorily explained by two mechanisms of conduction, i.e. the band conduction and the conduction in the acceptor level [58]. Given our

results published in the manuscript [H6] I assumed that for the $\text{Zn}_{1-x}\text{Mn}_x\text{SnSb}_2+\text{MnSb}$ samples with $x > 0.066$, there is an additional conduction channel or an additional type of carriers, both associated with the MnSb precipitates, with the concentration and mobility which differ significantly from the parameters characteristic of the semiconductor matrix.

The last element of the studies of the electrical properties of the $\text{Zn}_{1-x}\text{Mn}_x\text{SnSb}_2+\text{MnSb}$ crystals consisted of the magnetoresistance studies in the range of strong magnetic fields. At temperatures from $T = 10$ K to 300 K the magnetoresistance of all the studied $\text{Zn}_{1-x}\text{Mn}_x\text{SnSb}_2+\text{MnS}$ samples showed only a small positive component associated with the orbital movement of carriers in a magnetic field. At temperatures lower than 10 K and for low values of the magnetic field, $|B| < 0.1$ T, I observed large changes of the $\rho_{xx}(B)$ dependencies. At higher values of the magnetic field, $|B| > 0.1$ T, the slope of the magnetoresistance curves is much smaller and only positive classical magnetoresistance is observed. The maximum value of the positive magnetoresistance is close to 460% for the sample with $x = 0.027$ at $T = 1.4$ K. Moreover, the observed magnetoresistance depends on the average chemical composition, x . The amplitude of the negative magnetoresistance is reduced with increasing temperature T , and at $T \approx 10$ K the effect disappears.

I attempted to analyze and interpret the observed low-temperature magnetoresistance. There are several possible explanations for this effect. In systems with strong spin-orbit interaction there exists the effect of reducing the probability of backscattering below its classical value. This phenomenon is called weak antilocalization (WAL¹²) [67]. The ZnSnSb_2 chemical compound is characterized by the strong spin-orbit coupling energy of about 0.87 eV [68,69] for the energy gap changing from 0.7 eV at $T = 300$ K to 0.4 eV at $T = 77$ K [70,71]. The magnetoresistance observed in the examined samples at $T < 10$ K can be related to the WAL phenomenon and can be described by the Hikami-Larkin-Nagaoka theory [72]. I performed an analysis of the experimental magnetoresistance curves obtained at $T < 10$ K in view of the WAL theory [72]. The analysis showed that the WAL phenomenon does not describe well the experimental results due to the necessity of using the fitting parameters with values that do not have a physical justification. Therefore, I looked for another possible explanation for the observed strong magnetoresistance. Finally, I interpreted the observed magnetoresistance effect as the phenomenon of the destruction of superconductivity by the magnetic field. This interpretation explains the magnetoresistance of this composite. This stage adds another point to the verification of the thesis T6.

c.2.2.d. Control of the electrical properties of the $\text{Zn}_{1-x}\text{Cd}_x\text{GeAs}_2$ crystals

Interesting results of the studies of the electrical properties including the change of the conductivity type of the crystals and fascinating magnetoresistive effects observed for the $\text{Zn}_{1-x-y}\text{Cd}_x\text{Mn}_y\text{GeAs}_2$ crystals in the manuscript [H4] caused a number of questions as to which of the observed effects are due to the presence of the MnAs clusters, which are connected with the addition of the Cd ions to the crystals. Motivation contained in the thesis T4 led to my interest in the samples that do not contain magnetic impurities, i.e. the $\text{Zn}_{1-x}\text{Cd}_x\text{GeAs}_2$ crystals with the Cd content, x , varying from 0 to 1. I have received two series of crystals; in each of the series the chemical composition of the crystals should change every $\Delta x \approx 0.1$. This enabled me to: (i) carry out systematic studies of the structural and the electric properties for a range of crystals having different chemical compositions, and (ii) to check the reproducibility of the results for crystals of the two series. The results of the studies, which I obtained for the

¹² *weak anti-localization*

above samples have been published by me in the manuscript [H7] and completed the verification of the thesis T4.

The diffraction studies done with the use of the HRXRD technique and the data analysis by Rietveld method allowed me to indicate that for the $\text{Zn}_{1-x}\text{Cd}_x\text{GeAs}_2$ crystals with $x = 0$ and $x = 1$ we observe a single chalcopyrite phase. For intermediate chemical compositions we observe two tetragonal chalcopyrite phases with the values of the parameters of the crystal lattice in the range between the values observed for the single phase crystals. Both sets of lattice parameters obtained for both phases show a nearly linear increase with the average Cd content, x , suggesting that the Vegard rule for both the observed phases is satisfied to some extent. The values of the slope coefficients for all the dependencies of the lattice parameters on x are smaller than could be expected based on the literature data for the $\text{ZnGeAs}_2\text{-CdGeAs}_2$ system. This is a proof that with increasing Cd content, x , in the samples the Cd content in each phase is also increasing. In addition, the percentage of each of the two phases observed in the $\text{Zn}_{1-x}\text{Cd}_x\text{GeAs}_2$ samples is a monotonic function of the Cd content in the alloy.

The final stage of the studies of the structural properties of the $\text{Zn}_{1-x}\text{Cd}_x\text{GeAs}_2$ crystals was focused over detailed microscopic studies aiming to illustrate both phases present in the crystals, to determine their chemical composition, and perform microscopic analysis of the stoichiometry of the two phases. Microscopic studies were performed using the SEM by my colleagues' MSc. A. Reszka and prof. B.J. Kowalski in the IF PAN. The SEM results indicated in accordance with the HRXRD data, that in the $\text{Zn}_{1-x}\text{Cd}_x\text{GeAs}_2$ crystals we are dealing with two different phases with different Cd contents in most of the samples except those with $x = 0$ and $x = 1$, where only a single phase is present. SEM maps show that the chemical compositions observed of the two phases are either rich in Zn or Cd atoms. Detailed measurements performed on selected points on the surface of the samples indicated that the Cd content in each of the observed phases increases as a function of the average Cd content, x . This finding explains the results of the HRXRD studies showing the increase in the lattice parameters for both phases present in the $\text{Zn}_{1-x}\text{Cd}_x\text{GeAs}_2$ samples with an increase in x .

The structural properties of the $\text{Zn}_{1-x}\text{Cd}_x\text{GeAs}_2$ crystals allowed us to establish that in the case of these samples we have the composite system consisting of two nonmagnetic phases. Therefore, a potential impact of the structural quality of the crystals on their electrical properties has become a very interesting problem. This issue is included in the thesis T5 and studied in detail in the manuscript [H7]. All the studies and the data analysis of the electrical properties of the $\text{Zn}_{1-x}\text{Cd}_x\text{GeAs}_2$ crystals I performed personally.

A very important issue requiring systematic studies is the influence of the changing Cd contents on the magnetotransport properties of the $\text{Zn}_{1-x}\text{Cd}_x\text{GeAs}_2$ crystals. In order to explore this issue I made a series of magnetotransport measurements (see Fig. 12). The observed ρ_{xx} dependencies indicate that the resistance of the

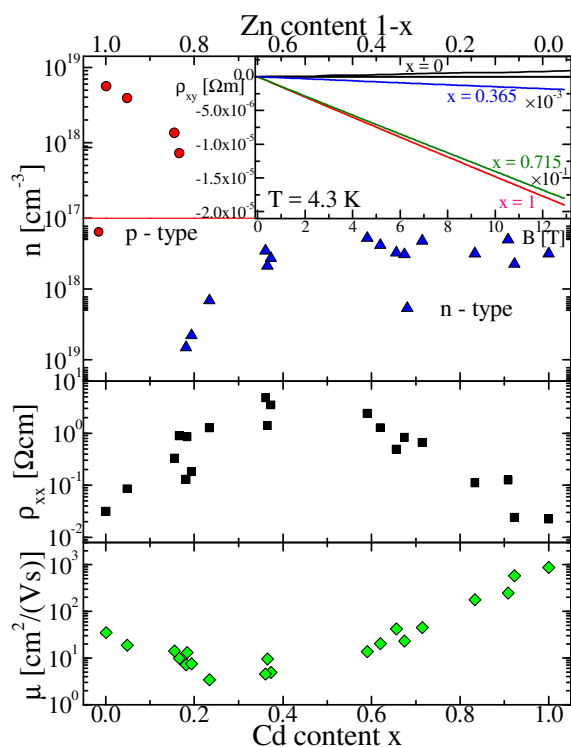


Fig. 12. Electrical properties of the $\text{Zn}_{1-x}\text{Cd}_x\text{GeAs}_2$ crystals obtained at $T = 300$ K: carrier concentration n , resistivity ρ_{xx} , and carrier mobility μ as functions of the Cd content, x .

$\text{Zn}_{1-x}\text{Cd}_x\text{GeAs}_2$ crystals varies by three orders of magnitude with x . The lowest resistance values are observed for the samples with $x = 0$ and $x = 1$ and therefore in the threefold compounds. It is very likely that the presence of the two phases observed in the samples with $0 < x < 1$ and scattering of carriers at interfaces is responsible for the reduction in the conductivity of these samples. This interpretation is justified by the fact that the $\rho_{xx}(x)$ dependence is an increasing function of x to about 0.2, where the resistance reaches the maximum value. For x from 0.2 to about 0.6 the resistance does not change significantly. On the other hand, for $x > 0.6$, the resistance is a decreasing function of x , reaching a minimum value for the sample with $x = 1$. The temperature dependences of the conductivity $\sigma_{xx}(T)$ observed by me for all the $\text{Zn}_{1-x}\text{Cd}_x\text{GeAs}_2$ crystals are typical for thermally activated carrier transport. I carried out the data analysis of the experimental $\sigma_{xx}(T)$ dependencies based on the theory of thermal excitations in semiconductors so that I could determine the conductivity activation energy, E_a . The obtained E_a value is about 20-30 meV for all the studied samples. The band structures of both compounds i.e. CdGeAs_2 and ZnGeAs_2 are similar. Both compounds have a straight energy gap at the Γ point of the Brillouin zone with the bandgap energy, E_g , equal to 0.53 eV for the CdGeAs_2 [73] and 1.15 eV for the ZnGeAs_2 [74]. The large difference between the E_g for the CdGeAs_2 and the ZnGeAs_2 and the E_a value determined by me indicates that the most likely the thermal activation of charge carriers occurs between the defect subband and the conduction band or the valence band, depending on the type of the conducting carriers in the material.

The next stage of the studies of the electrical properties of the $\text{Zn}_{1-x}\text{Cd}_x\text{GeAs}_2$ crystals consisted of the Hall effect measurements. The obtained $\rho_{xy}(B)|_{T=\text{const.}}$ dependencies were linear (see the inset to Fig. 12) indicating the absence of the two-carrier electrical transport in the material. This enabled the precise calculation of the $n(T)$ and $\mu(T)$ dependencies for all the crystals investigated in the manuscript [H7]. The samples with $x \leq 0.18$ show p-type conductivity with $n \approx 6 \times 10^{18} \text{ cm}^{-3}$ for $x = 0$. The $n(x)$ dependence shows a decrease with x from the value of about $n \approx 7 \times 10^{17} \text{ cm}^{-3}$ for $x = 0.166$ and then I observe the change to the n-type of the conductivity, for the sample with $x = 0.181$. For $x > 0.18$, all samples show n-type conductivity in the whole investigated range of chemical compositions and temperatures. The $n(T)$ dependencies show relatively small change of n with temperature. This indicates clearly that the carrier transport in the $\text{Zn}_{1-x}\text{Cd}_x\text{GeAs}_2$ system is dominated by the carrier excitation processes from defect levels. *Rapid change in the conductivity type is related to the creation of a large population of defects for the samples with $x \approx 0.2$.*

Based on the magnetotransport data I have calculated the temperature dependence of the carrier mobility, μ . The $\mu(x)$ dependence obtained at $T = 300 \text{ K}$ (see Fig. 12) shows a decrease for $x \leq 0.233$. The $\mu(x = 0)$ value is similar to the value for the $\text{Zn}_{1-x}\text{Mn}_x\text{GeAs}_2$ crystals studied in detail in the manuscripts [H1] and [H3]. The decreasing $\mu(x)$ dependence is most likely related to the increasing influence of the grain boundaries on the conduction of polycrystalline samples. For $x > 0.233$ I observed the increased $\mu(x)$ dependence to a maximum value for $x = 1$. The relatively high mobility values observed for the samples with $x = 1$ are higher than the values reported for the $\text{Cd}_{1-x}\text{Mn}_x\text{GeAs}_2$ crystals in the manuscript [H2] and much higher than the values observed in the $\text{Zn}_{1-x-y}\text{Cd}_x\text{Mn}_y\text{GeAs}_2$ composites with $y \approx 0.85$ in the manuscript [H4]. The $\mu(x)$ dependence can be understood in relation to the differences in the carrier effective mass for holes in ZnGeAs_2 and electrons in CdGeAs_2 . The effective mass of the holes in ZnGeAs_2 has values from $0.21m_e$ to $0.29m_e$ [46]. The effective mass of the conduction electrons in the CdGeAs_2 equals $0.027m_e$ [75]. It is therefore possible that the observed $\mu(x)$ dependence for the $\text{Zn}_{1-x}\text{Cd}_x\text{GeAs}_2$ crystals can be attributed to the presence of

different fractions of the Zn-rich and Cd-rich phases. That leads to local changes in the carrier effective mass and also modifies the resultant Hall mobility, which I studied experimentally.

I observed in the manuscript [H7] the increasing $\mu(T)$ dependence for all the studied samples. Such a $\mu(T)$ dependence is characteristic for the heterogeneous semiconductors in which the carrier transport is dominated by the carrier scattering processes at the grain boundaries. This is called temperature-activated carrier mobility [76,77]. Low activation energies observed in the $\text{Zn}_{1-x}\text{Cd}_x\text{GeAs}_2$ samples I studied are characteristic of this type of transport in the polycrystalline material.

The last element of the studies of the electrical properties of the $\text{Zn}_{1-x}\text{Cd}_x\text{GeAs}_2$ crystals consisted of the magnetotransport research in the range of strong magnetic fields. As a result of the studies I obtained very important magnetoresistance results indicating the presence of localization phenomena in this material. This allowed the verification of these T3 and T4. Selected magnetotransport results are gathered in Fig. 13. The results of magnetoresistance measurements I obtained indicate that there are two main physical mechanisms affecting the $\rho_{xx}(B)$ dependence in the $\text{Zn}_{1-x}\text{Cd}_x\text{GeAs}_2$ samples. Therefore I observe a small positive classical magnetoresistance proportional to the square of the magnetic field. This effect is related to the orbital motion of the charge carriers in the presence of a magnetic field. For the samples with $x \geq 0.833$ I observe the negative magnetoresistance at temperatures lower than 100 K and at low values of the magnetic field $|B| < 3$ T. In disordered systems such as the studied $\text{Zn}_{1-x}\text{Cd}_x\text{GeAs}_2$ samples the electrons movement is diffusive. Electrons in such a system experience a number of scattering events due to the presence of defects. These scattering events do not depend on the magnetic field. In contrast, the magnetic field destroys the weak localization (WL¹³) phenomenon [78]. The negative magnetoresistance observed in the studied $\text{Zn}_{1-x}\text{Cd}_x\text{GeAs}_2$ crystals is most likely related to the WL. There are several theories of quantum corrections to the conductivity in the presence of a three-dimensional WL. In particular, the theory proposed by Baxter [79] seems to be the most suitable approach to describe the experimental magnetotransport data for the $\text{Zn}_{1-x}\text{Cd}_x\text{GeAs}_2$

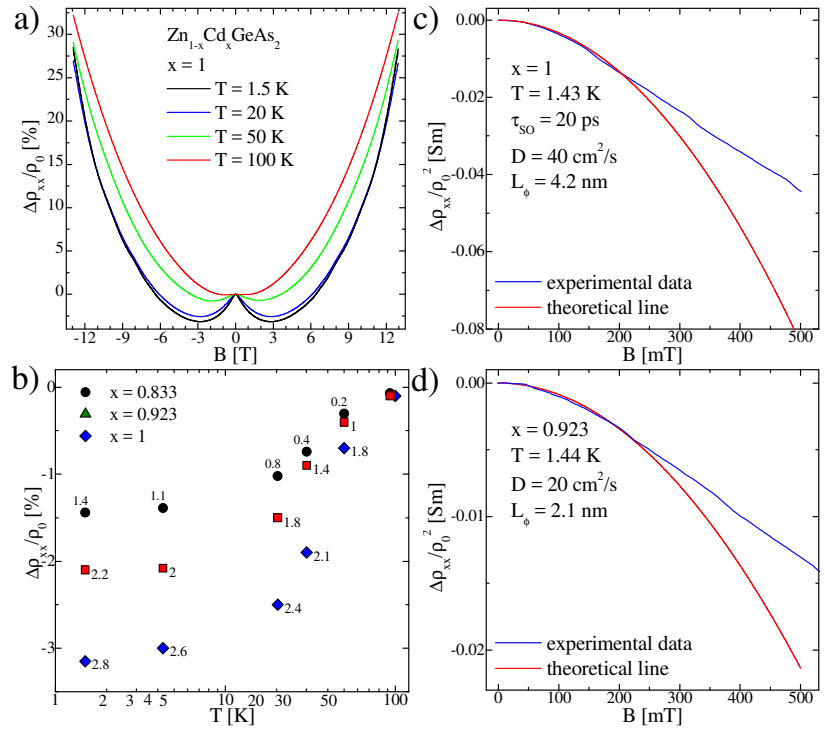


Fig. 13. Selected magnetotransport results obtained for the $\text{Zn}_{1-x}\text{Cd}_x\text{GeAs}_2$ crystals with different chemical composition: (a) magnetoresistance curves obtained at different temperatures for the sample with $x = 1$, (b) temperature dependence of the amplitude of the negative component to the magnetoresistance for the crystals with different x , and (c-d) magnetoresistance curves obtained experimentally and calculated theoretically for two selected samples.

¹³ weak localization

crystal. I performed in the manuscript [H7] the analysis of the $\rho_{xx}(B)$ dependencies based on the WL theory [79] (see Figs. 13c and 13d). The theoretical curves fitted to the experimental results for the $Zn_{1-x}Cd_xGeAs_2$ samples with $x \geq 0.833$ have the spin coherence length parameter equal to less than 5 nm. Thus, WL phenomenon occurring in our samples has a short range and is strongly attenuated by conventional scattering processes of charge carriers present both in the volume of the semiconductor and at the grain boundaries.

The phenomenon of the charge carrier localization that I have observed is a very important research topic. Furthermore, the examined non-magnetic $Zn_{1-x}Cd_xGeAs_2$ crystals showed that the magnetotransport effects observed in the crystals containing MnAs clusters are associated with the processes in the semiconductor matrix, and are strongly correlated with the presence of clusters and their properties. These conclusions are therefore an important contribution to the verification of the thesis T6.

c.2.2.e. Magnetoresistance of the $Cd_{1-x-y}Mn_xZn_ySnAs_2$ composite crystals

The last representatives of the family of group II-IV- V_2 semiconductors, whose electrical properties I examined in order to verify the thesis T6 were composite $Cd_{1-x-y}Mn_xZn_ySnAs_2$ crystals i.e. the crystals with an average Mn content, $x \geq 0.076$. I conducted a series of studies of the Hall effect for all the $Cd_{1-x-y}Mn_xZn_ySnAs_2$ crystals. The results and their analysis gave very important results, i.e. for the samples containing MnAs clusters I observed a very high carrier mobility. The highest value of the carrier mobility observed by me for the group of samples with $x \geq 0.076$ was equal to $\mu = 6860 \text{ cm}^2/(\text{V}\cdot\text{s})$ for the sample with $x = 0.076$ and $y = 0.004$. The carrier mobility values observed in the composite crystals I studied in the manuscript [H8] are the highest values for the group of II-IV- V_2 composite semiconductors. In this way we have reached a significant progress in improving the electrical properties of group II-IV- V_2 materials.

For all the $Cd_{1-x-y}Mn_xZn_ySnAs_2$ crystals containing the MnAs clusters I observed the presence of the SDH oscillations at $T < 50 \text{ K}$ (see Fig. 14). *The oscillating nature of the $\rho_{xx}(B)$ curves is visible on the background of a linear magnetoresistance in all the ferromagnetic samples with $x \geq 0.076$ studied in the manuscript [H8]. The contribution to the magnetoresistance linear as a function of the magnetic field in the samples containing the MnAs clusters was interpreted by me as the presence of the geometric magnetoresistance associated with the scattering of carriers in the material having two phases significantly different in terms of the electrical conductivity. This result is important since I observed a large linear magnetoresistance, which is proportional to the concentration of the MnAs clusters in the alloy. Thus I achieved the ability to control the magnetotransport effects of the $Cd_{1-x-y}Mn_xZn_ySnAs_2$ composites positively verifying the thesis T6.*

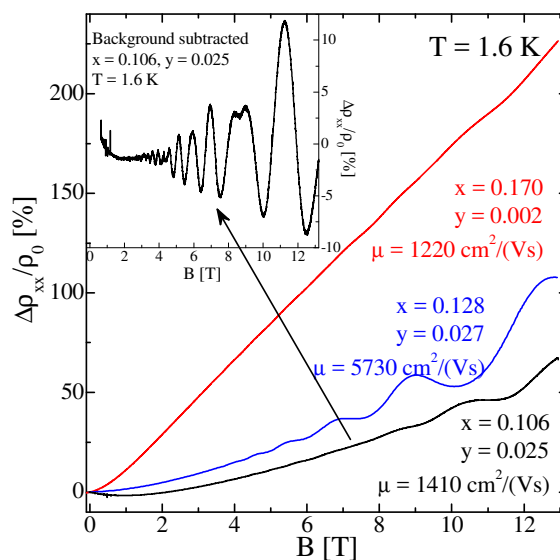


Fig. 14. Magnetotransport results obtained for the $Cd_{1-x-y}Mn_xZn_ySnAs_2$ crystals with different chemical compositions.

c.2.2.f. Summary

I performed the detailed studies of the structural, magnetic, and electrical properties of the selected ferromagnetic metal – semiconductor composites containing magnetic clusters (manuscripts [H4-H8]). Research of the composite materials enabled a positive verification of the three research theses (T4-T6) and significantly extended the current knowledge about this new group of materials with the following findings:

- I have shown that it is possible to obtain a range of II-IV-V₂ group materials with Mn in the form of a composite semiconductor - ferromagnetic metal: (i) Zn_{1-x-y}Cd_xMn_yGeAs₂ in the range of Cd content, x , from 0 to 0.18 and from 0.82 to 1, and Mn from $y = 0.033$ to 0.109, (ii) ZnSnAs₂-MnAs with the MnAs cluster concentration changing from 10% to 47%, (iii) Zn_{1-x}Mn_xSnSb₂+MnSb with the average Mn content, x , changing from 0.027 to 0.138, and (iv) Cd_{1-x-y}Mn_xZn_yGeAs₂ with the average Mn content, x , changing from 0.076 to 0.170.
- I have demonstrated that the magnetic and electrical properties of the Zn_{1-x-y}Cd_xMn_yGeAs₂ crystals vary over a wide range of values with the changes in the concentration of magnetic and non-magnetic dopants in the alloy. I observed the presence of ferromagnetic ordering for all the crystals with the specific parameters subjected to change with x and y . However, the most important results are the change of the sign, the change of the physical mechanism, and the change of temperature range at which the magnetoresistive effects are observed. These changes result from the presence of MnAs clusters in these crystals.
- I have shown that with the change in the amount of Cd in the Zn_{1-x-y}Cd_xMn_yGeAs₂ crystals the change of the conductivity type from p-type ($n = 0.8-1.9 \times 10^{18} \text{ cm}^{-3}$) for the samples with $x \approx 0.085$ to n-type ($n = 5.5-11 \times 10^{19} \text{ cm}^{-3}$) for the samples with $x \approx 0.012$ is possible. This is a result of the change of the dominant type of electrically active defects in the material. All the Zn_{1-x-y}Cd_xMn_yGeAs₂ crystals are characterized by the low carrier mobility values ($\mu \leq 11 \text{ cm}^2/(\text{V}\cdot\text{s})$) and no $\mu(T)$ dependence. This is due to the large defect concentration in these crystals.
- I discovered the phenomenon of self-organization of the MnAs clusters for the ZnSnAs₂-MnAs nanocomposites. I have shown that the self-assembly of the MnAs clusters allows to control the magnetic and electrical properties of the ZnSnAs₂-MnAs nanocomposites.
- I have conducted the research of the influence of the presence of the MnSb clusters on the properties of the Zn_{1-x}Mn_xSnSb₂+MnSb composites. I discovered the presence of different magnetic states of the MnSb clusters in the semiconductor matrix: (i) the ferromagnetic state and (ii) the cluster-glass state. I have shown that a large magnetic anisotropy of the MnSb clusters whose positions in the semiconductor crystal lattice are random is responsible for the observation of two types of magnetic order in this material.
- I observed low values of the effective Mn content in the Zn_{1-x}Mn_xSnSb₂+MnSb composites. This effect is related with the presence of the significant structural disorder in the material. The parameters characterizing the magnetization hysteresis curves of the Zn_{1-x}Mn_xSnSb₂+MnSb crystals have very low values for all the studied samples. It is associated with the presence of the cluster-glass type behavior of the examined samples.
- The strong structural disorder of the Zn_{1-x}Mn_xSnSb₂+MnSb composites leads to a strong p-type conductivity with carrier concentrations with values from $5 \times 10^{20} \text{ cm}^{-3}$ for $x = 0.138$ to $1.3 \times 10^{22} \text{ cm}^{-3}$ for $x = 0.027$. The carrier mobility does not exceed $35 \text{ cm}^2/(\text{V}\cdot\text{s})$.
- I have shown that the electrical properties of the composite Zn_{1-x}Cd_xGeAs₂ crystals with x varying from 0 to 1 strongly depend on the chemical composition. I observed changes in the resistance of the crystals by three orders of magnitude with changes in x . Moreover, for $x \leq 0.18$ I observed the p-type conductivity with $n \approx 6 \times 10^{18} \text{ cm}^{-3}$ for $x = 0$, next I observed

the change in the conductivity type to n-type for $x = 0.181$. For $x > 0.18$ all the $\text{Zn}_{1-x}\text{Cd}_x\text{GeAs}_2$ crystals show n-type conductivity. The $\mu(x)$ dependence shows a decrease for $x \leq 0.233$. Decreasing $\mu(x)$ dependence is related to the growing influence of the grain boundaries in the polycrystalline samples on their conduction. For $x > 0.233$ I observed an increase in the $\mu(x)$ dependence to a maximum value close to $1000 \text{ cm}^2/(\text{V}\cdot\text{s})$ for $x = 1$.

- I obtained significant magnetoresistance results indicating the presence of localization phenomena in the $\text{Zn}_{1-x}\text{Cd}_x\text{GeAs}_2$ crystals with $x \geq 0.833$ in the form of negative magnetoresistance at $T < 100 \text{ K}$ and $|B| < 3 \text{ T}$. The data analysis revealed that the weak-localization present in the $\text{Zn}_{1-x}\text{Cd}_x\text{GeAs}_2$ crystals has a short range and is probably strongly attenuated by the classical charge carriers scattering processes present both in the volume and at the grain boundaries in the semiconductor.
- I discovered the phenomenon of ferromagnetism of the composite $\text{Cd}_{1-x-y}\text{Mn}_x\text{Zn}_y\text{SnAs}_2$ crystals with $x \geq 0.076$. The carrier mobility values observed in the composite crystals are in the range up to $6800 \text{ cm}^2/(\text{V}\cdot\text{s})$, and are the highest for the group of composite II-IV-V₂ semiconductors. For all the $\text{Cd}_{1-x-y}\text{Mn}_x\text{Zn}_y\text{SnAs}_2$ crystals containing MnAs clusters I observed the presence of the SDH oscillations at $T < 50 \text{ K}$. The contribution to the magnetoresistance linear as a function of the magnetic field in the crystals containing the MnAs clusters I interpreted as the geometrical magnetoresistance associated with the scattering of carriers in the material consisting of the two phases significantly different in terms of their electrical conductivity.

c.3. Conclusions

I performed the studies of II-IV-V₂ semiconductors obtained in the form of homogeneous materials (manuscripts [H1-H3] and [H8]) and semiconductor - ferromagnetic metal composites (manuscripts [H4-H8]) in light of the verification of the six research theses T1-T6. The research that I conducted enabled me to present a number of conclusions:

- It is possible to obtain homogeneous diluted semimagnetic semiconductor materials based on II-IV-V₂ compounds.
- In the crystals with p-type conductivity it is possible to induce long-range magnetic RKKY interactions with a significant value of the magnetic exchange constant equal to $J_{\text{pd}} = (0.75 \pm 0.09) \text{ eV}$.
- In all the examined group II-IV-V₂ semimagnetic semiconductors I detected the presence of the short-range magnetic superexchange interactions via an anion. The strength of these interactions and their effect on the magnetism depends strongly on the type of the semiconductor.
- The II-IV-V₂ crystals, depending on the type, have different defect concentrations and structures. This determines the transport and magnetotransport properties of the crystals.
- It is possible to control the magnetic and magnetotransport properties of II-IV-V₂ group composites with MnAs and MnSb. A key influence on the above properties is the carrier localization on the defect states and the scattering processes at the ferromagnetic grain boundaries.
- The aggregation of magnetic impurities into ferromagnetic clusters with a defined spatial distribution in the semiconductor lattice is very difficult to achieve but possible for the ZnSnAs_2 -MnAs nanocomposites.
- It is possible to change the type of the conductivity and to control the magnetotransport properties of the $\text{Zn}_{1-x}\text{Cd}_x\text{GeAs}_2$ crystals by changing the chemical composition.
- It is possible to obtain and investigate the ferromagnetic composites that exhibit quantum oscillations, effects characteristic of the materials with a high structural quality.

c.4. Bibliography

- [1] S.A. Wolf, D.D. Awschalom, R.A. Buhrman, J.M. Daughton, S. von Molnar, M.L. Roukes, A.Y. Chtchelkanova, and D.M. Treger, *Science* **294**, 1488–1495 (2001).
- [2] I. Zutic, J. Fabian, S. Das Sarma, *Rev. Mod. Phys.* **76**, 323–410 (2004).
- [3] D. D. Awschalom, M.E. Flatté, *Nature Physics* **3**, 153 (2007).
- [4] T. Story, R. R. Galazka, R. B. Frankel oraz P. A. Wolf, *Phys. Rev. Lett.* **56**, 777 (1986).
- [5] J. Kossut, W. Dobrowolski, Handbook of Magnetic Materials, North-Holland, Amsterdam, 1993.
- [6] W. Dobrowolski, J. Kossut, T. Story, Handbook of Magnetic Materials, Elsevier, New York, 2003.
- [7] T. Dietl, *Nature Mater.* **9**, 965 (2010).
- [8] A. Janotti, Su-Huai Wei, S.B. Zhang, S. Kurtz, *Phys. Rev. B* **63**, 195210 (2001).
- [9] V.M. Novotortsev, S.F. Marenkin, S.A. Varnavskii, L.I. Koroleva, T.A. Kupriyanova, R. Szymczak, L. Kilanski, B. Krzymanska, *Russ. J. Inorg. Chem.* **52**, 22 (2008).
- [10] I.V. Fedorchenko, A.V. Kochura, S.F. Marenkin, A.N. Aronov, L.I. Koroleva, L. Kilanski, R. Szymczak, W. Dobrowolski, S. Ivanenko, E. Lahderanta, *IEEE Trans. Magn.* **48**, 1581 (2012).
- [11] C.K. Sinclair, in Proceedings of the Eighth International Symposium on High Energy Spin Physics, edited by K. J. Heller, AIP, New York, 2000, p. 65-68.
- [12] D.S. Chemla, *Phys. Rev. Lett.* **26**, 1441 (1971).
- [13] A. Twardowski, *Acta. Phys. Pol. A* **98**, 203 (2000).
- [14] L. Kilanski, M. Górka, W. Dobrowolski, E. Dynowska, M. Wójcik, B. J. Kowalski, J. R. Anderson, C. R. Rotundu, D. K. Maude, S. A. Varnavskiy, I. V. Fedorchenko, and S. F. Marenkin, *J. Appl. Phys.* **108**, 073925 (2010).
- [15] L. Kilanski, I. V. Fedorchenko, M. Górka, E. Dynowska, M. Wójcik, B. J. Kowalski, J. R. Anderson, C. R. Rotundu, S. A. Varnavskiy, W. Dobrowolski, and S. F. Marenkin, *Phys. Stat. Sol. B* **7**, 1601 (2011).
- [16] S. C. Erwin, I. Zutic, *Nature Mater.* **3**, 410 (2004).
- [17] S. Picozzi, *Nature Mater.* **3**, 349 (2004).
- [18] G.A. Medvedkin, T. Ishibashi, T.N. Hayata, Y. Hasegawa, K. Sato, *Jpn. J. Appl. Phys.* **39**, 165 (2000).
- [19] S. Choi, G.B. Cha, S.C. Hong, S. Cho, Y. Kim, J.B. Ketterson, S.Y. Jeong, G.C. Yi, *Solid State Comm.* **122**, 165 (2002).
- [20] S. Cho, S. Choi, G.B. Cha, S.C. Hong, Y. Kim, Y.J. Zhao, A.J. Freeman, J.B. Ketterson, B.J. Kim, Y.C. Kim, and B.C. Choi, *Phys. Rev. Lett.* **88**, 257203 (2002).
- [21] P. Mahadevan, A. Zunger, *Phys. Rev. Lett.* **88**, 047205 (2002).
- [22] Yu-Jun Zhao, S. Picozzi, A. Continenza, W.T. Geng, A.J. Freeman, *Phys. Rev. B* **65**, 094415 (2002).
- [23] L. Kilanski, W. Dobrowolski, E. Dynowska, M. Wojcik, B.J. Kowalski, N. Nedelko, A. Slawska-Waniewska, D.K. Maude, S.A. Varnavskiy, I.V. Fedorchenko, S.F. Marenkin, *Solid State Comm.* **151**, 870 (2011).
- [24] A. Lewicki, A. I. Schindler, I. Miotkowski, J.K. Furdyna, *Phys. Rev. B* **41**, 4653 (1990).
- [25] J. A. Gaj, R. Planel, and G. Fishman, *Solid State Commun.* **29**, 435 (1979).
- [26] S. F. Marenkin, V. M. Novotortsev, K. K. Palkina, S. G. Mikhailov, and V. T. Kalinnikov, *Inorg. Mater.* **40**, 93 (2004).
- [27] V. H. Pfister, *Acta Crystallogr.* **11**, 221 (1958).
- [28] E. Dynowska, L. Kilanski, W. Paszkowicz, W. Dobrowolski, I.V. Fedorchenko, and S.F. Marenkin, *X-Ray Spectrom.* **44**, 404-409 (2015).

- [29] M. Romcevic, N. Romcevic, J. Trajic, L. Kilanski, W. Dobrowolski, I.V. Fedorchenko, and S.F. Marenkin, *J. Alloys Comp.* **688**, 56-61 (2016).
- [30] V. M. Novotortsev, K. K. Palkina, S. G. Mikhailov, A. V. Molchanov, L.I. Ochertyanova, and S. F. Marenkin, *Inorg. Mater.* **41**, 439 (2005).
- [31] S. V. Gudenko, B. A. Aronzon, and V. A. Ivanov, *JETP Lett.* **82**, 532 (2005).
- [32] J. Spalek, A. Lewicki, Z. Tarnawski, J. K. Furdyna, R. R. Galazka, and Z. Obuszko, *Phys. Rev. B* **33**, 3407 (1986).
- [33] M. Gorska and J. R. Anderson, *Phys. Rev. B* **38**, 9120 (1988).
- [34] B. E. Larson, K. C. Haas, H. Ehrenreich, and A. E. Carlsson, *Solid State Commun.* **56**, 347 (1985).
- [35] S. von Molnar, H. Munekata, H. Ohno, and L. L. Chang, *J. Magn. Magn. Mater.* **93**, 356 (1991).
- [36] M. Zajac, J. Gosk, M. Kaminska, A. Twardowski, T. Szyszko, and S. Podsiadlo, *Appl. Phys. Lett.* **79**, 2432 (2001).
- [37] T. Moriya and A. Kawabata, *J. Phys. Soc. Jpn.* **34**, 639 (1973).
- [38] T. Moriya and A. Kawabata, *J. Phys. Soc. Jpn.* **35**, 669 (1973).
- [39] R. A. Lee and T. V. Ramakrishnan, *Rev. Mod. Phys.* **57**, 287 (1985).
- [40] D. V. Baxter, R. Richter, M. L. Trudeau, R. W. Cochrane, and J. O. Strom-Olsen, *J. Phys. France* **50**, 1673 (1989).
- [41] L. Kilanski, A. Zubiaga, F. Tuomisto, W. Dobrowolski, V. Domukhovski, S. A. Varnavskiy, and S. F. Marenkin, *J. Appl. Phys.* **106**, 013524 (2009).
- [42] F. Tuomisto and I. Makkonen, *Rev. Mod. Phys.* **85**, 1583 (2013).
- [43] I. Makkonen, M. Hakala, and M. J. Puska, *Phys. Rev. B* **73**, 035103 (2006).
- [44] T. R. Paudel and W. R. L. Lambrecht, *Phys. Rev. B* **78**, 085214 (2008).
- [45] J. S. Blakemore, *J. Appl. Phys.* **53**, R123 (1982).
- [46] J.L. Shay and J.H. Wernick, *Ternary Chalcopyrite Semiconductors: Growth, Electronic Properties, and Applications* (Pergamon Press, Oxford, 1975).
- [47] I. V. Fedorchenko, A. N. Aronov, L. Kilanski, V. Domukhovski, A. Reszka, B. J. Kowalski, E. Lahderanta, W. Dobrowolski, A. D. Izotov, and S. F. Marenkin, *J. Alloys Compd.* **599**, 121 (2014).
- [48] J. H. Song, Y. Cui, and J. B. Ketterson, *J. Appl. Phys.* **111**, 07E125 (2012).
- [49] M. Bolzan, I. Bergenti, G. Rossetto, P. Zanella, V. Dediu, and M. Natali, *J. Magn. Magn. Mater.* **316**, 221 (2007).
- [50] A. Gerber, A. Milner, B. Groisman, M. Karpovsky, A. Gladkikh, and A. Sulpice, *Phys. Rev. B* **55**, 6446 (1997).
- [51] J. S. Helman and B. Abeles, *Phys. Rev. Lett.* **37**, 1429 (1976).
- [52] R. P. Panguluri, G. Tsoi, B. Nadgorny, S. H. Chun, N. Samarth, and I. I. Mazin, *Phys. Rev. B* **68**, 201307(R) (2003).
- [53] H. G. Johnson, S. P. Bennett, R. Barua, L. H. Lewis, and D. Heiman, *Phys. Rev. B* **82**, 085202 (2010).
- [54] V. Guttal and D. Stroud, *Phys. Rev. B* **71**, 201304(R) (2005).
- [55] V. Guttal and D. Stroud, *Phys. Rev. B* **73**, 085202 (2006).
- [56] I.V. Fedorchenko, A.N. Aronov, S.F. Marenkin, N.P. Simonenko, N.M. Boeva, A.V. Kochura, E. Lahderanta, *J. Alloy. Compd.* **626**, 9-15 (2015).
- [57] N.F. Mott, *Metal-Insulator Transitions*, Taylor and Francis, London, 1990.
- [58] J. T. Asubar, Y. Agatsuma, Y. Jinbo, T. Ishibashi, N. Uchitomi, *IOP Conf. Ser. Mater. Sci. Eng.* **21**, 012031 (2011).

- [59] A.C. Beer, *Solid State Physics Supplement 4: Galvanomagnetic Effects In Semiconductors*, Academic, New York, 1963.
- [60] W. J. Takei, D. E. Cox and G. Shirane, *Phys. Rev.* **129**, 2008 (1963).
- [61] A. V. Kochura, B. A. Aronzon, K. G. Lisunov, A. V. Lashkul, A. A. Sidorenko, R. De Renzi, S. F. Marenkin, M. Alam, A. P. Kuzmenko and E. Lahderanta, *J. Appl. Phys.* **113**, 083905 (2013).
- [62] M. R. Cimberle, R. Masini, F. Canepa, G. Costa, C. Artini, A. Vecchione, M. Polichetti, M. Gombos, M. G. Adesso, *J. Magn. Magn. Mater.* **316**, e529 (2007).
- [63] S. Prasad and N. S. Gajbhiye, *J. Alloys Compd.* **265**, 87 (1998).
- [64] V. M. Novotortsev, I. S. Zakharov, A. V. Kochura, S. F. Marenkin, R. Laiho, E. Lahderanta, A. Lashkul, A. G. Veresov, A. V. Molchanov, and G. S. Yur. *Russ. J. Inorg. Chem.* **51**, 1627 (2006).
- [65] V. M. Novotortsev, A. V. Kochura, S. F. Marenkin, I. V. Fedorchenko, S. V. Drogunov, A. Lashkul, and E. Lahderanta, *Russ. J. Inorg. Chem.* **56**, 1951 (2011).
- [66] H. Akinaga, S. Miyanishi, W. Van Roy, J. De Boeck, and G. Borghs, *Appl. Phys. Lett.* **73**, 3285 (1998).
- [67] G. Bergmann, *Solid State Commun.* **42**, 815 (1982).
- [68] Y. I. Polyganov, Y. M. Basalev, M. L. Zolotarev, and A. S. Poplavnoi, *Fiz. Tekh. Poluprovodn.* **23**, 279 (1989).
- [69] Y. I. Polyganov, Y. M. Basalev, M. L. Zolotarev, and A. S. Poplavnoi, *Sov. Phys.—Semicond.* (Engl. transl.) **23**, 173 (1989).
- [70] L. I. Berger, L. V. Kradinova, V. M. Petrov, and V. D. Prochukan, *Izv. Akad. Nauk SSSR Neorg. Mater.* **9**, 1258 (1973).
- [71] L. I. Berger, L. V. Kradinova, V. M. Petrov, and V. D. Prochukan, *Inorg. Mater* (Engl. transl.) **9**, 1118 (1973).
- [72] S. Hikami, A. I. Larkin, and Y. Nagaoka, *Prog. Theor. Phys.* **63**, 707 (1980).
- [73] V. G. Yarzhemsky, S. V. Murashov, V. I. Nefedov, E. N. Muravev, A. V. Molchanov, A. A. Bagaturyants, A. A. Knizhnik, and V. A. Morozova, *Inorganic Materials* **42**, 924 (2006).
- [74] G.S. Solomon, M.L. Timmons, and J.B. Posthill, *J. Appl. Phys.* **65**, 1952 (1989).
- [75] K.P. Ghatak, M. Mondal, *Zeitschrift fr Physik B* **69**, 471 (1988).
- [76] J.Y. Seto, *J. Appl. Phys.* **46**, 5247 (1975).
- [77] J.H. Werner, in "Polycrystalline Semiconductors III-Physics and Technology", Ed.: H. P. Strunk, J. Werner, B. Fortin and O. Bonaud. p. 213, Scitec Publ., Switzerland, Zug, Switzerland, 1993.
- [78] G. Bergmann, *Phys. Rep.* **107**, 1 (1984).
- [79] D.V. Baxter, R. Richter, M.L. Trudeau, R.W. Cochrane, and J.O. Strom-Olsen, *J. Phys. France* **50**, 1673 (1989).


27.02.2017.

5. Overview of other scientific - research achievements

5.a. Summary of scientific achievements before earning the master's degree

I started the academic work in 2005 as a student of the fifth-year of the MSc-engineering studies at the Technical Physics specialization at the Faculty of Technical Physics, Computer Science and Applied Mathematics of the University of Lodz by doing the master of science thesis under the direction of Dr. P. Gorski. This work started my passion for solid state physics. The result of the thesis titled "Determination of the quadratic electro-optic coefficient $|g_{2211}-g_{1111}|$ in the RDP crystal at room temperature", was the publication in the scientific notebooks of the Technical University of Lodz:

M1. P. Gorski, L. Kilański, R. Ledzion, and W. Kucharczyk, "What is the true order of magnitude of the quadratic electrooptic coefficient $|g_{1111}-g_{1122}|$ in RDP crystal", *Scientific Bulletin of the Technical University of Lodz* **1010**, 5-8 (2007).

My master thesis as well as the manuscript [M1] contains interesting results that constitute an important contribution to the understanding of the optical properties of the birefringent RDP crystals. Studies of the problems of solid state physics have become a motivation for me to focus my future work in the direction of solid state physics.

5.b. Summary of scientific achievements before receiving the title of doctor

Scientific work after receiving a Master of Science degree I continued from 2006 as a graduate student of the International Doctoral Studies that operates at the Institute of Physics, Polish Academy of Sciences in Warsaw. My tutor was Prof. Witold Dobrowolski, the head of the Semimagnetic Semiconductor Physics Laboratory working in the Department of Semiconductor Physics in the IF PAN. The main issues on which I focused within the framework of my doctoral studies were structural, magnetic and electrical properties of semiconductors containing transition metals and rare earth impurities. Up till my doctoral studies there was a large interest in the semiconductor materials belonging to the two groups of compounds, i.e. the IV-VI and II-IV-V₂ groups of the periodic table. So far, the literature reports on research of the properties of these materials often showed fragmented research or contradictory results which caused the need to systematize the knowledge of these semimagnetic semiconductors. In particular, I made the explanation of the following physical problems. As a result it was possible to publish a number of scientific papers:

1. Crystals belonging to the IV-VI group of the periodic table doped with the magnetic Mn ions are an important object of research. I have made research on several $\text{Ge}_{1-x-y}\text{Sn}_x\text{Mn}_y\text{Te}$ crystals with different chemical compositions in order to study: (i) the impact of the Sn ions on the temperature and the type of the magnetic transitions to the ordered state (published in manuscripts [D1-D3]) and (ii) the effect of magnetic ordering on the electrical properties of the crystals shown in manuscripts [D4-D5].

D1. L. Kilański, M. Arciszewska, V. Domukhovski, W. Dobrowolski, V. E. Slynko, and I. E. Slynko, "AC Magnetic Susceptibility Studies of $\text{Ge}_{1-x-y}\text{Sn}_x\text{Mn}_y\text{Te}$ Mixed Crystals", *Acta Phys. Pol. A* **114**, 1145-1150 (2008).

D2. L. Kilański, M. Arciszewska, W. Dobrowolski, V. Domukhovski, V. E. Slynko, and E. I. Slynko, "Spin-glasslike behavior in rhombohedral $(\text{Ge},\text{Mn})\text{Te}-(\text{Sn},\text{Mn})\text{Te}$ mixed crystal", *J. Appl. Phys.* **103**, 103901-1-8 (2009).

D3. L. Kilański, R. Szymczak, W. Dobrowolski, K. Szalowski, V. E. Slynko, and E. I. Slynko, "Magnetic interactions in spin-glasslike $\text{Ge}_{1-x-y}\text{Sn}_x\text{Mn}_y\text{Te}$ dilute magnetic semiconductors", *Phys. Rev. B* **82**, 094427 (2010).

- D4.** L. Kilanski, R. Szymczak, W. Dobrowolski, V. E. Slynko, and E. I. Slynko, "Magnetotransport studies of spin-glass (Ge,Mn)Te-(Sn,Mn)Te mixed crystals", *Acta Phys. Superf.* **9**, 88-89 (2009).
- D5.** L. Kilanski, R. Szymczak, W. Dobrowolski, A. Podgórn, A. Avdonin, V. E. Slynko, and E. I. Slynko, "Negative magnetoresistance and anomalous Hall effect in GeMnTe-SnMnTe spin-glass-like system", *J. Appl. Phys.* **113**, 063702 (2013).

The studies I conducted in manuscripts [D1-D3] enabled me to examine the spin-glass type state observed in the $\text{Ge}_{1-x-y}\text{Sn}_x\text{Mn}_y\text{Te}$ crystals. I also showed the ability to control the temperature of the transition to the ordered state through changes in the chemical composition. I calculated for the first time in this compound the Mn ion – conducting carrier interaction exchange constant, J_{pd} . On the other hand, in the manuscripts [D4-D5] I showed a strong anomalous Hall effect in the $\text{Ge}_{1-x-y}\text{Sn}_x\text{Mn}_y\text{Te}$ crystals and I have calculated a number of parameters describing the magnitude of this effect. I showed a number of magnetoresistance studies along with the interpretation associated with the influence of magnetic impurities.

2. I have examined the problem of the influence of the mutual doping of the crystals belonging to the IV-VI group of the periodic table with Mn and Eu ions in the $\text{Ge}_{1-x-y}\text{Mn}_x\text{Eu}_y\text{Te}$ crystals on their magnetic and electrical properties [D6]. I conducted the studies of the influence of the substitutional ion content on: (i) the temperature and the type of the magnetic phase transition, (ii) the domain structure, and (iii) the anomalous Hall effect and magnetoresistance.

- D6.** L. Kilanski, M. Górska, R. Szymczak, W. Dobrowolski, A. Podgórn, A. Avdonin, V. Domukhovski, V. E. Slynko, and E. I. Slynko, "Cluster Altered Magnetic and Transport Properties in $\text{Ge}_{1-x-y}\text{Mn}_x\text{Eu}_y\text{Te}$ ", *J. Appl. Phys.* **116**, 083904 (2014).

I obtained a number of valuable scientific results allowing me to examine the ferromagnetic order and the cluster-glass state in the $\text{Ge}_{1-x-y}\text{Mn}_x\text{Eu}_y\text{Te}$ crystals. In addition, I made the Hall effect studies, which made possible to estimate the strength of this effect and the parameters characterizing normal and anomalous Hall effect. I made an analysis of the magnetoresistance effects showing their correlation with the magnetic properties of the crystals.

3. We have started for the first time the studies of the structural, magnetic, and electric properties of the $\text{Zn}_{1-x}(\text{Mn},\text{Co})_x\text{GeAs}_2$ crystals with different chemical compositions. This enabled obtaining of valuable scientific results and resolving a number of scientific problems contained in manuscripts [D7-D11].

- D7.** L. Kilanski, M. Gorska, V. Domukhovski, W. Dobrowolski, J. R. Anderson, C. R. Rotundu, S. A. Varniavskii, and S. F. Marenkin, " $\text{Zn}_{1-x}(\text{Mn},\text{Co})_x\text{GeAs}_2$ Ferromagnetic Semiconductor: Magnetic and Transport Properties", *Acta Phys. Pol. A* **114**, 1151-1157 (2008).

- D8.** V. M. Novotortsev, S. F. Marenkin, S. A. Varnavskii, L. I. Koroleva, T. A. Kupriyanova, R. Szymczak, L. Kilanski, and B. Krzymanska, "Ferromagnetic semiconductor $\text{ZnGeAs}_2(\text{Mn})$ with a Curie point of 367 K", *Russian Journal of Inorganic Chemistry (Zhurnal Neorganicheskoi Khimii+)* **53**, 22-29 (2008).

- D9.** L. I. Korolewa, B. J. Pawlow, D. M. Zaszirinskij, S. F. Marenkin, S. A. Warniavskij, R. Szymczak, W. Dobrowolski, and L. Kilanski, "Magnetic and electrical properties of $\text{ZnGeAs}_2:\text{Mn}$ chalcopyrite", *Physics of the Solid State (Fiz. Tverd. Tela+)* **49**, 2121-2125 (2007).

- D10.** L. Kilanski, A. Zubiaga, F. Tuomisto, W. Dobrowolski, V. Domukhovskiy, S. A. Varnavskiy, and S. F. Marenkin, "Native vacancy defects in $Zn_{1-x}(Mn,Co)_xGeAs_2$ studied with positron annihilation spectroscopy", *J. Appl. Phys.* **106**, 013524-1-6 (2009).
- D11.** L. Kilanski, M. Górska, W. Dobrowolski, E. Dynowska, M. Wójcik, B. J. Kowalski, J. R. Anderson, C. R. Rotundu, D. K. Maude, S. A. Varnavskiy, I. V. Fedorchenko, and S. F. Marenkin, "Magnetism and magnetotransport of strongly disordered $Zn_{1-x}Mn_xGeAs_2$ semiconductor: The role of nanoscale magnetic clusters", *J. Appl. Phys.* **108**, 073925 (2010).
- D12.** L. Kilanski, I. V. Fedorchenko, M. Górska, E. Dynowska, M. Wójcik, B. J. Kowalski, J. R. Anderson, C. R. Rotundu, S. A. Varnavskiy, W. Dobrowolski, and S. F. Marenkin "Paramagnetic regime in $Zn_{1-x}Mn_xGeAs_2$ diluted magnetic semiconductor", *Phys. Stat. Sol. B* **7**, 1601 (2011).

Initial studies [D7-D9] related to the properties of the $Zn_{1-x}(Mn,Co)_xGeAs_2$ crystals allowed me to observe the presence of ferromagnetism for the samples with Mn (for $x > 0.053$) and paramagnetism in the crystal with $x = 0.053$. The crystal with Co was diamagnetic. I discovered a number of defect states in the above-mentioned crystals in the manuscript [D10]. Publication of the results contained in [D10] was made possible by receiving the scholarship for the internship at the Helsinki University of Technology, during which I made positron measurements. I have shown for the first time in the manuscript [D11], and in opposition to the literature data that the ferromagnetism of the crystals with $x > 0.053$ is associated with the presence of the MnAs precipitates. Moreover, in the manuscript [D11] I discovered and described the giant magnetoresistance associated with the granular nature of the crystals with MnAs. The research of the magnetotransport properties was extended to the range of high magnetic field due to obtaining the travel grant in 2008 for a short internship at the Laboratory of High Magnetic Fields in Grenoble, France. Moreover, I made a detailed study of the paramagnetic $Zn_{1-x}Mn_xGeAs_2$ crystal with $x = 0.053$ in the manuscript [D12].

4. We performed a series of studies of the $ZnSiAs_2$ crystals containing Mn magnetic impurities. This enabled the examination of a number of interesting magnetic and transport effects published in manuscripts [D13-D16].
- D13.** L. I. Koroleva, D. M. Zashchirinski, T. M. Khapaeva, S. F. Marenkin, I. V. Fedorchenko, R. Szymczak, B. Krzymanska, W. Dobrowolski, and L. Kilanski, "Manganese-Doped $ZnSiAs_2$ Chalcopyrite: A New Advanced Material for Spintronics", *Physics of the Solid State (Fiz. Tverd. Tela+)* **51**, 303-308 (2009).
- D14.** S. F. Marenkin, V. M. Novotortsev, I. V. Fedorchenko, S. A. Warniavskij, L. I. Koroleva, D. M. Zashchirinski, T. M. Khapaeva, R. Szymczak, B. Krzymanska, W. Dobrowolski, and L. Kilanski, "Novel Ferromagnetic Mn-doped $ZnSiAs_2$ Chalcopyrite With Curie Point Exceeded Room Temperature", *Solid State Phenomena* **152-153**, 311-314 (2009).
- D15.** V. M. Novotortsev, S. F. Marenkin, L. I. Koroleva, T. A. Kupriyanova, I. V. Fedorchenko, R. Szymczak, L. Kilanski, V. Domuchovski, and A. V. Kochura, "Magnetic and Electric Properties of Manganese-Doped $ZnSiAs_2$ ", *Russian Journal of Inorganic Chemistry (Zhurnal Neorganicheskoi Khimii+)* **54**, 1350-1354 (2009).
- D16.** S. F. Marenkin, V. M. Novotortsev, I. V. Fedorchenko, S. A. Warniavskij, L. I. Koroleva, D. M. Zashchirinski, T. M. Khapaeva, R. Szymczak, B. Krzymanska, W. Dobrowolski, and L. Kilanski, "Room-Temperature Ferromagnetism in Novel Mn doped $ZnSiAs_2$ Chalcopyrite", *J. Phys.: Conf. Ser.* **153**, 012058-1-4 (2009).

A series of papers [D13-D16] devoted to the structural, magnetic and electrical properties of the ZnSiAs_2 crystals containing Mn magnetic impurities allowed me to observe and explain a number of important properties that this system has. In particular, we made detailed magnetometric studies of the crystals which allowed obtaining the knowledge and understanding of the magnetism of Mn ions present both in the MnAs clusters and uniformly dissolved in the semiconductor matrix.

5. The studies of the systems based on the II-IV- V_2 semiconductors I focused on the possibility of obtaining the composites containing the MnAs precipitates. A key result of this subject, which I received for the $\text{CdGeAs}_2\text{:MnAs}$ crystals was published in the manuscript [D17].

D17. L. Kilański, W. Dobrowolski, E. Dynowska, M. Wójcik, B. J. Kowalski, N. Nedelko, A. Slawska-Waniewska, D. K. Maude, S. A. Varnavskiy, I. V. Fedorchenko, and S. F. Marenkin, "Colossal linear magnetoresistance in $\text{CdGeAs}_2\text{:MnAs}$ micro-composite ferromagnet", *Solid State Comm.* **151**, 870 (2011).

Manuscript [D17] made it possible to show that obtaining composites based on the CdGeAs_2 semiconductor is possible. The main result of this work was the discovery of the presence of the coupling between the MnAs clusters and inducing in the samples the colossal linear magnetoresistance with values of several hundred percent. This effect has been studied in detail by me in the manuscript [D17]. This research was supported by the magnetotransport studies at high magnetic fields performed due to the fact that I received in 2009 the second travel grant for a short research internship at the Laboratory of High Magnetic Fields in Grenoble, France.

6. I was also involved in the works devoted to the studies of the structural, magnetic, and optical properties of the ZnO nanocrystals systems doped with the transition metal oxides [D18-D19].

D18. U. Narkiewicz, D. Sibera, I. Kuryliszyn-Kudelska, L. Kilański, W. Dobrowolski and N. Romcevic, "Synthesis by Wet Chemical Method and Characterization of Nanocrystalline ZnO Doped with Fe_2O_3 ", *Acta Phys. Pol. A* **113**, 1695-1700 (2008).

D19. I. Kuryliszyn-Kudelska, W. D. Dobrowolski, L. Kilański, B. Hadzic, N. Romcevic, D. Sibera, U. Narkiewicz, and P. Dziawa, "Magnetic properties of nanocrystalline ZnO doped with MnO and CoO", *J. Phys.: Conf. Ser.* **200**, 072058-1-5 (2010).

My contribution in the preparation of the manuscripts [D18-D19] was minor and consisted of making a part of the magnetometric measurements.

The research carried out by me during my doctoral studies yielded interesting and very important results, which, thanks to the financial support could be carried out without hindrance. I have received support from the Office of the Marshal of the Mazovia District by granting for a period of seven months the Mazovia Doctoral Scholarship. In addition, the research I conducted during doctoral studies was supported by the Ministry of Science and Higher Education by the promoter grant for Prof. W. Dobrowolski titled: "New materials for spintronics - II-IV- V_2 and IV-VI group semiconductors containing transition metal ions". I finished the doctoral studies in IF PAN ahead of schedule in June 2010, defending dissertation titled "Magnetism of the CuFeS_2 and NaCl structure semiconductors on examples of $(\text{Cd,Zn})\text{MnGeAs}_2$ and GeSnMnEuTe " performed under the direction of Prof. W. Dobrowolski.

After defending the PhD thesis in June 2010 I started to work as an assistant in the IF PAN in the group led by Prof. W. Dobrowolski. I broke this work after two months due to receiving funding of the annual postdoctoral fellowship at the Aalto University in Finland.

This internship was funded by the EU under the Marie Curie Post-Doctoral Fellowship and the Initial Training Network RAINBOW.

5.c. Postdoctoral probation in the Laboratory of Positron Defect Spectroscopy

After obtaining the title of doctor I had the postdoctoral internship in the Aalto University in Espoo, Finland, in the Laboratory of Positron Defect Spectroscopy led by prof. F. Tuomisto. This internship allowed me to undertake the research of the structural defects in a number of different materials and allowed the publication of the manuscripts [S1-S6] and the manuscript [H3].

- S1. L. Kilański, F. Tuomisto, R. Szymczak, and R. Kruszka, "Magnetically active vacancy related defects in irradiated GaN layers", *Appl. Phys. Lett.* **101**, 072102 (2012).
- S2. H. Nykanen, S. Suihkonen, L. Kilański, M. Sopanen, and F. Tuomisto, "Low energy electron beam induced vacancy activation in GaN", *Appl. Phys. Lett.* **100**, 122105 (2012).
- S3. H. Nykänen, S. Suihkonen, L. Kilański, M. Sopanen, and F. Tuomisto, "Ga-vacancy activation under low energy electron irradiation in GaN-based materials", *Mater. Res. Soc. Symp. Proc.* Vol. 1432.
- S4. T.P. Jili, E. Sideras-Haddad, D. Wamwangi, F. Tuomisto, and L. Kilański, "Defects identification in FeTiO₃ using positron annihilation technique", in Proceedings of SAIP2012: The 57th Annual Conference of the South African Institute of Physics, 81-84 (2012).
- S5. F. Tuomisto, C. Rauch, M. Wagner, A. Hoffmann, S. Eisermann, B. Meyer, L. Kilański, M. Tarun and M. McCluskey, "Nitrogen and vacancy clusters in ZnO", *J. Mater. Res.* **28**, 1977 (2013).
- S6. F. Linez, M. Ritt, C. Rauch, L. Kilański, S. Choi, J. Raisanen, J. S. Speck, and F. Tuomisto, "He implantation induced defects in InN", *J. Phys.: Conf. Ser.* **505**, 012012 (2014).

The research that I conducted in Finland enabled me to publish several papers that helped to solve a number of scientific problems. A very important problem that I solved in the manuscript [S1] was to explain the reasons behind the observation of a presence of significant magnetic moments in the GaN layers that have been irradiated via beam of high energy helium ions. I conducted detailed studies of the magnetic properties of the GaN layers that have been irradiated in a controlled manner. In conjunction with the positron studies it allowed me to explain the observed magnetic properties as coming from the structural defects with nonzero magnetic moment. The studies of structural defects of the GaN layers under controlled creation of defects I continued in the manuscripts [S2,S3]. In the above mentioned papers I showed that irradiation of the GaN layers with the electron beam leads to the creation of structural defects, and consequently to changes in their optical properties. During the internship I also studied the IV-VI and the II-IV-V₂ group crystals. Part of these results I published in the manuscript [H3]. I also carried out a part of the research published in manuscripts [S4-S6]. This work focused on the studies of defect structure in different materials.

5.d. Summary of scientific achievements while working as an assistant professor, not forming part of habilitation dissertation

After returning from the postdoctoral fellowship in Finland I won the competition for the position of the assistant professor in the group of Prof. W. Dobrowolski in IF PAN. I began the work in this position in August 2011. My work focused on the issues related to the

subject of the habilitation. However, I also carried out the research in different areas and subjects which are gathered below:

1. Magnetic exchange interactions and the phenomenon of aggregation of dopants into clusters in the crystals belonging to the IV-VI group of the periodic table doped with magnetic ions of chromium. I conducted a series of studies of a few selected semiconductors with Cr ions which allowed me to make a series of scientific discoveries published in manuscripts [P1-P8] and in the review manuscript [P9]. These papers were made in collaboration with Dr. A. Podgórn, for whose doctoral dissertation I was the secondary supervisor. This research I carried out in part in frame of the statutory work in the IF PAN. These studies were also funded under the HOMING PLUS grant titled: "Homogeneous vs. composite ferromagnetic semiconductors for spintronics applications: structural, electrical and magnetic properties ", of which I was the principal investigator.
- P1.** L. Kilański, M. Górka, W. Dobrowolski, M. Arciszewska, V. Domukhovski, J. R. Anderson, N. P. Butch, A. Podgórn, V.E. Slynko, and E.I. Slynko, "The Role of Frustration in Magnetism of $\text{Ge}_{1-x}\text{Cr}_x\text{Te}$ Semimagnetic Semiconductor", *Acta Phys. Pol. A* **119**, 654 (2011).
- P2.** L. Kilański, M. Górka, W. Dobrowolski, M. Arciszewska, V. Domukhovski, J.R. Anderson, N.P. Butch, A. Podgórn, V.E. Slynko, and E.I. Slynko, "The Role of Frustration in Magnetism of $\text{Ge}_{1-x}\text{Cr}_x\text{Te}$ Semimagnetic Semiconductor, *Acta Physica Polonica A* **119**, 654 (2011), ERRATUM", *Acta Phys. Pol. A* **119**, 904 (2011).
- P3.** L. Kilański, A. Podgórn, W. Dobrowolski, M. Górka, B. J. Kowalski, A. Reszka, V. Domukhovski, A. Szczerbakow, J. R. Anderson, N. P. Butch, V. E. Slynko and E. I. Slynko, "Magnetic Interactions in $\text{Ge}_{1-x}\text{Cr}_x\text{Te}$ Semimagnetic Semiconductors", *J. Appl. Phys.* **112**, 123909 (2012).
- P4.** A. Podgórn, L. Kilański, W. Dobrowolski, M. Górka, A. Reszka, V. Domukhovski, B. J. Kowalski, J. R. Anderson, N. P. Butch, V. E. Slynko and E. I. Slynko, "Spinodal Decomposition of Magnetic Ions in Eu-Codoped $\text{Ge}_{1-x}\text{Cr}_x\text{Te}$ ", *Acta Phys. Pol. A* **122**, 1012 (2012).
- P5.** L. Kilański, A. Podgórn, M. Górka, W. Dobrowolski, V. E. Slynko, E. I. Slynko, A. Reszka oraz B. J. Kowalski, "Magnetic Properties of $\text{Sn}_{1-x}\text{Cr}_x\text{Te}$ Diluted Magnetic Semiconductors", *Acta Phys. Pol. A* **124**, 881 (2013).
- P6.** L. Kilański, M. Szymański, B. Brodowska, M. Górka, R. Szymczak, A. Podgórn, A. Avdonin, A. Reszka, B. J. Kowalski, V. Domukhovski, M. Arciszewska, W. Dobrowolski, V. E. Slynko, and E. I. Slynko, "Magnetic order and magnetic inhomogeneities in SnCrTe-PbCrTe solid solutions", *Acta Phys. Pol. A* **126**, 1203 (2014).
- P7.** L. Kilański, M. Górka, R. Szymczak, A. Podgórn, A. Avdonin, A. Reszka, B. J. Kowalski, V. Domukhovski, W. Dobrowolski, V. E. Slynko, and E. I. Slynko, "Magnetic and magnetotransport properties of $\text{Sn}_{1-x-y}\text{Cr}_x\text{Eu}_y\text{Te}$ crystals: The role of magnetic inhomogeneities", *J. Alloys Comp.* **658**, 931-938 (2016).
- P8.** A. Podgórn, L. Kilański, M. Górka, R. Szymczak, A. Avdonin, M. Arciszewska, W. Dobrowolski, A. Reszka, B. J. Kowalski, V. Domukhovski, V. E. Slynko, and E. I. Slynko, "Magnetic order and the role of inhomogeneities in $\text{Ge}_{1-x-y}\text{Pb}_x\text{Cr}_y\text{Te}$ bulk nanocomposite crystals", *J. Alloys Comp.* **686**, 184-193 (2016).
- P9.** L. Kilański, R. Szymczak, E. Dynowska, M. Górka, A. Podgórn, W. Dobrowolski, V. E. Slynko, E. I. Slynko, M. Romčević, and N. Romčević, "Magnetic Interactions and Magnetotransport in $\text{Ge}_{1-x}\text{TM}_x\text{Te}$ Diluted Magnetic Semiconductors", in Proceedings of the III Advanced Ceramics and Applications Conference, p. 69-84, Ed. W.E. Lee, Atlantis Press (2016).

We have published a number of valuable results related to the doping of GeTe crystals with Cr ions. The main findings published in the manuscripts [P1-P3] devoted to $\text{Ge}_{1-x}\text{Cr}_x\text{Te}$ were: (i) examination of the orbital component to the total magnetic moment of Cr in GeTe, (ii) estimation of the value of the J_{pd} constant for GeTe, (iii) determination of the effectiveness of doping the GeTe matrix with Cr ions and other ions. The next stage of research was an attempt to doping GeTe with Cr and Eu ions. The properties of the $\text{Ge}_{1-x-y}\text{Cr}_x\text{Eu}_y\text{Te}$ crystals allowed for the first time in this group of compounds the identification of the so called spinodal decompositions, i.e. the clusters with the same structure as the matrix and containing magnetic impurities with much higher content than the average chemical composition of the crystals described in the manuscript [P4]. My next manuscripts [P5-P8] concerned problems of the properties of other magnetic IV-VI semiconductors with Cr. The results confirmed the presence of such spinodal precipitates [P5] and Cr_2Te_3 clusters [P6-P8] that dominate the magnetic properties of crystals. The results of my previous research devoted to the IV-VI semiconductors are summarized in the review manuscript [P9].

2. A very important part of my research work was to carry out in cooperation with a number of scientists from Poland and abroad several different studies of selected semiconductors belonging to the II-IV- V_2 group with magnetic Mn ions, published in manuscripts [P10-P23]. These studies significantly increased the knowledge about the properties of the II-IV- V_2 group semiconductors contained in manuscripts [H1-H8]. In manuscripts [P10-P23] my participation was not often dominant. The manuscripts [P10-P23] undertake an analysis of the structural, magnetic, electrical, and optical properties of the range of selected materials, most of which was characterized by the presence of clusters in the semiconductor lattice.

- P10.** I. V. Fedorchenko, A. V. Kochura, S. F. Marenkin, A. N. Aronov, L. I. Koroleva, L. Kilański, R. Szymczak, W. Dobrowolski, S. Ivanenko, and E. Lahderanta, "Advanced Materials for Spintronic Based on $\text{Zn}(\text{Si,Ge})\text{As}_2$ Chalcopyrites", *IEEE Trans. Magn.* **48**, 1581 (2012).
- P11.** M. Romčević, N. Romčević, W. Dobrowolski, L. Kilański, J. Trajić, D. V. Timotijević, E. Dynowska, I. V. Fedorchenko, and S. F. Marenkin, "Optical properties and plasmon - two different phonons coupling in $\text{ZnGeAs}_2+\text{Mn}$ ", *J. Alloys Compd.* **548**, 33, (2013).
- P12.** T. R. Arslanov, A. Yu. Mollaev, I. K. Kamilov, R. K. Arslanov, L. Kilański, V. M. Trukhan, T. Chatterji, S. F. Marenkin, and I. V. Fedorchenko, "Emergence of pressure-induced metamagnetic-like state in Mn-doped CdGeAs_2 chalcopyrite", *Appl. Phys. Lett.* **103**, 192403 (2013).
- P13.** I. V. Fedorchenko, A. N. Aronov, L. Kilański, V. Domukhovski, A. Reszka, B. J. Kowalski, E. Lahderanta, W. Dobrowolski, A.D. Izotov, S.F. Marenkin, "Phase equilibria in the ZnGeAs_2 - CdGeAs_2 system", *J. Alloys. Comp.* **599**, 121 (2014).
- P14.** M. Romcevic, L. Kilański, N. Romcevic, B. Hadzic, W. Dobrowolski, I. V. Fedorchenko, and S. F. Marenkin, "Raman spectra of ZnGeAs_2 highly doped with Mn", *Mater. Res. Bull.* **59**, 300 (2014).
- P15.** L. Kilański, W. Dobrowolski, R. Szymczak, E. Dynowska, M. Wójcik, M. Romčević, N. Romčević, I.V. Fedorchenko, and S. F. Marenkin, "Chalcopyrite Semimagnetic Semiconductors: from Nanocomposite to Homogeneous Material", *Sci. Sinter.* **46**, 271 (2014).
- P16.** L. I. Koroleva, V. Yu. Pavlov, D. M. Zashchirinskii, S. F. Marenkin, S. A. Varnavskii, R. Szymczak, V. Dobrovol'skii, and L. Kilański, "Erratum to: "Magnetic and Electrical

- Properties of the ZnGeAs₂: Mn Chalcopyrite” [Physics of the Solid State 49 (11), 2121 (2007)]”, *Fiz. Tverd. Tela (Phys. Solid State)* **56**, 2367 (2014).
- P17.** L. I. Koroleva, V. Yu. Pavlov, D. M. Zashchirinskii, S. F. Marenkin, S. A. Varnavskii, R. Szymczak, V. Dobrowolski, and L. Kilanski, "Erratum to: “Magnetic and Electrical Properties of the ZnGeAs₂: Mn Chalcopyrite” [Physics of the Solid State 49 (11), 2121 (2007)]”, *Fiz. Tverd. Tela (Phys. Solid State)* **56**, 2589 (2014).
- P18.** T. R. Arslanov, A. Yu. Mollaev, I. K. Kamilov, R. K. Arslanov, L. Kilanski, R. Minikaev, A. Reszka, S. Lopez-Moreno, A. H. Romero, M. Ramzan, P. Panigrahi, R. Ahuja, V. M. Trukhan, T. Chatterji, S. F. Marenkin, and T. V. Shoukavaya, “Pressure control of magnetic clusters i strongly inhomogeneous ferromagnetic chalcopyrites“, *Scientific Reports* **5**, 7720 (2015).
- P19.** E. Dynowska, L. Kilanski, W. Paszkowicz, W. Dobrowolski, I. V. Fedorchenko, and S. F. Marenkin, "X-ray powder diffraction study of chalcopyrite type Cd_{1-x}Mn_xGeAs₂ crystals", *X-Ray Spectrom.* **44**, 404–409 (2015).
- P20.** N. Romcevic, M. Romcevic, W. D. Dobrowolski, L. Kilanski, M. Petrovic, J. Trajic, B. Hadzic, Z. Lazarevic, M. Gilic, J. L. Ristic-Djurovic, N. Paunovic, A. Reszka, B. J. Kowalski, I. V. Fedorchenko, S. F. Marenkin, "Far-infrared spectroscopy of Zn_{1-x}Mn_xGeAs₂ single crystals: Plasma damping influence on plasmon - Phonon interaction", *J. Alloys Comp.* **649**, 375 (2015).
- P21.** T. R. Arslanov, L. Kilanski, S. López-Moreno, A. Yu Mollaev, R. K. Arslanov, I. V. Fedorchenko, T. Chatterji, S. F. Marenkin, and R. M. Emirov, "Changes in the magnetization hysteresis direction and structure-driven magnetoresistance of a chalcopyrite-based magnetic semiconductor", *J. Phys. D: Appl. Phys.* **49**, 125007 (2016).
- P22.** M. Romcevic, N. Romcevic, J. Trajic, L. Kilanski, W. Dobrowolski, I. V. Fedorchenko, and S. F. Marenkin, "Defects in Cd_{1-x}Mn_xGeAs₂ lattice", *J. Alloys Comp.* **688**, 56-61 (2016).
- P23.** T. R. Arslanov, R. K. Arslanov, L. Kilanski, T. Chatterji, I. V. Fedorchenko, R. M. Emirov, and A. I. Ril, "Low-field-enhanced unusual hysteresis produced by metamagnetism of the MnP clusters in the insulating CdGeP₂ matrix under pressure", *Phys. Rev. B* **94**, 184427 (2016).

The papers listed above, putted in the chronological order by the date of their publication, led to examination of a number of scientific problems: (i) the optical properties studied by the Raman scattering technique were used to identify the phonons for a number of phases present in the crystals [P14,P22] as well as allowed the observation of the plasmon-phonon interactions [P11,P20], (ii) the studies of the magnetic and electrical properties of the composite crystals made as a function of the applied pressure made possible to show the presence of meta-magnetic phase transitions in these crystals [P10,P12,P18,P21,P23], (iii) in cooperation with technologists from Russia we created phase diagrams and described in detail a number of structural properties of crystals [P13] and (iv) we published the excellent quality diffraction patterns of the Cd_{1-x}Mn_xGeAs₂ crystals [P19]. I also published the review manuscript [P15], which presented the summary of a series of discoveries for the selected II-IV-V₂ crystals.

3. I undertook, together with my PhD student A. Podgórn, an extensive study of the structural, magnetic, and electrical properties of the Ge_{1-x}Pb_xTe crystals doped with Mn or Cr ions. Our results allowed the publication of three papers [P24-P26]. This research I carried out in part in the framework of the statutory work in the IF PAN. This research was also supported by the POMOST grant titled: "Magneto-optical studies of spintronics

materials based on IV-VI ferromagnetic semiconductors", headed by Dr. B. Brodowska. I was the main contractor for this project.

P24. A. Podgórn, L. Kilański, W. Dobrowolski, M. Górka, V. Domukhovski, B. Brodowska, A. Reszka, B. J. Kowalski, V. E. Slynko and E. I. Slynko, "Anomalous Hall Effect in $\text{Ge}_{1-x-y}\text{Pb}_x\text{Mn}_y\text{Te}$ Composite System", *Acta Phys. Pol. A* **126**, 1180 (2014).

P25. A. Podgórn, L. Kilański, K. Szałowski, M. Górka, R. Szymczak, A. Reszka, V. Domukhovski, B.J. Kowalski, B. Brodowska, W. Dobrowolski, V.E. Slynko, E.I. Slynko, "Magnetic properties of $\text{Ge}_{1-x-y}\text{Pb}_x\text{Mn}_y\text{Te}$ cluster-glass system", *J. Alloys Comp.* **649**, 142 (2015).

P26. A. Podgórn, L. Kilański, M. Górka, R. Szymczak, V. Domukhovski, A. Reszka, B.J. Kowalski, B. Brodowska, W. Dobrowolski, V.E. Slynko, and E.I. Slynko, "Anomalous Hall Effect and Magnetoresistance in $\text{Ge}_{1-x-y}\text{Pb}_x\text{Mn}_y\text{Te}$ Cluster-Glass System", *J. Alloys Comp.* **658**, 265-271 (2016).

Our results showed that: (i) the studied system does not allow to create the homogenous solid solution but dissipates into two crystalline phases, (ii) we estimated the magnetic exchange interaction constants, J_{pd} , for the two magnetic subsystems showing mutual magnetic interactions, (iii) we have examined the anomalous Hall effect and magnetoresistance of the above-mentioned materials allowing to correlate these results with the magnetic properties of the alloys.

4. In collaboration with researchers from Russia we also made a preliminary study of the structural, magnetic, and electrical properties of the systems of thin layers of II-IV-V₂ semiconductors evaporated on the semiconductor substrate [P27].

P27. I.V. Fedorchenko, A. Rumiantsev, T. Kuprijanova, L. Kilański, R.A. Szymczak, W. Dobrowolski, and L.A. Koroleva, "Making Ferromagnetic Heterostructures $\text{Si}/\text{Zn}_{1-x}\text{Mn}_x\text{SiAs}_2$ and $\text{Ge}/\text{Zn}_{1-x}\text{Mn}_x\text{GeAs}_2$ ", *Solid State Phenomena* **168-169**, 313-316 (2011).

The studies gathered in the above-mentioned manuscript had the opening character and opened a larger research program. My role in the creation of the manuscript [P27] was not dominant.

5. I also conducted the research of ZnO nanocrystals doped with Fe_2O_3 [P28] and amorphous glasses doped with magnetic ions [P29]. My role in these studies was not dominant.

P28. I. Kuryliszyn-Kudelska, B. Hadzic, D. Sibera, L. Kilański, N. Romcevic, M. Romcevic, U. Narkiewicz, and W. Dobrowolski, "Nanocrystalline ZnO Doped with Fe_2O_3 - Magnetic and Structural Properties", *Acta Phys. Pol. A* **119**, 689 (2011).

P29. I. S. Yahiaa, K. A. Aly, Yasser B. Saddeek, W. Dobrowolski, M. Arciszewska, and L. Kilański, "Optical constants and magnetic susceptibility of $x\text{La}_2\text{O}_3$ -30PbO-(70-x) B_2O_3 glasses", *J. Non-Cryst. Solids.* **548**, 33 (2013).

5.e. Development of instrumentation for magnetometric measurements

In the framework of the ongoing work focused on the research of the magnetic properties of IV-VI crystals doped with magnetic ions I undertook the execution of works related to the development of two new measurement systems used to study the magnetism of these materials. This research was financed by the SONATA grant titled: "Ultra-precise studies of the magnetic properties of the complex ferromagnetic semiconductors", of which I am the principal investigator. The development of instruments for the magnetometric research enabled me to build a system for the magneto-optical measurements and the magnetometer with the sample vibrating due to the presence of the gradient of the

alternating magnetic field. These devices are currently used by me for the studies of the magnetic materials obtained in the form of thin films and nanostructures.

5.f. Future plans and directions of research

In the future, I plan to direct my research interests toward the following issues:

- The research of the possibilities of inducing ferromagnetism by changing the doping efficiency and changes in the electrical parameters in the homogeneous $\text{Zn}_{1-x}\text{Mn}_x\text{GeAs}_2$, $\text{Cd}_{1-x}\text{Mn}_x\text{GeAs}_2$, and $\text{Cd}_{1-x-y}\text{Mn}_x\text{Zn}_y\text{SnAs}_2$ crystals. So far, I could not observe the ferromagnetism in these compounds. However, in the manuscripts [H1-H3,H8] I showed that the effective Mn content in these materials has a high value, the J_{pd} exchange constant may have high values, and it is possible to obtain a strong p-type conductivity. These features together should allow the induction of ferromagnetism resulting from the RKKY interactions.
- The research of the possibility of achieving a controlled growth of the ferromagnetic clusters on the surface of thin layers based on II-IV-V₂ semiconductors. That would allow me the microscopic examination of the magnetic properties of the clusters while maintaining their effect on the macroscopic properties of the material. These tasks constitute a development of the work contained in my publications [H4-H8]. Such an approach will be an important step to achieve greater understanding of the physical mechanisms responsible for the observed properties of composite materials based on the II-IV-V₂ chalcopyrite compounds.
- The research of the topological states of the topological insulators based on the II-IV-V₂ semiconductors, i.e. CdSnAs_2 crystals. These task is an extension of my initial work devoted to the $\text{Cd}_{1-x-y}\text{Mn}_x\text{Zn}_y\text{SnAs}_2$ crystals published in the manuscript [H8] towards examining the thin strained CdSnAs_2 layers that according to the theoretical literature reports should exhibit behavior characteristic of the three-dimensional topological isolators. The second research topic is the research of the influence of the magnetic impurities on the topological states in the CdSnAs_2 crystals.
- Another very important topic that I would like to take in the future is to undertake further studies of the magnetic properties of the nonmagnetic objects, i.e. defect states having the nonzero orbital angular momentum. This work, which I started in the manuscript [S1] would have to rely on the irradiation of semiconductors with the controlled proton beam that shall cause formation of structural defects in the material. This, in turn, combined with the use of research techniques allowing the studies of structural defects will allow a thorough understanding of these very interesting magnetic states. Even more interesting is the research to introduce into such materials the dopant magnetic ions and to study the magnetic material consisting of two magnetic subsystems.

Łukasz Kilański
27.02.2017v.